Species diversity of Fusarium head blight and deoxynivalenol (DON) levels in western Canadian wheat fields
and
generating *Leptosphaeria maculans* isolates carrying single avirulent (*Avr)* genes

By

Sachithrani Kanchana Kannangara

A Thesis
Submitted to the Faculty of Graduate Studies of
The University of Manitoba
In partial fulfillment of the requirements of the Degree of

MASTER OF SCIENCE

Department of Plant Science
University of Manitoba
Winnipeg, Manitoba, Canada

©Copyright by Sachithrani Kanchana Kannangara 2022

ACKNOWLEDGEMENTS

It is a pleasure to thank those who made this thesis possible. First and foremost, I would like to express my sincere gratitude to my supervisor, Dr. Dilantha Fernando, for accepting me as a graduate research student. I would like to thank him for his continuous encouragement, dedicated involvement, support, and excellent guidance throughout my studies, research work, and thesis writing. Further, I would like to thank my committee members, Dr. Paul Bullock, Dr. Ana Badea, and Dr. Sean Walkowiak, for their tremendous support and guidance.

I gratefully acknowledge the members of my lab. My special thanks to Ms. Paula Parks, who always helped me find materials and for her guidance in lab work. Your friendly and kind words encouraged me all the time. Further, I thank Dr. Abbot Oghenekaro, Dr. Zhongwei Zou, Dr. Shuaglong Huang, and Dr. Fei Liu for their advice and expertise offered for my lab experiments. My gratitude expands to Dr. Liang Zhao for his support in reviewing my thesis. I thank my dearest friends Ms. Rasanie Padmathilake and Ms. Arshani Alukumbura, for being there for me and support they given to me. Further, I thank Ms. Sierra Walker for her hard work of *Fusarium* spore counting.

I would gratefully thank members of Dr. Paul Bullock's lab, Dr. Paul Bullock, Dr. Manasah Mkhabela, and Taurai Matengu for their support in sample collection, processing, and sharing data with me. I am thankful to Dr. Sean Walkowiak and his lab members in the Canadian Grain Commission for supporting me to genotype my samples under challenging times of the year with all COVID restrictions. Further, I thank Dr. Matthew Bakker for his guidance to conduct qPCR assays and allowing me to use his laboratory. Moreover, I acknowledge Mr. Isuru Dharmasena from the Department of Statistics for his support and guidance in analyzing data. Moreover, I convey my gratitude to the Department of Plant Science for providing a very conducive academic atmosphere, and my gratitude extends to the general staff for their tremendous support and cooperation during this study. Finally, I would like to express my deepest and heartfelt thanks to my beloved husband, parents, sisters, and friends. This dissertation could not have been completed without their sincere love, patience, support, and devotion.

TABLE OF CONTENTS

LIST OF TABLES

LIST OF FIGURES

ABSTRACT

Kannangara, Sachithrani K. M.Sc., The University of Manitoba, February 2022. Species diversity of Fusarium head blight and deoxynivalenol (DON) levels in western Canadian wheat fields and generating *Leptosphaeria maculans* isolates carrying single avirulent (Avr) genes. Advising Professor: Dr. W. G. Dilantha Fernando.

Wheat and canola are two major economically important food crops grown in western Canada, accounting for billions of dollars in revenue. Fusarium head blight (FHB) in wheat and blackleg in canola are the most destructive diseases that cause economic losses annually. Both diseases are caused by fungal pathogens, where FHB is primarily caused by *Fusarium graminearum*, while *Leptosphaeria maculans* causes the blackleg disease. This project's first objective is to evaluate the *Fusarium* species diversity and deoxynivalenol (DON) levels in western Canadian wheat fields in 2019 and 2020. The analysis of deoxynivalenol (DON) revealed that spring wheat grain contained higher DON levels than winter wheat grain samples. Additionally, for spring wheat, a significantly lower DON content was found in the grain than in the chaff collected from the same wheat heads for both years. The species diversity analysis showed that *F. graminearum* was the most frequent *Fusarium* species found in the infected samples except the samples from Alberta, while the highest percentage of *F. graminearum* was found in the spring wheat samples from Manitoba. The analysis of chemotype diversity of infected samples showed that 3ADON is the dominant chemotype in FHB disease. For the blackleg disease, a growing concern among blackleg researchers is that resistance (*R*) genes are identified, the same gene as two different genes by two independent laboratories, as not all research laboratories use a standard set of well-characterized isolates. To standardize the *R* gene identification and novel *R* gene discovery, the second objective of this thesis is to develop a procedure to generate *L. maculans* isolates that only carry a single avirulent (*Avr*) gene. Mating between two *L. maculans* isolates showed less efficiency in achieving the above objective. Thus, gene editing with the clustered regularly interspaced short palindromic repeat (CRISPR)/Cas9 was utilized. Seven transformed isolates displayed reduced virulence on the canola cultivar Westar, even though they were not mutated at the target gene.

1.0 General introduction

Western Canada produces a dominating portion of Canadian wheat and canola (AAFC, 2020). In 2020, wheat was cultivated on 23.4 million acres of land, and the number is 22.5 million acres for canola (Statistics Canada, 2021). Canada produces 13% of world's wheat exports (Canadian Cereals, 2020), and Canada is the top canola producer globally. Moreover, wheat and canola play a significant role in the export market of Canada, where 63% of the total wheat product (AAFC, 2020) and 90% of canola yield were exported in 2020 (Canola Council of Canada, 2021). The total value of canola exports was recorded as 11.9 billion Canadian dollars in 2020 (Statistics Canada, 2021). As wheat and canola production is expected to be increasing annually to fulfill the demand created by rising populations, improving the yield of wheat and canola farmlands is vital to both Canadian economy and escalating demand.

Pathogen and pest damage significantly reduce crop productivity and have been responsible for the highest percentage of yield loss (Fernando et al., 2021). Presence of causal agents, susceptible crops and suitable environment for diseases are main components for disease occurrence and persistence (Aboukhaddour et al., 2020). Highly evolving pathogen populations has ability to overcome crop resistance increase the severity of the disease (Amarasinghe et al., 2013; Liban et al., 2016; Van de Wouw et al., 2019). In addition, the cropping system and geographical and climatic properties in western Canada further promoted disease development. Therefore, disease management highly relies on our more profound understanding of crop, pathogen, and their interactions. This study has investigated causal agents of Fusarium head blight (FHB) in wheat and blackleg in canola, which are devastating diseases in western Canada.

Fusarium head blight is a fungal disease caused by *Fusarium* species. The severity of the disease is highly affected by inoculum availability, *Fusarium* species diversity in the field and environmental conditions during anthesis (Figueroa et al., 2018). Even though many studies were conducted on identifying *Fusarium* species and chemotypes in western Canada, the diversity of *Fusarium* species in commercial farmer's fields has not been studied widely (Guo et al., 2008). Thus, the first part of the study focuses on evaluating *Fusarium* species diversity for FHB in wheat fields from western Canada. This study used molecular methods including PCR assays to identify

Fusarium species and chemotypes in spring wheat grain, chaff and winter wheat grain samples collected from western Canada. The results indicated that *F. graminearum* was the most frequent *Fusarium* species associated with the disease. Also, the results confirmed that the 3ADON chemotype is becoming prevalent in western Canada. Moreover, chaff removal reduced the DON levels and *Fusarium* diversity in spring wheat grains. The results will help evaluate the FHB pressure based on species and chemotypes in western Canada and validate the disease forecasting models developed explicitly for western Canada.

Some canola varieties contain resistant genes or *R* genes against blackleg caused by *L. maculans*. Thus, *L. maculans* has a high evolutionary potential to overcome these *R* genes, resulting in a quick breakdown of R genes even within a few years (Van de Wouw et al., 2014b). Therefore, identifying novel *R* genes in canola is essential to control blackleg. However, a growing concern among blackleg researchers is that resistance (*R*) genes are not correctly named as not all research laboratories use a standard set of well-characterized isolates. Further, another concern is the lack of an effective method to create a set of isolates carrying a single *Avr* gene. Therefore, the second part of this study aims to standardize the process of R gene identification and novel R gene discovery by developing a strategy to generate *L. maculans* isolates that only carry a single *Avr* gene.

Meiotic segregation ensures genetic variations in progeny during sexual reproduction or mating between two compatible hyphae (Balesdent et al., 2013). Thus, mating was performed in a laboratory setting and screened for loss of *Avr* genes in the progeny. However, results showed that mating between *L. maculans* isolates was less effective in getting isolates carrying a single *Avr* gene due to fewer pseudothecia production. Thus, the gene-editing tool of the clustered regularly interspaced short palindromic repeats (CRISPR)/Cas9 was used to knockout the *AvrLm5* gene of the *D3 L. maculans* isolate. The CRISPR vector was constructed to target the *AvrLm5* gene and delivered to *D3* via *Agrobacterium* mediated transformation. The results showed that successfully transformed isolates were not mutated on the *AvrLm5* gene sequence. Interestingly, transformed isolates showed phenotype changes, including reduced virulence on canola cultivar, Westar. Further studies will be necessary to determine genetic differences between those transformants and wild-type *D3* isolates.

2.0 Literature review

2.1 Agriculture in western Canada

Agriculture contributes significantly to the Canadian economy. In 2020, there were 2.1 million people employed in the agriculture and agri-food industries. The agriculture and agri-food industry contributes 7.4% of Canada's gross domestic product (GDP), worth over 139 billion dollars. Specifically, crop production accounts for 34.4 billion dollars of GDP and created 124 thousand jobs in 2020. The major Canadian crop commodities include canola, wheat, soybeans, vegetables and potatoes (AAFC, 2020b).

Western Canada produce largest portion of cereal crops and oilseeds grown in Canada (AAFC, 2020). The major crops include wheat, canola, barley, corn, and soybean. Among them, wheat and canola are grown most extensively. In 2020, wheat was grown on 23.4 million acres, and canola on 22.5 million acres (Statistics Canada, 2021). In western Canada, the province of Saskatchewan is the most significant contributor to wheat and canola production. In 2020, the total net worth was recorded as 5.3 billion dollars for canola and 3.3 billion dollars for wheat (AAFC, 2020b). Further, western Canadian cereals and oilseeds play a significant role in the export market of Canada.

2.2 Wheat

Wheat, which belongs to the family Poaceae, is one of the most important cereal crops globally, and it includes common wheat (*Triticum aestivum* L.), durum (*T. durum*) and club wheat (*T. compactum*). Common wheat (wheat) is the most widely cultivated species of wheat (FAOSTAT, 2019). Wheat is consumed by 40% of the world's population as their staple food. In addition, various food items are made from wheat as the primary raw material, including bread, noodles, pastries, and cakes. On a daily basis, wheat products provide an average of 500 kcal per capita in Canada (Grote et al., 2021). Wheat is grown as a cash crop due to its high yield per area and high demand. As temperate climates are most suitable for wheat production, the European Union, China, India, Russia, United States, and Canada are the top wheat producers in 2020/2021. In 2020/2021, total global wheat production volume is recorded as 772.64 million metric tons, an increase of over 30 million tons compared to 2019/2020 (Shahbandeh, 2021).

The demand for wheat is increasing annually with the world population growth. The annual population growth rate is calculated as 1.3% from 1990 to 2020, and the estimated population for 2050 is nine billion (Johnson, 1999). Therefore, the increase in wheat production is crucial for feeding the world. Canada contributed 13% of total wheat production around the world (Canadian Cereals, 2020), and in recent years Canadian wheat production has been increasing yearly by 5% on average. The latest information indicated that in 2020-21, the acreage of wheat was 7,892 k ha, and the average yield will be 3.7 ton/ha as predicted by AAFC.

Western Canada is the main production region of Canadian wheat, and Saskatchewan is the top production province, followed by Alberta and Manitoba (Campbell, 2015). There are different classes of wheat grown in Canada, including Canada Western Red Spring (CWRS), Canada Prairie Spring (CPS), Canada Western Soft White Spring (CWSWS), Canadian Northern Hard Red (CNHR), Canadian Eastern Red Spring (CERS) and others. CWRS is the class with the largest growing area in western Canada (Dexter et al., 2006). The wheat cultivars of these classes are bred for targeting higher yield and resistance to biotic and abiotic stress. Moreover, wheat plays a significant role in the export market, as 63% of the total product was exported in 2019 (AFCC, 2020). Improving the productivity of wheat farmlands is vital for the Canadian economy and to meet escalating demand.

2.2.1 Challenges in wheat production

The Canadian prairies are known as the world's breadbasket because of their significant contribution to world wheat production. Wheat was the first staple crop domesticated in Europe, West Asia, and North Africa (Tack et al., 2015) and first introduced to Canada during 1605 at Port Royal, Nova Scotia. Since then, wheat has been grown extensively in Canada (Fernando et al., 2021). Usually, successful wheat cultivation needs 300 mm to 500 mm of annual rainfall and 15 – 21 °C of temperature throughout the growing season (Canadian Cereals, 2020). The vast flat prairie land also facilitates the use of large agricultural machinery for seeding, spraying, and harvesting. Further, wheat prefers humus-rich deep soil, thus fields are supplemented with necessary fertilizers or manure. Mostly, spring wheat seeds are sowed directly to ploughed fields in May, while winter wheat seeding starts in fall and undergoes a dormancy period. As a result, winter wheat will be

harvested in summer, while spring wheat is harvested from August to the end of September (GeoforCXC, 2021).

Abiotic and biotic stresses have significantly challenged wheat production by reducing the expected yield and causing losses in grain quality. Most abiotic stresses are triggered by extreme weather conditions such as frost, flooding, heat, salinity, and drought stress (Brar et al., 2019; Dresselhaus & Hückelhoven, 2018). Also, some biotic stresses are associated with environmental conditions, which may be favourable to pathogens and pests. Fungal pathogens cause severe diseases in wheat, such as wheat rust, blotch, and FHB (Figueroa et al., 2018). Other than fungi, bacteria and viruses may also cause wheat diseases, such as yellow ear rot and yellow dwarf (Prescott et al., 2015). Further, insect pests such as aphids, stink bugs, and grasshoppers may damage the crop foliage. Moreover, the soil-borne nematodes such as seed gall nematode, root-knot, and cereal cyst nematodes feed on the crop, causing severe damage to plant productivity (Prescott et al., 2015).

Global warming and climate change have made a significant challenge for wheat breeders and farmers in searching for more resistant cultivars to both biotic and abiotic stress as they may may negatively affect the quantity and quality of the yield. Different strategies have been adopted to overcome these challenges. For example, farmers apply cultural practices, crop rotation, fungicides, herbicide application, and growing resistant cultivars (Champeil et al., 2004). At the same time, plant scientists are working to overcome these challenges through advanced breeding techniques to create resilient cultivars (Fernando et al., 2021). Since conventional breeding is time-consuming and labour-intensive, the advancement of biotechnology has been a promising way of improving wheat pest resistance. This process is accelerated with currently available state-of-the-art technologies such as high-throughput sequencing, gene identification, annotation, and gene editing (Buerstmayr et al., 2020; Fernando et al., 2021).

Better management of fungal diseases is crucial to achieving the expected yield target, as 15-20% annual yield loss may occur due to fungal infections (Figueroa et al., 2018). In Canada, wheat breeding projects target a minimum resistance level against all five top-priority wheat diseases, which are FHB (primary causal agent: *Fusarium graminearum*), leaf rust (primary causal agent:

Puccinia triticina), stem rust (primary causal agent: *Puccinia graminis*), stripe rust (primary causal agent: *Puccinia striiformis*), and common bunt (primary causal agent: *Tilletia caries*) (Brar et al., 2019). The following sections introduce FHB, including history, epidemiology, impact, and management strategies.

2.2.2 Fusarium head blight

Fusarium head blight (FHB) or scab is a fungal disease that affects small grain cereal species such as wheat, oats, barley, triticale, and rye (Parry et al., 1995; Sutton, 1982). Fusarium head blight has caused significant epidemics in history, causing millions of tons of yield loss by damaging the crop. The disease is recorded worldwide, including in North America, Europe, and East Asia (Bottalico & Perrone, 2002; Leonard & Bushnell, 2003). Fusarium head blight was first observed in England in 1884, while FHB was found in North America at the beginning of the 1900s in Minnesota and North Dakota, USA. By 1996, FHB was widespread across the wheat fields of eastern parts of the USA and caused an estimated $56 million loss (McMullen et al., 1997). Besides the yield loss, the infected grains will be unsuitable as human or animal feed due to contamination of mycotoxins produced by the pathogen (Desjardins, 2006). Thus, FHB is one of the most studied diseases of wheat (Audenaert et al., 2009; Buerstmayr et al., 2020; Fernando et al., 2021).

Fusarium head blight is identified as a priority-one disease in wheat by the Canadian Grain Commission due to its high impact on annual yield loss. *Fusarium* species were first reported in Canada in 1923 in Manitoba on corn stubble. However, the most virulent FHB pathogen, *F. graminearum,* was not observed in Canada until 1948. Eventually, the FHB disease became more severe in western Canadian prairies as the percentage of *F. graminearum* gradually increased among the pathogen population. The disease spreaded from Manitoba to Saskatchewan and recently to Alberta (Clear & Patrick, 2010). Severe FHB epidemics reported in 1993 in western Canada brought out FHB as the most concerning problem in the Canadian wheat industry. The no-till cropping systems adopted in recent decades aided the inoculum survival and also facilitated the disease occurrence during conducive conditions for pathogen (McMullen et al., 1997). From 1991 to 2016, the increased minimum and zero-tillage practices before sowing may supported the drastic increase of FHB disease severity. The most recently, the highest mean percentage of sample

containing *Fusarium* damaged kernel (FDK) was reported in 2016 in western Canada (Canadian Grain Commission, 2020). Further, the disease severity increased from 34% to 59% in Manitoba, 36% to 93% in Saskatchewan, and 27% to 88% in Alberta in 2019 (Aboukhaddour et al., 2020). In addition, limited knowledge about the disease epidemiology caused devastating FHB epidemics in history, resulting in severe damage to the wheat industry. Currently, FHB is still responsible for significant yield loss annually. Therefore, a better understanding of FHB will be beneficial for the agriculture industry of Canada (Desjardins, 2006; McMullen et al., 1997).

2.2.3 Fusarium head blight causing agents

The *Fusarium* genus belongs to Ascomycota (Phylum), Hypocereales (order), and Nectriaceae (Family), is ubiquitous, and is known to cause infections in both plants and animals. Specifically, to plants, the *Fusarium* genus includes many pathogenic fungal species that cause different agriculturally destructive diseases. For example, *F. oxysporum* strains are soil-borne plant pathogens that cause wilting in crop plants, including tomatoes, bananas, cabbage and cucumber (Arie, 2019). *F. solani* causes root rot in soybeans, peas and many crops in the Solanaceae family (Coleman, 2016). *F. graminearum* infects cereal hosts such as wheat, corn and non-cereal crops such as soybeans, field peas and canola (Gilbert & Fernando, 2004). In general, *Fusarium* species cause devastating diseases in many crop species.

F. graminearum (teleomorph *Gibberella zeae*) is identified as the primary etiological agent of FHB of wheat in North America (Leonard & Bushnell, 2003; Parry et al., 1995; Ward et al., 2008). Although studies found that other *Fusarium* sp. are also associated with disease formation, their contribution to disease development is lower than *F. graminearum* (Parry et al., 1995). *F. graminearum* was isolated from crops infected with FHB worldwide, including Asia, Africa, America, Europe, and Oceania. All of these isolates are described to be part of the same *F. graminearum* species complex (*Fg* complex), as they could not separate using their morphological characters (Wang et al., 2011). In 2000, a study conducted by O'Donnell et al. (2000) found that the *Fg* complex separated into seven phylogenetic lineages using the genealogical concordance phylogenetic species recognition (GCPSR). They showed the presence of phylogenetically distinct species within the *Fg* complex occurred by limited gene flow during their evolution due to geographical separation. (O'Donnell et al., 2000). Later studies revealed 13 phylogenetically

distinct species through combining GCPSR, multilocus genotyping (MLGT) and molecular markers (O'Donnell et al., 2008). They have named the new clades and showed that those isolates were endemic to specific global regions. However, *F. graminearum sensu stricto* was found from all of those regions (O'Donnell et al., 2008; Starkey et al., 2007; Yli-Mattila et al., 2009). Specifically, Canadian *F. graminearum* isolates found in infected samples from the western Canadian fields were classified as *F. graminearum sensu stricto* (Amarasinghe et al., 2019; Kelly & Ward, 2018).

2.2.4 Disease cycle and epidemiology

Fusarium spp. that cause FHB are hemibiotroph fungi that can survive on crop residues. They can also become phytopathogens in the presence of suitable host plants under favourable environmental conditions. Therefore, the infected cereal crop residues such as wheat or corn may start a new disease cycle (Figure 2.1). *Fusarium* produce both asexual (macroconidia or/and microconidia in sporodochia) and sexual spores (ascospores in perithecia). Studies showed that crop residues that remained on the field had perithecia even after two years of decomposition. However, no spore production was observed when infected residues were buried in the ground (Gilbert & Fernando, 2004; Khonga & Sutton, 1988). Thus, the no-tillage agricultural system enhances disease persistence by facilitating the survival of fungal fruiting bodies (Khonga & Sutton, 1988).

Fusarium head blight pathogen infection is triggered mainly by warm and humid weather (McMullen et al., 1997). The primary inoculum of FHB comprises ascospores released from the perithecia and conidia liberated from sporodochia (Sutton, 1982). A temperature between 15 to 25 °C is ideal for spore formation and dissemination (Gilbert & Fernando, 2004). The conidia are released and dispersed by splash created by rainfall (Paul et al., 2004). Further, past studies showed that rainfall events also increase the air-borne ascospore concentration measured afterward (Inch et al., 2005). Periods of high humidity provide suitable conditions for ascospore dispersal and germination on wheat spikelets (Parry et al. 1995, Gilbert and Fernando 2004). In addition, the ascospores are dispersed by the wind as a gradient downwind from the infected loci to neighbouring crops (Fernando et al., 1997). In addition, insect vectors such as wheat midges act

as vectors of FHB as they transmit *Fusarium* macroconidia from the source to wheat spikes (Mongrain et al., 2000).

Spore germination occurs on the wheat spikes (Sung & Cook, 1981). The fungal spores should land on wheat spikes during their susceptible period, which lasts for a short time, starting from anthesis to the soft dough stage of grain formation. This period usually lasts for 10 to 20 days in common wheat (Pritsch et al., 2000; Schroeder & Christensen, 1963). High relative humidity facilitates germ tube formation and subsequent mycelium growth (Bai Guihua & Shaner, 1994; Parry et al., 1995). The macroconidia of *F. graminearum* began to germinate within 6 to 12 hours on host tissues (Pritsch et al., 2000). In addition to the environmental conditions, the time required for germ tube formation differs among the *Fusarium* species. Since the spore germination does not coincide with infection, the ecological factors following infection also affect the disease severity (Beyer et al., 2004; Palmero Llamas et al., 2008). Thus, the disease severity of FHB highly depends on the susceptible host and environmental factors (Gilbert & Fernando, 2004; Klem et al., 2007; Sung & Cook, 1981).

The penetration and colonization occur through stomatal openings of the glume and through cracks in anthers. During infection, *F. graminearum* produces infection structures including appressoria which facilitate the penetration by secreting lytic enzymes (Boenisch & Schäfer, 2011). Conidiophores bearing macroconidia were observed on the surface of the glume within the next 48 to 76 hours after inoculation (Pritsch et al., 2000). At this point, fungal hypha is well distributed and established around the plant plasma membrane. However, degradation of plant organelle starts at 120 hours post inoculum due to over colonization of fungi (Kheiri et al., 2019). As a result, the host cells start necrosis showing visual symptoms (Figueroa et al., 2018). Further, fungal mycelium infects neighbouring spikelets through the vascular bundles of the rachilla and rachis (Leonard & Bushnell, 2003).

2.2.5 Development of disease symptoms

FHB disease symptoms could be observed at the early milk stage on wheat kernels as water-soaked brown colour spots, especially on the glume or rachis. These symptoms will gradually spread through the grain during disease progress (Figure 2.2). Salmon pink-coloured mycelia can be

observed on the base of the spikelet at the beginning, and progressively it will spread over the entire head. The fungus also proliferates on seeds, seeds become shrunken and bleached due to the degradation of starch and proteins (Parry et al., 1995; Sutton, 1982). The production of mycotoxins by the pathogen is most dangerous and can be symptom-less on the plant, yet mycotoxins are of utmost importance to human and animal health concerns (Amarasinghe et al., 2019; Amarasinghe et al., 2015). Further, the production of mycotoxins may decrease the host defence mechanisms and cause cell death, increasing the disease severity (Figueroa et al., 2018).

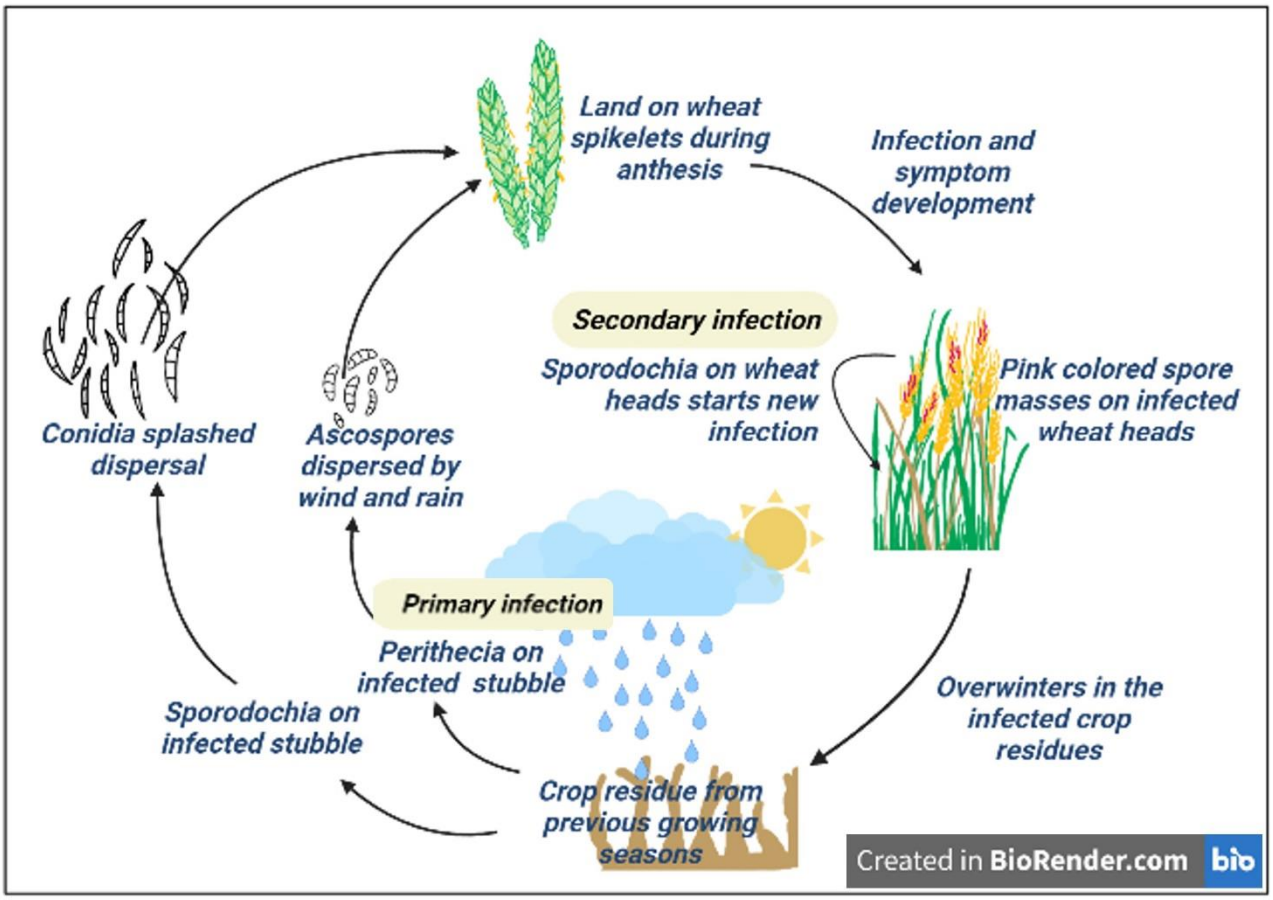

Figure 2.1 *Fusarium* disease cycle. Inoculum released from infected crop residues to land on susceptible wheat during anthesis. The pathogen invades the host tissues initiating the disease and development of symptoms. (Created with BioRender.com)

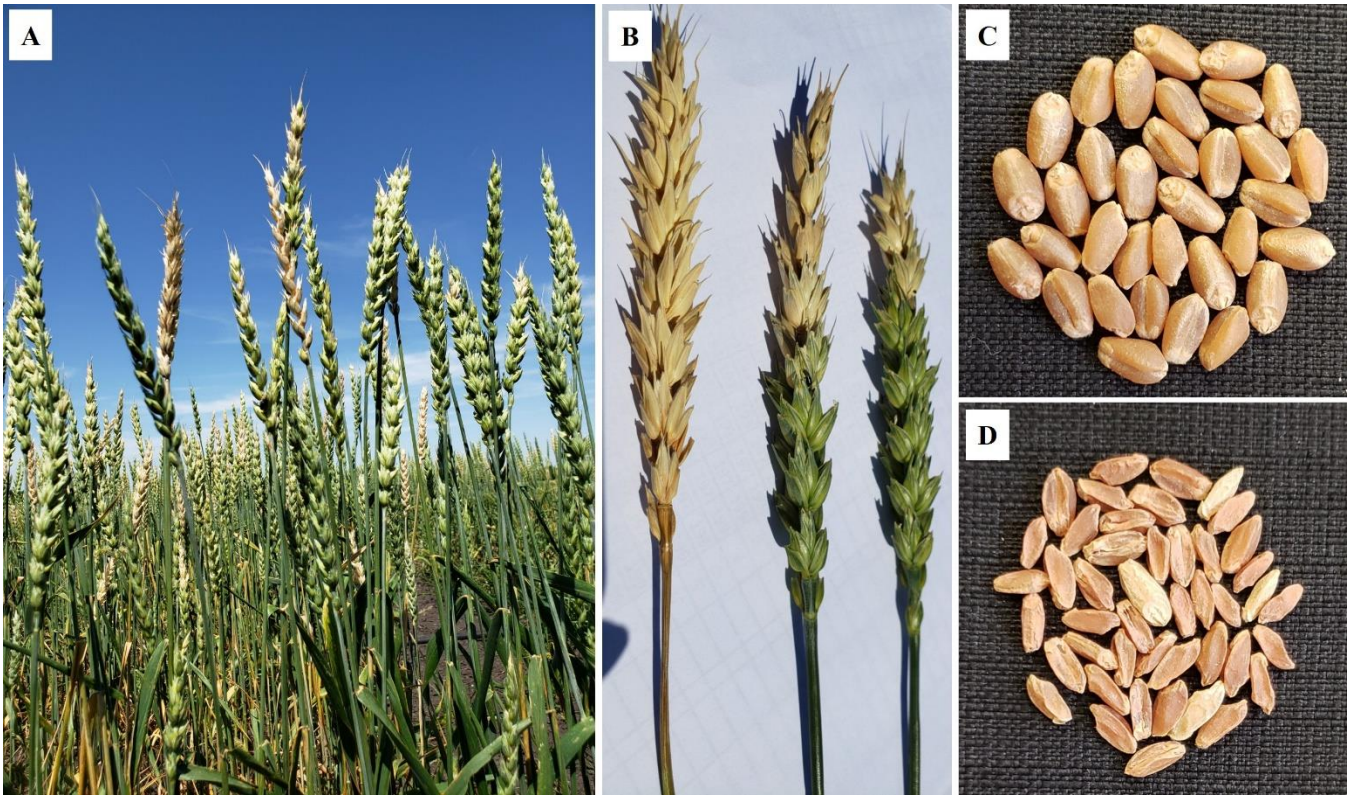

Figure 2.2 Visual symptoms of Fusarium Head Blight. A: FHB infected wheat field with discoloured spikelets. B: Premature bleaching of wheat heads, C: Healthy wheat kernels compared to D: FHB damaged kernels which are bleached and shrunken.

2.2.6 Mycotoxins

Fusarium species can produce several types of mycotoxins, including trichothecenes, zearalenone (ZON), fumonisins, moniliformin and butanolide (Desjardins, 2006; Jurado et al., 2005). Among them, trichothecenes are the most studied mycotoxin type which cause great impact on agricultural production systems for wheat. There are four types of trichothecenes (type A, B, C and D) produced by phytopathogenic fungi. However, only type A and B trichothecenes are associated with FHB (Foroud & Eudes, 2009). There are several forms of type A trichothecenes. *Fusarium* species produce type A trichothecenes such as T-2 toxin, HT-2 toxin, diacetoxyscirpenol, and neosolaniol. For example, *F. sporotrichioides* and *F. poae* make type A trichothecene during infection (Foroud & Eudes, 2009; Mateo et al., 2002). In contrast, type B trichothecenes are produced by all members of the *F*g complex during the invasion of host tissues (Amarasinghe et al., 2019; O'Donnell et al., 2008). When comparing their toxicity between type A and type B

trichothecenes, type A trichothecenes, especially T-2 toxins, have higher toxicity in mammals than type B trichothecenes (Bottalico & Perrone, 2002; Foroud & Eudes, 2009).

F. graminearum produces two forms of type B trichothecenes, deoxynivalenol (DON) and nivalenol (NIV). DON has two forms of acetylated derivatives, 3-acetyl-DON (3ADON) and 15-acetyl-DON (15ADON) (Amarasinghe et al., 2015; Goswami & Kistler, 2005). The production of these mycotoxins enhances the virulence of the pathogen. A study conducted on a mutant strain of *F. graminearum* with a disrupted trichothecene synthase (*Tri5*) gene showed a lower disease severity of this pathogen under both greenhouse and field conditions (Bai et al., 2001). This non-DON producing strain only caused disease on the initial infection site but could not spread to nearby spikes (Bai et al., 2001). Further, DON produced inside the plant tissues inhibits the protein synthesis in plant cells by binding to the ribosome-60S subunit to disturb cell signaling and cause cell death (Desjardins, 2006). NIV is more toxic than DON and frequently produced by Asian populations of *F. graminearum*. Interestingly, no *F. graminearum* is found with the capacity to produce both DON and NIV due to known gene variations in trichothecene biosynthesis pathway (Goswami & Kistler, 2005). In addition to DON and NIV, recently *F. graminearum* population was found in North America producing a different type of trichothecene analog, 3α-acetoxy, 7α, 15-dihydroxy-12,13-epoxytrichothec-9-ene (NX-2), which chemical structure was silimar to 3ADON chemotype (Kelly and Ward 2018). In Canada, NX-2 producing *F. graminearum* was reported in low frequencies (Fernando et al., 2021).In Canadian fields, DON is identified as the primary mycotoxin produced by the *F. graminearum* (Amarasinghe et al., 2019; McMullen et al., 1997). Even though 15ADON was more prevalent in Canadian *Fusarium* populations previously, the frequency of 3ADON is significantly increasing in western Canada, as indicated by many surveys identifying a shift of chemotype (Amarasinghe et al., 2019; Guo et al., 2008; Ward et al., 2002, 2008). These 3ADON producing populations are more virulent and toxigenic than 15ADON producing populations (Ward et al., 2008). In western Canada, NIV-producing *Fusarium* species are rare (Miller & Richardson, 2013), while both DON and NIV can be found in FHB infected fields in Asia and Europe (Ichinoe et al., 1983). A recent study conducted by Amarasinghe et al. (2015) indicated the risk of NIV contamination in Canadian fields by showing the presence of NIV producing *Fusarium* sp.; *Fusarium cerealis*.

These mycotoxins could be present in the infected wheat grains, flour, and even in processed food, increasing contamination risk (Dexter et al., 1997). DON level in end products is strictly regulated due to their toxicity. Wheat millers only accept DON levels below 2 ppm in wheat grains for human consumption and below 5-10 ppm for livestock feed (US Food and Drug Administration, 2010; Government of Canada, 2017). High DON levels in wheat may threaten human health by direct consumption of DON-contaminated food, or indirectly by consuming contaminated livestock products such as milk, eggs, or meat. The Codex Alimentarius Commission set up international food standards for maximum DON levels in cereal-based food at 0.2 mg per kg, 1 mg per kg for wheat flour or flakes and 2 mg per wheat which may further process before consumption (FAO, 2021). High DON levels in the human diet cause vomiting, nausea, diarrhea, abdominal pain, headache, dizziness and fever (Sobrova et al., 2010). For animals, an undesired level of DON presence in the feed may cause toxic effects such as feed refusal, vomiting, decreased resistance to infection/disease, and impaired reproductive function (Government of Canada, 2017). Thus, the high levels of DON and other mycotoxins reduce grain quality, lower grain price, and can even result in total loss of commercial value (Gilbert & Tekauz, 2000).

DON accumulation on grain is highly correlated with the presence of *F. graminearum* and FHB severity in the field (Demeke et al., 2005; Paul et al., 2005). Moreover, disease epidemiology-related environmental factors such as rainfall, temperature, relative humidity may influence the DON accumulation (Wegulo, 2012). For example, 15-20 °C temperature and high moisture level during the anthesis stage were identified as significant factors which increase the DON accumulation (Cowger et al., 2009). At the same time, other factors influencing DON accumulation include cultivar resistance, the crop's growth stage, availability of inoculum, tillage system, previously grown crop type, and fungicide application (Wegulo, 2012).

2.2.7 Fusarium head blight forecasting systems

Since weather conditions highly impact FHB disease occurrence and severity, agronomists have generated weather-based FHB forecasting models. Moreover, additional information related to other conditions such as the severity of FHB, mycotoxin contamination, inoculum dispersal and narrow window of pathogenicity towards the susceptible crop makes risk assessing models more suitable for mitigating the disease (De Wolf et al., 2003). There are two types of forecasting

models, empirical and mechanistic models. The empirical models are more common and simple and can be developed quickly by integrating weather parameters and FHB data collected from specific regions. On the other hand, mechanical models are more complex and generated by combining data collected over an extended period (Prandini et al., 2009). Although these models are more efficient in the designed area, they can be readily adapted to another region after modifying the parameters (Giroux et al., 2016; Prandini et al., 2009).

Many FHB forecasting models have been developed worldwide, including Argentina, Belgium, Canada, Italy, and the USA (Prandini et al., 2009). In Canada, Hooker et al. (2002) developed a model to predict DON accumulation in mature wheat heads by analyzing the rainfall, temperature, FHB occurrence and final DON content. They utilized stepwise multiple regression procedures to select the vital weather variables and their timing at 50% head emergence (Hooker et al., 2002). Later, they developed web-available software, DONcast®, which provides wheat producers with a prediction tool about DON accumulation to increase the efficiency in fungicide spray (available at https://www.weatherinnovations.com/).

The developed models could be beneficial for releasing FHB risk maps to guide growers in making farming decisions. For example, the Departments of Agriculture in Manitoba, Saskatchewan and Alberta publish FHB risks maps for each province annually (Manitoba Agriculture, 2021). The Saskatchewan maps were created with a model that included temperature and relative humidity in the previous five days plus two days forecast. On the other hand, Manitoba and Alberta maps use a model which contains the hours of precipitation and the hours with temperature ranging from 15 to 30 °C during the previous seven days. As a result, the modeled FHB risk levels are slightly different between provinces (Manitoba Agriculture, 2021). The Fusarium Risk Tool is another web-based software offered by the National Fusarium Head Blight Prediction Center, USA (available at https://www.wheatscab.psu.edu/) developed with decades of data since 2004 using weather data (hourly temperature, humidity, and rainfall), crop growth stage and disease observations from different states. This model is utilized to predict the FHB risk level (disease severity more than 10%) for spring wheat and winter wheat according to the location of the field, flowering date and the variety grown. Currently, this model is utilized by 23 states, and the estimated model accuracy is 80% (De Wolf et al., 2003; McMullen et al., 2012). Further, the

knowledge about air-borne inoculum availability is an essential factor for developing risk assessment models to manage the disease (Inch et al., 2005).

In conclusion, FHB forecasting models allow producers to evaluate the disease severity. Thus, it will allow farmers to predict the need for fungicide application well ahead of visible disease symptoms in the field. Furthermore, these models will help create a live, area-specific FHB Alert System, which will provide excellent protection against this devastating disease (McMullen et al., 2012). For example, the system could notify the farmers about high-risk events by sending an auto-generated multimedia message or notification to their mobile phones.

2.2.8 Identification of *Fusarium* species and their chemotype

Monitoring of the *Fusarium* populations is essential in disease management as the FHB disease severity differs with the type of *Fusarium* species. In addition, the species composition varies among different fields, and the pathogen species and their chemotypes determine the FHB disease severity. For example, a higher percentage of *F. graminearum* or *F. culmorum* causes more severe damage to crops than less pathogenic *F. sporotrichoides* or *F. poae* (Wang et al., 2011). Similarly, *Fusarium* species producing the 3ADON chemotype cause high disease severity because they are more virulent than 15ADON producing *Fusarium* species (Ward et al., 2008). Thus, studying *Fusarium* species diversity could provide more significant insights for FHB disease management. Furthermore, identification of chemotype diversity of *Fusarium* facilitates inference of pathogen genetic diversity due to genetic recombination, population age, and cropping systems. The chemotype diversity in different areas may also help predict disease distribution patterns (Guo et al., 2008). In addition, knowledge about mycotoxins may be used to prevent contamination through the food chain (Jurado et al., 2005; Klem et al., 2007). Therefore, the information about FHB population diversity will help farmers in disease management and increase their willingness to adhere to control measures (Panthi et al., 2014).

Traditionally, *Fusarium* species are identified by their macroscopic characteristics such as colony morphology and microscopic characters such as the shape of macroconidia (Aoki & O'Donnell, 1999). Moreover, selective media for *Fusarium* provides an accurate and convenient identification. For example, the Segalin and Reis agar (SRA-FG) was created as a semi-selective media to detect

F. graminearum (Karelov et al., 2021; Segalin & Reis, 2010). However, these traditional identification methods are time-consuming, laborious and less accurate than molecular identification (Aoki & O'Donnell, 1999; Demeke et al., 2005).

The molecular and biochemistry-based technologies provide handy tools in identifying different chemotypes and species. These technologies include ELISA (enzyme-linked immunosorbent assay), gas chromatography, mass spectroscopy, polymerase chain reaction (PCR), and sequencing. The ELISA, gas chromography, and mass spectroscopy techniques are specifically used to identify and quantify the chemotypes or toxins produced by the *Fusarium* species. The ELISA technique is an immunochemical method that has been readily used for DON determination in ground grain samples (Panthi et al., 2014). There are commercially available chemotype identification kits for ELISA, such as Veratoxin 5/5 kits (Biognost, Neogen, Leest, Belgium) that provide high accuracy in DON identification (Amarasinghe et al., 2016; Audenaert et al., 2009). The gas chromatography or mass spectroscopy techniques (GC-MS /LC-MS/MS) use biochemical properties to differentiate DON and its derivatives from other chemicals present. They are widely used in DON quantification due to the higher sensitivity, accuracy, specificity and preciseness of the technique (Foroud & Eudes, 2009; Krska et al., 2001).

PCR provides rapid, sensitive, and precise species identification by amplifying a target DNA strand. For instance, pure mycelial cultures can be subjected to species-specific PCR following DNA extraction (Demeke et al., 2005). These PCR techniques include genus-specific or species-specific primers which are designed to target common genes, including but not limited to trans-elongation factor EF-1α, β-tubulin gene, histone H3, and trichothecene biosynthesis genes; *Tri5* and *Tri101* or universal fungal barcoding gene; internally transcribed spacer (ITS) *ITS1* and *ITS2* (Amarasinghe et al., 2019; Amarasinghe et al., 2016; Demeke et al., 2005; O'Donnell et al., 2008; Wang et al., 2011). Sequence polymorphism within the genus is used to differentiate species. Furthermore, multiplex PCR assays can be used to characterize the chemotype of *Fusarium* sp. present in a specific population (Guo et al., 2008; Jurado et al., 2005; O'Donnell et al., 2008). Polymorphisms within the TRI-gene cluster, which contains the biosynthetic and regulatory genes for tricothecene production, was utilized to develop chemotype-specific multiplex primers to differentiate 3ADON, 15ADON and NIV (Ward et al., 2002). Moreover, quantitative PCR

(qPCR) techniques have been utilized to quantify the fungal abundance, which is more sensitive and accurate than conventional PCR. The qPCR also contains probe-based assays, providing rapid and high-throughput detection and quantification of *Fusarium* species and their chemotypes (Karelov et al., 2021; Nicolaisen et al., 2009; J. H. Wang et al., 2011). In addition, the next-generation sequencing techniques are used to identify *Fusarium* species by aligning the unknown sequence with the DNA databases of reference sequences (Fernando et al., 2021).

2.2.9 FHB disease management

As explained in previous sections, the FHB disease occurrence and persistence greatly rely on the presence of inoculum and favourable environmental conditions, including moderate temperature and high humidity. Fusarium head blight is considered a complex disease to manage because of this involvement of ecological conditions (Bai Guihua & Shaner, 1994). Nevertheless, several strategies are utilized for disease control, including soil cultivation, crop rotation, fungicide application and introducing resistant cultivars. The soil cultivation system significantly influences disease initiation due to the persistence of inoculum on crop debris remaining from the previous growing season. The highest severity of the disease is reported from cultivation systems which leave more residue on the field, especially in no-till cultivation fields (Khonga & Sutton, 1988; Klem et al., 2007). Crop rotation leaves inoculum to degrade in soil with non-host crops and thus reduce the disease severity. The studies have proven that longer crop rotations could significantly mitigate disease. However, FHB severity of wheat may increase if the following crop of rotation is a host for *Fusarium* spp, such as corn, durum wheat or oats. Thus, non-host crops such as canola, flax, alfalfa, or sugar beets are the best to rotate with wheat. Moreover, two years with non-host crops are recommended between two wheat cultivations (Champeil et al., 2004).

Breeding for disease resistance has been used from ancient history to today to produce better performing crops. Fusarium head blight disease resistance is a priority trait that breeders want to include in new wheat cultivars. The Prairie Recommending Committee for Wheat, Rye and Triticale (PRCWRT) recommended including a minimum FHB resistance level for cultivar registration (Aboukhaddour et al., 2020; Brar et al., 2019). Many quantitative genes control the FHB resistance of wheat. These genes are selected during breeding which is initially found by screening wild wheat relatives or native resistant to FHB. For example, the Canadian wheat

breeding programs use the resistant germplasm of the Chinese wheat variety (Sumai 3) for breeding spring wheat and a Brazilian cultivar (Fontana) for winter wheat breeding (Gilbert & Tekauz, 2011). The wheat breeders look for five types of FHB resistance including resistance to the initial infection (type I), resistance to spread from its initial infection site (type II), resistance to grain damage (type III), tolerance to yield loss (type IV) and resistance to DON accumulation by degrading the toxins within the host tissues (type V) (Fernando et al., 2021). The Canadian wheat varieties predominantly exhibit type I and type II resistance (Gilbert and Tekauz, 2011). Many studies have developed a set of molecular markers to identify these valuable quantitative trait loci (QTL), which can be used in Marker Assistant Selection (MAS) (Bai & Shaner, 2004; Buerstmayr et al., 2020; Fernando et al., 2021). Even though these resistant cultivars may not be 100% tolerant to FHB, they provide an efficient and cost-effective disease management tool against FHB (Bai & Shaner, 2004).

The application of fungicide is the most common strategy implemented by farmers to fight against phytopathogenic fungi. The fungicide application will provide partial protection from the disease and subsequent DON accumulation in grain (Amarasinghe et al., 2013). Moreover, several studies have been conducted on the biological control of FHB as it is more cost-effective and environmentally friendly than chemical fungicides. Biological control agents such as *Trichoderma* spp have been discovered to reduce the colonization of phytopathogenic fungi, including *Fusarium* spp. (Gilbert & Tekauz, 2000). Further, the development of biological control for FHB will be highly beneficial in organic wheat farming.

An integrated disease management system, including improved disease resistance (Anderson, 2001; Fernando et al., 2021), crop rotation, soil management, and using both chemical (fungicide) and biological controls (Fernandez et al., 2001), is essential to control FHB. However, studies prove that soil management and crop rotation are not that effective under disadvantageous environmental conditions such as dry and humid conditions, concluding that environmental conditions are the primary factor in FHB development (Fernandez et al., 2001). Hence, the FHB forecasting models have become an important and effective way of disease management. A forecasting system will provide precise data on disease progression to wheat producers in a reliable and timely manner. Therefore, it will help to reduce yield loss and mycotoxin contamination. FHB

risk prediction models are constructed depending on the previous weather data collections during the anthesis period, past FHB epidemics, and earlier records of mycotoxins (De Wolf et al., 2003). Thus, FHB risk assessment models combined with an integrated management system will more effectively protect the crop against FHB.

2.3 Canola

Many species from the *Brassica* genus, such as mustard, cabbage, kale, broccoli and cauliflower, have been consumed by humans from ancient history. These crops today came through tremendous crossing and hybridization during breeding for crop improvement. Previously, rapeseed (*Brassica napus*) was cultivated mainly to produce oils, which were applied as a mechanical lubricant (Bell, 1982). Later, it was developed for human consumption as a vegetable oil and as solid meal for livestock feed.

"Canola" rapeseed has a high economic value. It is the second greatest growing area of all oil crops in the world, with the being soybeans (Zhang & Fernando, 2018). The term canola is a trademark of the Canadian Canola Association, which stands for Canada oil. According to the Canadian Canola Association, canola includes varieties from the genus *Brassica* (*Brassica napus*, *Brassica rapa* or *Brassica juncea*) where the fatty acid profile of seeds should comprise less than 2% of erucic acid. In addition, the solid parts of the grain must contain less than 30 µmol of any combination of 3-butenyl glucosinolate, 4-pentenyl glucosinolate, 2-hydroxy-3 butenyl glucosinolate, and 2-hydroxy- 4-pentenyl glucosinolate per gram of air-dry, oil-free solid (Canola Council of Canada, 2021). The first canola variety of *B. napus* was developed in 1970 by Dr. Baldur Stephenson from the University of Manitoba via selection and breeding (Bell, 1982). Since then, canola cultivation has increased dramatically due to high demand.

Canola seeds contain 45% oil and have the lowest saturated fatty acid content compared to other vegetable oils. In addition, canola oil contains a high percentage of omega-3 fatty acids known to reduce blood cholesterol levels. Hence, canola oil is used as a heart-healthy cooking oil and is included in numerous commercial products. The solid parts of the seeds left after crushing are used to produce canola meal, which feeds livestock, poultry and fish (Canola Council of Canada, 2021). Canola meal is an excellent addition to animal feed due to its high protein content. Because of the

richness of protein, canola meal is identified as a potential plant-based protein for human consumptions (Bell, 1982). Moreover, canola oil can be utilized as a renewable energy source (biofuel), making a whole new market for canola (Canola Council of Canada, 2021).

Canola is one of the most cultivated cash crops in western Canada. In 2020, 20.8 million acres were seeded with canola, and the total production was reported as 18.7 million metric tons. Most of the canola was produced in Saskatchewan (55% of total production), followed by Alberta (28%) and Manitoba (17%). More than 90% of Canadian canola products are exported annually, including oil, seeds, and meal. The total value of canola exports was recorded as 11.9 billion Canadian dollars in 2020 (Statistics Canada, 2021). Currently, there are more than 207 000 jobs created around the Canadian canola industry (Canola Council of Canada, 2021).

2.3.1 Diseases of canola

Plant diseases are causing a substantial negative impact on the canola industry. The damage caused by pathogenic infections is increasing annually (Canola Council of Canada, 2021) mainly due to monoculture and extensive cultivation without proper rotations (Fitt et al., 2006). Many economically destructive canola diseases are caused by fungi. Examples include, blackleg (*Leptosphaeria maculans*), Sclerotinia stem rot (*Sclerotinia sclerotiorum*), Fusarium wilt (*Fusarium oxysporum*), powdery mildew (*Erysiphe cruciferarum*), root rot (*Rhizoctonia solani*, *Fusarium* species and *Pythium* species), Alternaria black spot (*Alternaria brassicae*, *A. alternata* and *A. raphani*), Verticillium stripe (*Vertiticillium longisporum*), and white rust (*Albugo candida*). Among them, the blackleg disease of canola (described in next section) and Sclerotinia stem rot are two major diseases in the Canadian fields. Sclerotinia stem rot infection occurs during flowering via air-borne ascospores and causes stem rot following the invasion of susceptible host tissues. In addition, *Sclerotinia sclerotiorum* can produce cold-hardy sclerotia, which can overwinter in the soil (Morrall & Dueck, 1982; Van de Wouw et al., 2016).

In addition to fungal diseases, there are also other canola diseases caused by protozoa and phytoplasma. Clubroot is a destructive disease caused by soil-borne protozoa, namely *Plasmodiophora brassicae*. The infection occurs in roots and causes swelling or gall formation, leading to the premature death of plants (Peng et al., 2014). In addition, infected leafhoppers carry

aster yellows phytoplasma (*Candidatus Phytoplasma asteris*), which cause damage to canola plants during the flowering season (Canola Council of Canada, 2021). These diseases became more frequent in 2020 than in previous years on the Canadian prairies, increasing the awareness of disease control (Canola Council of Canada, 2021).

2.3.2 Blackleg disease

Blackleg (Phoma stem canker) is the most destructive disease of Canola in Canada and is caused by the fungal pathogen *Leptosphaeria maculans* (Fernando et al., 2016). Although *L. maculans* is the primary infector of blackleg, it is reported to co-exist with *L. biglobosa*, especially in European and North American regions (West & Fitt, 2005). *L. biglobosa* is less virulent and less damaging compared to *L. maculans*. Previously, they were identified as virulent and less virulent forms of *L. maculans*, respectively (Fitt et al., 2006). Later, they were separated into two species (Mendis-Pereira, et al., 2003). *L. biglobosa* was found all around western Canada, but it caused minor damage to the crop (Canola Council of Canada, 2021).

The virulent *L. maculans* can mainly infect the susceptible canola plants at their cotyledon stage and damage the stem base, causing cankers. These cankers on a stem base cause severe damage to crops by interrupting the nutrient and water uptake of the plant (Fitt et al., 2006). However, *L. biglobosa*, which may co-exist with *L. maculans*, may cause stem cankers or lesions on the upper portion of the stem (Kutcher et al., 2011). *Leptosphaeria* produces ascospores and *L. maculans* ascospores can survive a more extended period than *L. biglobosa* under the same conditions (Fitt et al., 2006; Huang et al., 2003).

Blackleg is found in most rapeseed growing regions of the world. The first blackleg epidemic was recorded in 1966 (Gugel & Petrie, 1992). Since then, blackleg has been causing significant loss to the canola industry worldwide. Blackleg became a problem for Canadian growers in 1970 when disease caused its first critical yield loss in north-eastern Saskatchewan. After that incident, the epidemics caused yield loss every year (Kutcher et al., 2011). The condition was mitigated by introducing resistant cultivars, fungicide application, and maintaining a proper rotation (Peng et al., 2014). However, the pathogen showed its ability to overcome crop resistance over time (Van

de Wouw et al., 2014b; Zhang et al., 2016). Thus, blackleg resistant crops are needed to maintain sufficient canola production to meet demand.

2.3.2.1 The principal causative agent of blackleg

L. maculans is identified as the primary causative agent of blackleg (i.e. Phoma stem canker) in canola and other *Brassica* crops (Fitt et al., 2006). *L. maculans* is a haploid ascomycete fungus distributed in all canola growing regions except for China. It has caused severe blackleg epidemics in those regions, including Europe, Australia, and North America. Thus, studies about *L. maculans* gain much attention from the scientific community (West et al., 2001). *L. maculans* is a saprophytic fungus that lives on crop debris until a favourable environment and susceptible host emerges. The infection impacts the growth of many plant tissues, including cotyledons, leaves, stems, pods and roots, resulting in black colour lesions. In addition, *L. maculans* produces both sexual (pseudothecia) and asexual (pycnidia) fruiting bodies, which can initiate a new disease cycle (Zhang & Fernando, 2018).

In Canada, *L. maculans* was first isolated from infected crops in Saskatchewan in 1975. Then it was found in Alberta and Manitoba during 1983 and 1984, respectively (Gugel & Petrie, 1992). The first peak epidemic of *L. maculans* occurred in 1982 in Saskatchewan, where 56% of yield loss was observed in some fields. At this time, the most famous canola cultivar was Westar, which was widely grown in western Canadian prairies. Unfortunately, Westar did not carry any resistance against blackleg (Zhang & Fernando, 2018).

2.3.2.2 Mating types of *L. maculans*

Only the compatible mating types of *L. maculans* outcross during sexual reproduction. *L. maculans* have a single mating type locus known as MAT, which includes two alternative forms or idiomorphs (*MAT 1_1* and *MAT 1_2*). Mating only occurs between *MAT 1_1* and *MAT 1_*2 (Petrie & Lewis, 1985). In addition, the virulence of *L. maculans* highly correlate with sexual reproduction as the outcrossing creates genetic recombination during ascospore production (Cozijnsen & Howlett, 2003). Therefore, the mating type distribution in the *L. maculans* population is essential for disease management as it will reflect the possibility of recombination (Howlett et al., 2001).

Previously, the mating type of *L. maculans* was detected by an experimental procedure involving co-culturing the tester isolates with a defined isolate and checking the production of pseudothecia (Cozijnsen et al., 2000). Currently, the mating type specific-PCR assay is the most convenient and rapid method of determining the mating type of *L. maculans* (Cozijnsen & Howlett, 2003). Cozijinsen and Howlett (2003) introduced three multiplex PCR primers that amplify the *MAT* locus and result in a band length polymorphism for the two mating types.

2.3.3 Disease cycle and epidemiology

The blackleg disease cycle starts with the infection on canola seedlings by ascospores of *L. maculans,* causing leaf spots on the site of infection (Fitt et al., 2006; Hall, 1992). Air-borne ascospores are the primary inoculum of blackleg in Europe and Australia (Zhang & Fernando, 2018). Ascospores are released from pseudothecia during summer (usually starting from June in western Canada) and dispersed long distances by wind. Ascospore release usually happens when the canola seedlings emerge (Guo & Fernando, 2005). However, the primary inoculum of blackleg in western Canada was identified as pycnidiospores produced by pycnidia (Appendix A) (Dilmaghani et al., 2009; Ghanbarnia et al., 2011; Guo et al., 2005). Pycnidiospores only travel short distances as they are dispersed by rain-splash (Figure 2.3). Mycelium and pycnidiospores associated with infected seeds can also contribute as an inoculum (Hall, 1992). The occurrence of inoculum with infected seeds mixed with infected-dockage is a huge concern, particularly when the export destination has no reported *L. maculans*; for example, China (Zhang & Fernando, 2018).

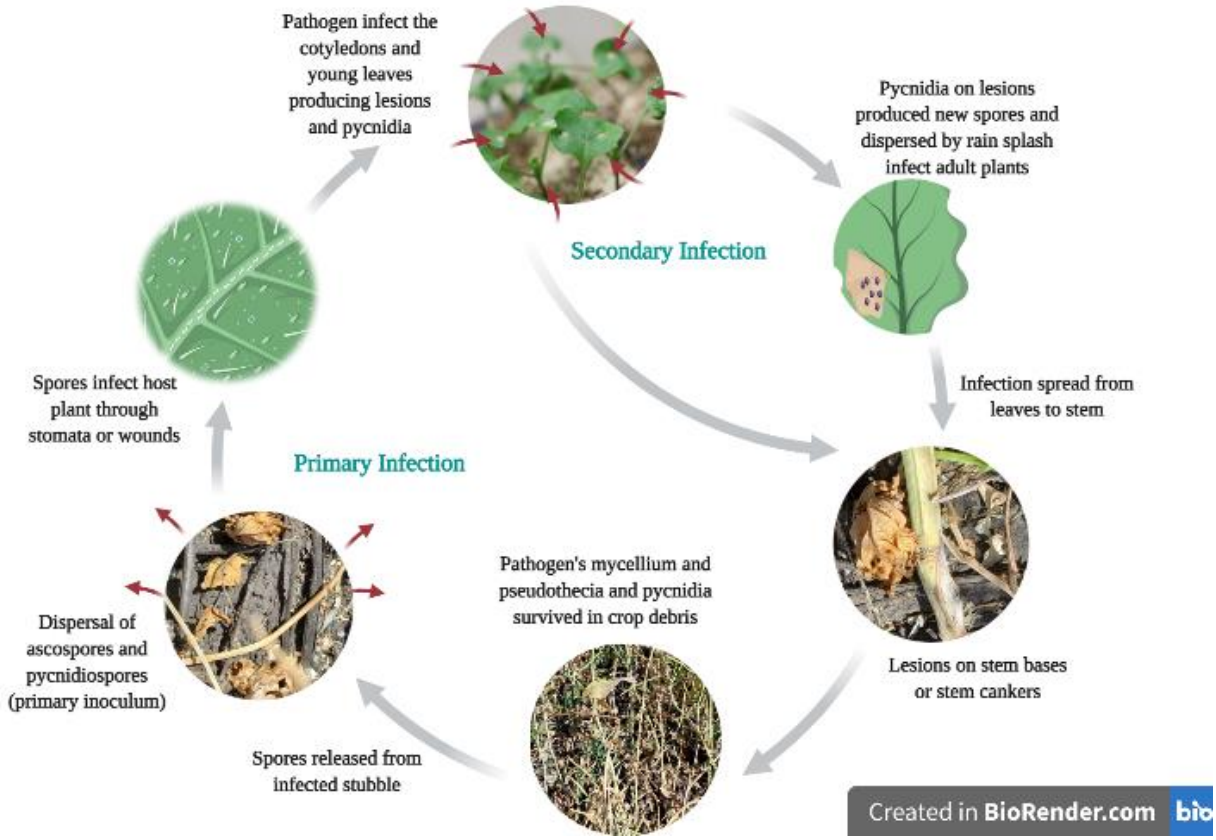

Figure 2.3 Blackleg disease cycle showing survival of *L. maculans* on infected stems from previous cropping season, which initiate the disease in susceptible canola cotyledons and progress into stem cankers, causing significant damage to yield. Image adopted according to Zhang & Fernando, (2018).

Later, the *L. maculans* infection spreads from leaves to the stem and produces lethal stem cankers at the stem base or the crown (West et al., 2001). Fungal growth from leaf to stem happens without showing any external symptoms. The fungal proliferation on stem base causes stem cankers known as Phoma stem canker or blackleg (Fitt et al., 2006; Hall, 1992). A secondary infection can occur by the pycnidiospores produced on leaf lesions of infected plants. However, the secondary infection is not as destructive as the primary infection.

Further, the crown canker occurs only when infection happens from the cotyledon to the eight leaf stage. Crown cankers are the most damaging than leaf lesions due to the cause of higher yield loss (Hall, 1992). Disease symptom development occurs rapidly in high-temperature regions such as

summers in Canada and Australia, increasing the disease severity (West et al., 2001). Therefore, knowledge of disease epidemiology is fundamental to control blackleg effectively.

2.3.4 Blackleg disease management

Scouting for the disease is the first step of disease management. Disease scouting will provide information about disease incidence and severity, which may be needed for effective and sustainable disease management. Before starting the seeding, farmers are advised to look for canola crop remains from the past growing seasons. Since the fungus can survive on crop debris on soil for 2 to 3 years, the likelihood of getting disease increases during shorter rotations. Further, pathogen infection can be recognized at the early growth stages if the cotyledons and early leaves contain lesions (Canola Council of Canada, 2021).

Moreover, the disease can be rated more accurately before swathing at the adult stage of the plant. The black-coloured basal cankers can be observed by pulling out random plants. Usually, disease rating is done by cutting a cross-section near the stem base and rating the darkening of tissues from a scale of 0 to 5, where 0 is no darkening and 5 is 100% darkening. In severe cases, lesions may be observed in the pods and upper parts of the stem (Canola Council of Canada, 2021; Zhang & Fernando, 2018).

Disease management consists of methods that prevent disease occurrence and progression, including using clean seeds, seed treatment, crop rotation, stubble management, application of foliar fungicides, and usage of resistant crop varieties (Fitt et al., 2006; West et al., 2001). Crop rotation is a very efficient and eco-friendly method for managing the blackleg as it will allow the decomposition of infected canola residues. Crop rotation will reduce the inoculum availability and slow down the breakdown of blackleg disease resistance in crops (Liban et al., 2016; Rashid et al., 2021). The Canola Council of Canada recommends that farmers keep 50 to 100m of buffer zone between canola fields to reduce pynidiospores and ascospores dispersal (Canola Council of Canada, 2021).

The utilization of genetic resistance is another environmentally friendly method of disease management and the most effective way of overcoming pathogen attacks. Canola plants contain

two types of genetic resistance, major gene or *R* gene resistance and adult plant resistance (APR) (Howlett et al., 2001). APR is also known as quantitative resistance, which occurs by minor genes (Howlett et al., 2001; Jestin et al., 2011). The major gene resistance, or *R* gene resistance, is that most studied and utilized in the fight against *L. maculans* (Zhang & Fernando, 2018). However, studies showed that combining *R* gene resistance and APR gave higher protection against the pathogen (Brun et al., 2010). Integrated pest management, which utilizes two or more protection modes, is the best strategy to control blackleg. For example, growing resistance varieties of canola together with good stubble management and correct usage of fungicides will significantly reduce the disease severity (Kutcher et al., 2011; West et al., 2001).

2.3.4.1 Gene for gene interactions

Gene for gene model explains the interaction between products of the pathogens avirulence (*Avr*) genes and their matching plant resistance (*R*) genes (Flor, 1971). Some plants develop a disease resistance against pathogens by pathogen-triggered immunity. The plants contain *R* proteins, which are identified as cell surface receptors or cytoplasmic receptors that recognize and bind to a specific pathogenic protein (i.e. effector protein) encoded by pathogen *Avr* genes (Cook et al., 2015). This binding of receptors to effectors results in hypersensitive cell senescence at the infection site and generates a barrier against the growth of the pathogen. Thus, the pathogen becomes avirulent for that plant (Flor, 1971). Breeders use this resistance mechanism to produce crop varieties with blackleg resistance.

2.3.4.2 Identification of *R* genes and *Avr* genes

Canola breeders extensively use *R* gene resistance to fight against blackleg pathogen (Delourme et al., 2004; Zhang et al., 2017). In *Brassica* sp., 18 *R* genes are identified: *Rlm1* to 11, *LepR1* to *R5*, *RlmS*, *BLMR1* and *BLMR2*. At the same time, 14 *Avr* genes are identified in *L. maculans* including *AvrLm1*, *AvrLm2*, *AvrLm3*, *AvrLm5-9*/*AvrLmJ1*, *AvrLm4-7*, *AvrLm6*, *AvrLm11* and *AvrLepR1* to *3* (Fernando et al., 2018; Liu et al., 2020b). The cotyledon inoculation assay was developed to identify *R* genes and their compatible *Avr* genes using the compatible or non-compatible interactions (Rimmer & Van Den Berg, 1992; Williams & Delwiche, 1980). A compatible reaction, where no lesions can be observed on the cotyledon, indicates that the host plant may contain the *R* gene, and the *R* gene has matched the *Avr* gene of the pathogen. On the

other hand, lesions on the cotyledons indicate a non-compatible reaction when the plant does not contain the matching R gene for pathogen *Avr* genes (Zhang et al., 2016). This simple test facilitates accurate phenotyping of plant *R* genes and pathogen *Avr* genes in a greenhouse within 11 to 14 days after inoculation. Moreover, PCR assays and DNA sequencing analysis are used to identify the genotype of *R* genes or *Avr* genes. Gene-specific primers are developed in the PCR assays for *Avr* gene identification, which enables rapid and efficient identification (Ghanbarnia et al., 2018; Plissonneau et al., 2016; Zhang et al., 2017).

2.3.4.3 Importance of identifying new *R* genes

Integrating currently available *R* genes into canola varieties will provide an efficient but not lasting solution for blackleg disease management, as the selection pressure created by *R* genes will increase the evolution of *L. maculans* isolates with different or mutated *Avr* genes. These virulent *L. maculans* populations will cause disease in the crop varieties that were previously resistant to blackleg (Ghanbarnia et al., 2018). The breakdown of *R* genes is happening rapidly due to the high evolutionary potential of *L. maculans* and the extensive usage of the same *R* gene (Van de Wouw et al., 2014b). Several studies have proved the adoption of *L. maculans* against *R* gene resistance. For example, the increased use of *Rlm1* resistant varieties makes it no longer resistant against pathogens as the *AvrLm1* carrying isolates tend to decrease in the population (Rouxel et al., 2003; Van de Wouw et al., 2014b). Zhang et al. (2016) also reported the breakdown of *Rlm3* over time with the intensive usage of a single gene. An exciting mechanism of overcoming the *R* gene resistance is the epistatic suppression of *AvrLm3* recognition by *Rlm3* when the pathogen also contains *AvrLm4-7* (Plissonneau et al., 2016). Another example is the suppression of *AvrLm9* by *AvrLm4-7* (Ghanbarnia et al., 2018). Thus, identifying new *R* genes and *Avr* genes are crucial for maintaining the crop resistance against blackleg.

2.3.5 CRISPR/Cas9 gene editing

Clustered Regularly Interspaced Short Palindromic Repeats (CRISPR) and CRISPR associate (Cas) proteins are an RNA-mediated adaptive defence mechanisms found in bacteria and archaea, which is a similar mechanism as RNAi interference found in eukaryotes (Wiedenheft et al., 2012). The CRISPR/Cas mechanism depends on small RNAs, which can accurately identify invading viruses or plasmids and protect the host by silencing the activity of foreign nucleic acid (Jinek et

al., 2012). This defence mechanism contains three steps. First, the host cells acquire the CRISPR loci by including a short fragment of foreign nucleotides (protospacer) into its chromosome at the proximal end of the CRISPR array. These CRISPR genes are expressed during a second infection to produce precursor CRISPR RNA or pre-crRNA. Secondly, Pre-crRNA undergoes post-translational modifications to generate crRNA, a complementary protospacer for invading target strands. In the final phase, the target is recognized by crRNA guided Cas protein complex and cleave the target DNA with the enzymatic activity of Cas protein (Wiedenheft et al., 2011). The Cas proteins need a transactivating CRISPR RNA (tracrRNA) to facilitate the binding of crRNA. Two RNA molecules form a duplex, cr:tracrRNA, guide the Cas to the target site (Cong & Zhang, 2015).

There are three types of CRISPR adaptive systems. They contain different features, including other Cas genes, the organization of Cas operons and CRISPR arrays. The type II CRISPR/Cas system is most straightforward when it contains the Cas9 endonuclease. Cas9 is a multidomain protein guided by a co-processed dual tracrRNA:crRNA molecule. Thus, the type II CRISPR/Cas9 system has been identified as a promising gene-editing tool as it can be easily engineered to target a desired nucleotide sequence (Chylinski et al., 2014).

The type II CRISPR gene-editing systems contain two main components, namely a guide RNA (gRNA) and a Cas endonuclease. The gRNA is custom-built for the target nucleotide sequence to guide the Cas endonuclease to the target site (Jinek et al., 2012). The gRNA is synthesized by connecting crRNA and tracrRNA by a linker loop. Thus, it is also called a single guide RNA (sgRNA). The Cas9 protein from *Streptococcus pyogenes* is widely used in gene editing, and it acts as a molecular scissor to cleave the target site (Chylinski et al., 2014; Cong & Zhang, 2015). The binding of gRNA to target DNA (protospacer) is achieved through base pairing to a short protospacer adjacent motif (PAM) sequence downstream of the target site. PAM sequence includes three nucleotides specific to Cas protein, for Cas9 it is 5′-NGG-3′. (Barrangou et al., 2007). After the PAM site is secured correctly, the gRNA base pairs with the target sequence. Then Cas9 endonuclease cleave double-stranded target DNA at three to four bases upstream of the PAM site. This CRISPR-induced double-strand break (DSB) will be repaired by cell repairing mechanisms,

either by non-homologous end joining (NHEJ) or homology-directed repair (HDR) (Gasiunas et al., 2012).

The NHEJ repair mechanism ligates the breakage of DNA. However, this process is error-prone and introduces inserts or deletes while repairing, resulting in missense mutation, nonsense mutation, or frameshift mutation. In some cases, the target DNA will no longer encode a functional protein. Therefore, NHEJ allows us to create knockout mutants. The efficiency of gene knockout can be increased by introducing a multi-guide sgRNA that can target the same gene and simultaneously make multiple DSBs. Alternatively, the homology-directed repair (HDR) pathway repairs a DSB by incorporating a donor DNA fragment into the DSB site. This donor template contains homology with target locus and should be presented to the cell with other CRISPR components. The cell repair mechanism may use this donor DNA to repair the broken strand with the HDR pathway. This mechanism can introduce precise mutations into the desired loci of the genome and create knock-ins (Maruyama et al., 2015).

2.3.5.1 CRISPR/Cas9 gene editing in *L. maculans*

L. maculans is the major causal agent of blackleg in canola and other relative crops (Fitt et al., 2006; Sun et al., 2006). Thus, studies of *L. maculans* gain much attention from the scientific community (West et al., 2001). Modern biotechnology and molecular biology have enabled a new era for studying the host-pathogen relationship. The availability of a genome sequence prompted molecular studies of *L. maculans,* including genome editing (Rouxel et al., 2011). However, the low rate of homologous integrations of constructs hindered the generation of gene deletion strains, which were commonly used to investigate gene functions (Idnurm et al., 2017b). Recent studies using CRISPR/Cas9 genome editing on *L. maculans* showed a silver lining in rapid and precise gene editing to create target mutations. Recently, CRISPR/Cas9 tools were successfully implemented to identify *L. maculans* genes involved in pathogenicity (Darma et al., 2019; Zou, et al., 2020; Urquhart & Idnurm, 2019) and fungicide resistance (Idnurm et al., 2017b). Moreover, creating virulent mutant isolates of *L. maculans* by knocking down an avirulent gene was also reported (Zou et al., 2020).

Identifying pathogenicity-related genes of *L. maculans* provide insights on pathogen management. The genes which show high transcript levels during infection are predicted to be correlated with blackleg disease progression. Usually, these highly expressed genes are identified through RNA expression profiling or transcriptomic analyses (Gervais et al., 2017; Haddadi et al., 2016; Lowe et al., 2014; Sonah et al., 2016). Urquhart and Idnurm (2019) tested this hypothesis using CRISPR/Cas9 to silence 11 previously identified high expression genes of *L. maculans* in 7-day post-inoculated canola cotyledons. However, the results showed that none of the selected genes are crucial for *L. maculans* pathogenicity on canola. This study highlighted the need for more advanced techniques than expression profiling to recognize pathogenicity-related genes (Urquhart and Idnurm, 2019).

The development of fungicide resistance in *L. maculans* is a persistent problem for disease management. For example, fungicide of dicarboximide iprodione (FRAC group 2; trade name Rovral® produced by Bayer Crop Science) is widely used to inhibit blackleg but is now overcome by the pathogen. The iprodione-resistant isolates of *L. maculans* are found to contain mutations in the high osmolarity glycerol response (HOG) pathway, which allows them to survive under hyper and hypo osmatic conditions. Idnurm et al. (2017b) confirmed that the *hos1* gene was important in iprodione resistance. The *hos1* gene encodes a predicted osmosensing histidine kinase which is an important gene in the HOG pathway. They used CRISPR/Cas9 to successfully mutate the *hos1* gene in *L. maculans*. Further, they showed that CRISPR/Cas9 technique is an effective mutational tool to characterize gene functions in *L. maculans* (Idnurm et al., 2017b).

2.3.5.2 Delivery and expression of CRISPR tools in *L. maculans*

To begin the CRISPR/Cas9-mediated gene editing, the associated genes (endonucleases and sgRNA) need to present inside the nucleus of the target organism. The widely used delivery method for filamentous fungi is *Agrobacterium*-mediated transformation (AMT) (Schuster & Kahmann, 2019). *Agrobacterium tumefaciens* is a plant pathogenic bacterium that can transfer its phytopathogenic T-DNA or transfer DNA into the host genome. The T-DNA is located on the *Ti* plasmid (tumour-inducing plasmid), containing virulence genes. The virulence DNA can be replaced with desired DNA without damaging the T region (genes related to transferring DNA to

another cell) to utilize the plasmid carrier of target DNA into the fungal cells (Michielse et al., 2005).

When investigating CRISPR/Cas9 gene-editing procedures of *L. maculans* used by past studies, Darma et al. (2019), Urquhart and Idnurm (2019), and Idnurm et al. (2017b) used two plasmid constructs to express Cas9 endonuclease and desired sgRNA separately. These plasmids were transformed to *L. maculans* through AMT and successfully transformed colonies selected with G418 and hygromycin resistance, respectively (Figure 2.4A). However, Liu et al. (2020a) constructed one plasmid containing Cas9 and sgRNA, where the transformants can be selected through hygromycin resistance (Figure 2.4B). This method was first introduced by Nødvig et al. (2015) to mutate a wild-type *Aspergillus aculeatus* strain. Both Liu et al. (2020a) and Zou et al. (2020) showed that the same method could be successfully implemented in *L. maculans*.

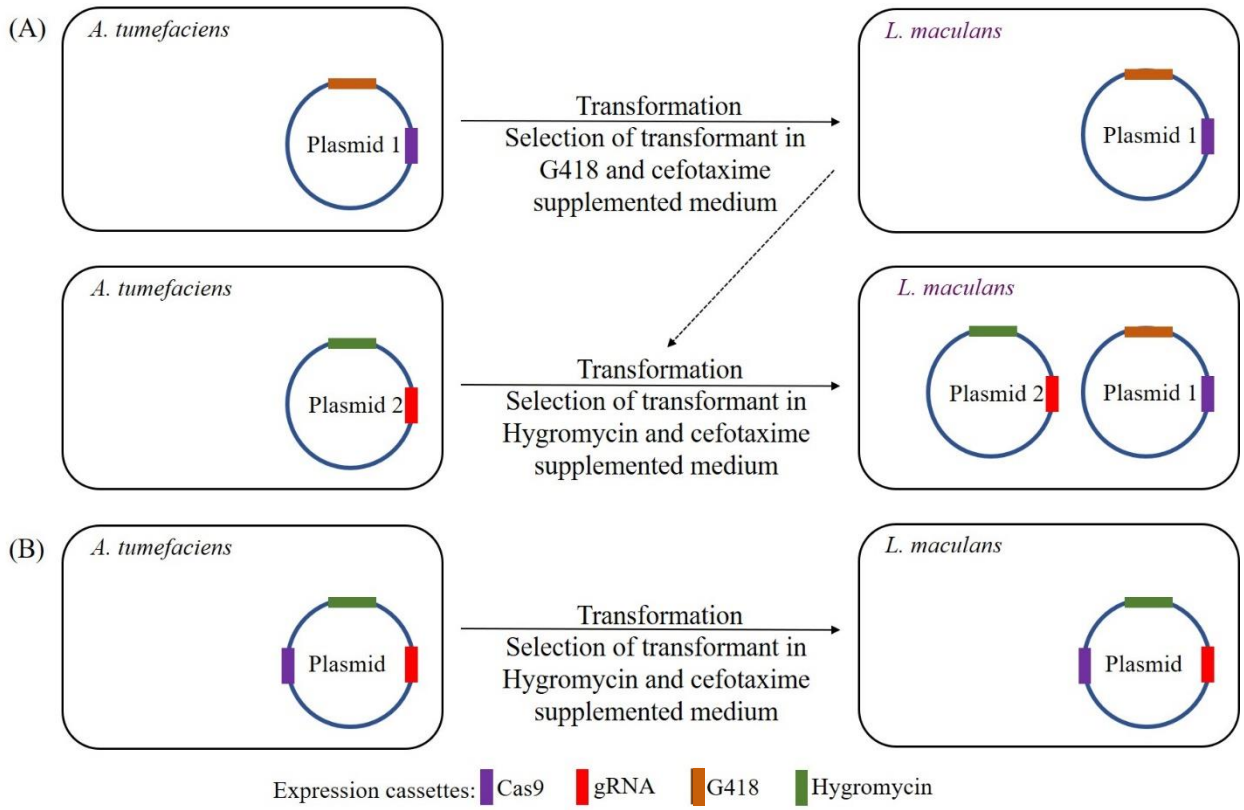

Figure 2.4 Delivery of CRISPR/Cas9 tools into *L. maculans*. A: *Agrobacterium* mediated transformation of two plasmids containing Cas9 and guide-RNA (gRNA) separately, while B: *Agrobacterium* mediated transformation of single plasmid construct containing Cas9 and gRNA.

The Cas9 protein and sgRNA need to be expressed inside the target organism to initiate the gene editing. The expression cassettes usually include two main components, a promoter and a terminator. The strength of the promoter is an important factor that affects the efficiency of the CRISPR/Cas9 system (Song et al., 2019). For example, Idnurm et al. (2017b) used a construct with an actin promoter of the *L. maculans* to express either the Cas9 or sgRNA. Zou et al., 2020 used two constructs, where sgRNA was expressed using a *gpdA* promoter and *trpC* terminator and Cas9 gene expressed by *Aspergillus nidulans tef1* promoter and *tef1* terminator.

Chapter One

3.0 Species diversity of Fusarium head blight and deoxynivalenol (DON) levels in western Canadian wheat fields

3.1 Abstract

Fusarium head blight (FHB) is the most destructive wheat disease in the Canadian prairies and is primarily caused by *Fusarium graminearum*. Chemotype diversity and weather conditions during anthesis severely impact the deoxynivalenol (DON) content in grain. This project aims to evaluate the diversity of *Fusarium* species and chemotypes of FHB in western Canadian producer fields. The grain analysis for deoxynivalenol revealed that 2019 spring wheat samples contained a range of 0.01 - 1.7, 0.01 - 8.5 and 0.01 - 1.7 ppm of DON level in fields of Manitoba, Saskatchewan, and Alberta, respectively. The 2020 growing season experienced milder levels of FHB toxin contamination than the year 2019. In spring wheat, the highest mean DON content was recorded from Manitoba samples (0.3 ppm in grain and 2.12 ppm in chaff), while both Saskatchewan and Alberta samples contained similar mean DON levels <0.2 ppm in grain and <1.00 ppm in the chaff. Winter wheat samples had less DON accumulation (<0.2 ppm) than spring wheat in all three provinces during both years. The chaff collected from the same spring wheat heads showed a significantly higher DON level than the level in grain ($P < 0.1$ for 2019 and $P < 0.001$ for 2020), suggesting that level of DON in chaff should be considered before used as animal feed. Most samples were contaminated with *F. graminearum*, with the highest *F. graminearum* percentage in the spring wheat fields in Manitoba. *F. avenaceum* and *F. poae* were higher in Alberta compared to the other two provinces. Most of the *F. graminearum* isolates were of the 3ADON chemotype in all three regions. Remarkably, the proportion of the 15ADON chemotype was significantly lower in Alberta than the other provinces, reflecting that the 3ADON chemotype is becoming the dominant chemotype in FHB. Further, the qPCR assays revealed that *F. graminearum* abundance on spring wheat stalks is significantly higher in Manitoba and Saskatchewan than in Alberta. This study confirmed that 3ADON producing *F. graminearum* is becoming more frequent in western Canadian producer fields.

3.2 Introduction

Wheat (*Triticum aestivum* L.) has a huge demand worldwide as it is a staple food in many nations. Canada produces 13% of total wheat exports in the world (Canadian Cereals, 2020). There are two main types of wheat grown in Canada, spring wheat and winter wheat. The majority of Canadian wheat is produced in western Canada (Campbell, 2015). Wheat plays a significant role in the export market of Canada, as 63% of the total product was exported in 2019 (AAFC, 2020). The demand for wheat is increasing drastically with the growth of the world population. Thus, farmers have to maximize the outcome of their crops to address the increasing demand. Both abiotic and biotic stresses may reduce the expected yield causing a massive loss for farmers. Most abiotic stresses are triggered by extreme weather conditions such as frost, salinity, flooding, heat, and drought stress (Dresselhaus & Hückelhoven, 2018). Pathogens and pests cause biotic stress under a favourable environment to complete their lifecycles. Among the diseases, Fusarium Head Blight (FHB) has been responsible for the highest percentage of yield loss (Fernando et al., 2021).

FHB is a fungal disease that has been reported in many wheat production regions, including North America, Europe, and East Asia. FHB affects both the quality and quantity of the yield of small grain cereal crops such as wheat, oat, corn, barley and durum (Leonard & Bushnell, 2003). *F. graminearum* (teleomorph *Gibberella zeae*) is the principal causative agent associated with FHB of wheat (McMullen et al., 1997; Parry et al., 1995), which causes significant losses in grain yield and grain quality by the contamination of mycotoxin (McMullen *et al*., 1997). *Fusarium* species were first reported in Canada in 1923 in Manitoba on corn stubble. However, *F. graminearum* was not observed in Canada until 1948. Since then, the percentage of *F. graminearum* found in diseased samples gradually increased, and FHB became more severe (Clear & Patrick, 2010). In addition, some *Fusarium* species, such as *F. graminearum* and *F. culmorum*, can produce mycotoxins. Mycotoxins negatively affect animal and human health (Amarasinghe et al., 2015).

F. graminearum overwinters on crop debris from previous growing seasons and produces sexual spores that are the primary inoculum of the disease. Airborne ascospores are released from crop debris and infect the wheat spikelet to start a new disease cycle (Sutton, 1982). Thus, the availability of inoculum during flowering determines the disease severity. The visible symptoms

of FHB begin to appear after days of floret infection, and the symptoms include premature bleaching and partially shattered heads. Further, pink coloured fungal mycelia may be visible on the base of the florets. The infected spikelet may not be filled and may be shrunken and bleached grain (Parry et al., 1995). Moreover, infected grains may get contaminated with fungal mycotoxins. In the western Canadian prairies, *F. graminearum* predominately DON. DON is found in two forms of acetylated derivatives which are 3-acetyl-DON (3-ADON) and 15-acetyl-DON (15-ADON) (Amarasinghe et al., 2015; Goswami & Kistler, 2005). In western Canada, NIV-producing *Fusarium* species are rare (Miller & Richardson, 2013). However, FHB infected fields in Asia and Europe contain both DON and NIV (Ichinoe et al., 1983). A recent study conducted by Amarasinghe et al. (2015) found NIV producing *F. cerealis* in Canadian fields. The production of DON and NIV enhances the virulence of the pathogen increasing the FHB disease incidence in wheat (Goswami & Kistler, 2005; Ji et al., 2015; Paul et al., 2005).

Cereal crop production in the Canadian prairies is profoundly affected by the FHB during favourable environmental conditions. FHB disease incidence and progression are high in warm and humid environments (Gilbert & Fernando, 2004; Klem et al., 2007; Sung & Cook, 1981). In addition, the *Fusarium* species associated with the disease varies in different location, and the disease severity depends on species found in the field and their chemotype. Thus, identifying the *Fusarium* species and chemotypes in different regions is essential to disease management decisions in predicting the disease severity (Starkey et al., 2007; J. H. Wang et al., 2011).

Fusarium species are identified by their macroscopic characteristics such as colony morphology and microscopic characters such as the shape of macroconidia (Aoki & O'Donnell, 1999). The polymerase chain reaction (PCR) provides a rapid, sensitive, and precise species identification by amplifying a target DNA strand (Demeke et al., 2005). The PCR technique uses specifically designed primers to differentiate *Fusarium* species and chemotypes (Amarasinghe et al., 2019; Amarasinghe et al., 2016; Demeke et al., 2005; O'Donnell et al., 2008; Wang et al., 2011). For example, polymorphisms within the *TRI* gene cluster was utilized to develop chemotype specific multiplex primers to differentiate 3ADON, 15ADON and NIV (Ward et al., 2002). Moreover, qPCR techniques quantify the fungal abundance, which is more sensitive and accurate than conventional PCR. Therefore, the probe-based assays will provide rapid and high-throughput

detection and quantification of *Fusarium* species and their chemotypes (Karelov et al., 2021; Nicolaisen et al., 2009; Wang et al., 2011).

Even though many studies were conducted on identifying *Fusarium* species and chemotypes in western Canada, few targeted *Fusarium* species diversity in farmer's fields (Guo et al., 2008). This chapter contained three main objectives in evaluating the *Fusarium* species diversity in western Canadian wheat fields. The first objective was identifying the associated *Fusarium* species and their chemotypes (3ADON, 15ADON and NIV). For this, wheat spikes were collected from participating spring wheat and winter wheat fields in Manitoba, Saskatchewan, and Alberta during the growing season of 2019 and 2020. The inoculum was determined by calculating the spore density in each field from flowering until the soft dough stage. Wheat spikes were processed manually to separate grain, chaff, and stalks. Both grain and chaff from spring wheat were subjected to mycotoxin testing by high-sensitive 5/5 Vomitoxin kits from Neogen. Further, the presence of *Fusarium* species and their chemotypes were tested by DNA-based methods (PCR). Secondly, the impact of chaff removal on DON levels and *Fusarium* diversity in grains was studied. The grain and chaff of spring wheat was compared by DON concentrations, percentages of *Fusarium* species, and chemotypes. Thirdly, this study confirmed the presence of *Fusarium* in stalks by quantifying the abundance of *F. graminearum* on spring wheat stalks. A probe-based quantitative PCR assay was developed to determine the abundance of *F. graminearum* in three sections of spring wheat stalks.

This study indicated that spring wheat samples were more contaminated with FHB than winter wheat. Further, grain samples from Manitoba and Saskatchewan showed higher DON contamination and a higher percentage of *F. graminearum* than Alberta. The majority of the *F. graminearum* isolates contained the 3ADON chemotype. The proportion of samples with the 15ADON chemotype was significantly lower in Alberta, indicating that the 3ADON is becoming the dominant chemotype in FHB disease. Moreover, the chaff collected from the same spring wheat heads showed higher DON content than the grain for both years (Kannangara et al., 2021). Further, *F. graminearum* abundance in Manitoba and Saskatchewan stalk samples was significantly higher than the samples of Alberta.

3.3 Materials and methods

3.3.1 Sample collection

Wheat spikes were harvested from a random selection of grower's fields in a 50 x 50 m area free of any fungicide applications to detect the presence of *Fusarium* species and the mycotoxin diversity. Samples were collected in the 2019 and 2020 growing season in Manitoba, Saskatchewan, and Alberta (Figure 3.1). All wheat plants from within eight quarter-square meter samples were collected, separately stored in mesh bags, and transported to Winnipeg, Manitoba. Spring wheat heads were to collect grains, chaff, and stalks. Only grains were collected from winter wheat samples (Table 3.1). Before processing, randomly selected wheat stalks were collected from spring wheat samples. Then each sample was ground roughly using a sharp rotating rod to shatter grain from the wheat head. The grain was separated from chaff using a windmill created at the laboratory. All the equipment used were sanitized with 1% bleach and alcohol between each sample.

3.3.2 DON levels in samples

The DON content in winter wheat grain, spring wheat grain and spring wheat chaff samples were analyzed by the Agriculture and Food Laboratory, University of Guelph, ON. The 5/5 Vomitoxin ELISA kits (Neogen, USA) were used to measure 3ADON and 15ADON content in each sample following sample grinding and homogenization.

Table 3.1 Number of samples for the study in 2019 and 2020

Province	Grain samples				Chaff samples		Stem samples	
	2019		2020		2019	2020	2019	2020
	SW	WW	SW	WW	SW	SW	SW	SW
Manitoba (MB)	21	7	22	6	4	22	5	16
Saskatchewan (SK)	14	6	14	10	13	8	10	8
Alberta (AB)	10	9	10	7	6	10	6	10

SW: spring wheat, WW: winter wheat and each sample represents one field

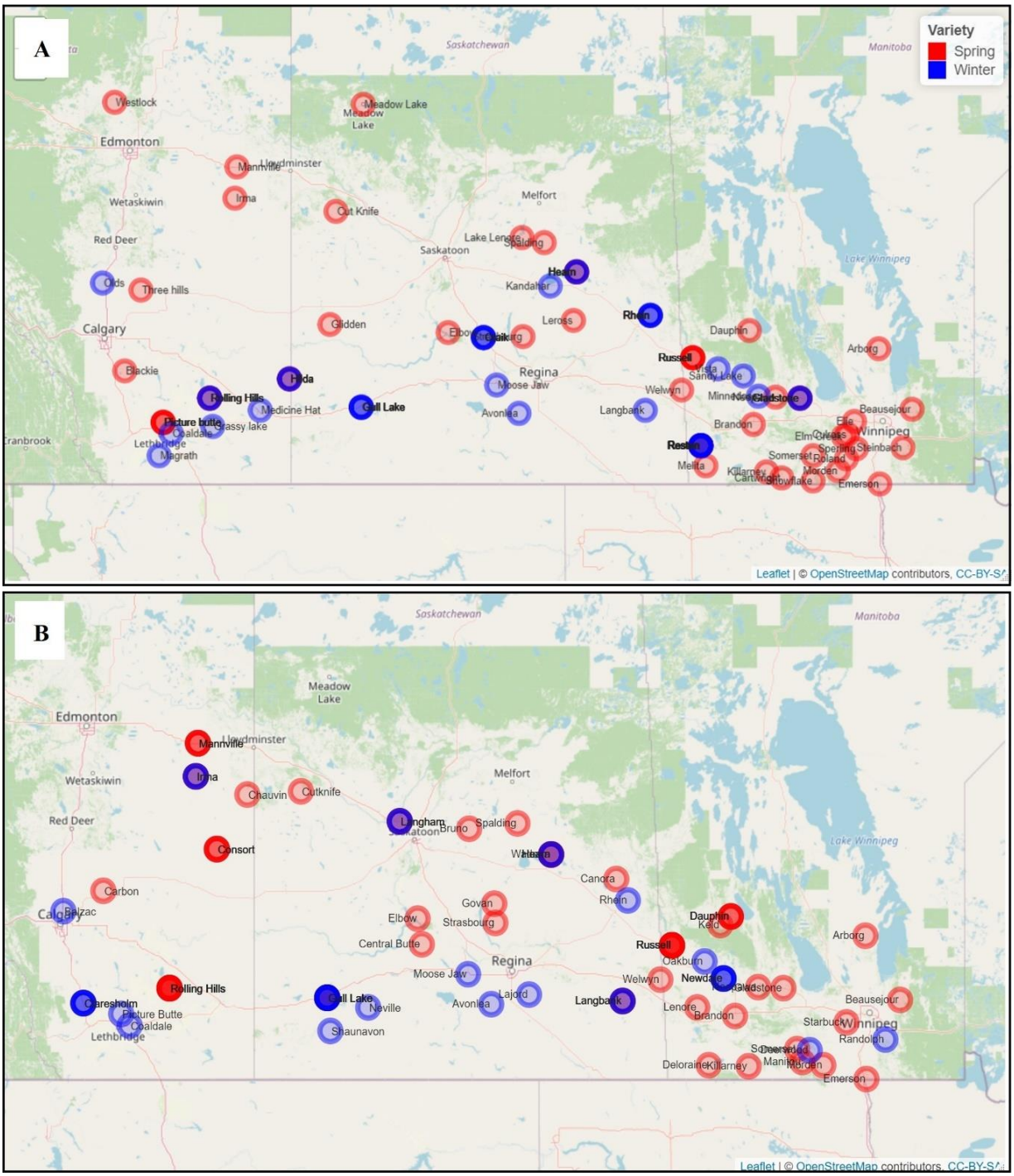

Figure 3.1 Map of western Canada indicating sampling collection sites in for A: 2020 and B: 2019. The red dots represent spring wheat, and the blue dots represent winter wheat.

DON levels in spring wheat grain and chaff were compared by ANOVA analysis using the R statistical software (version 4.1). The Levene test was used to check the assumption of homogeneous variance in the data sets for 2019 and 2020.

3.3.3 Calculation of spore availability during the flowering week

Two spore traps were set up in each field from the start of anthesis until the soft dough stage to monitor inoculum availability. Each spore trap was made out of a rectangular-shaped foam wrapped with Vaseline-coated double-sided tape on all four sides of the foam to capture airborne spores. Spore counts were taken by counting spores in 1 cm^2 of the Vaseline tape from one side of the spore trap under a light microscope and multiplying by the whole area (0.5 cm X 1.9 cm) of the Vaseline tape on the spore trap. Three independent replicates were counted separately from each spore trap, and then they were used to calculate the mean spore count. The spore density (number of spores per m^3 of air) was calculated by dividing the mean spore count by air volume passing across one side of each trap.

The volume of air passing across the area (0.5cm x 1.9cm) was calculated by first estimating the average daily wind speed for the period when the spore traps were in the field (i.e., from date of installation to date of removal). The wind speed data for each field was obtained from the nearest weather stations. In Alberta, the wind speed data were recorded at 2 m height, while in Manitoba and Saskatchewan, the wind speeds were recorded at 10 m height. However, the spore traps were installed at 1 m height in the fields. Thus, the wind speed values were extrapolated down to 1 m by using the log law wind profile formulae with roughness length set at 0.1 m (Stull & Ahrens, 2000). The total wind run (i.e., how much wind has passed) (m) for the day was then calculated by multiplying the average wind speed (m/s) at 1 m by 86 400 s (number of seconds in 24 hours). Next, the air volume (m^3) was calculated by multiplying the wind run by sampled area (0.005 m x 0.019 m). Since the spore traps have four sides, the wind run (m^3) was divided by 4, assuming that the wind came from different directions and passed in an equal amount over each of the 4 sides of the spore traps. Finally, the total air volume (m^3) was calculated by multiplying the air volume per day by the number of days the spore traps were in the field.

3.3.4 Determination of *Fusarium* species and chemotype diversity in 2019 by culturing

The grain and chaff samples from 2019 were cultured on potato dextrose agar (PDA) to determine the *Fusarium* contamination. Species-specific DNA markers identified *Fusarium* species following the isolation DNA from fungal hyphae growing on the medium. The detailed procedure is explained below.

3.3.4.1 Isolation of *Fusarium* sp. from grains

Isolation of the *Fusarium* species from grains was carried out by culturing the diseased grains followed by single hyphal tip isolation. Briefly, 12 infected seeds were selected from each sample, and they were surface sterilized with 1% bleach before culturing individually on PDA with 1mg/mL streptomycin followed by incubation at 25℃ for 4 - 7 days under fluorescent light until the appearance of *Fusarium* colonies (red/pink/orange colour and fluffy in texture). Next, each new colony was sub-cultured on PDA media separately.

Sub-culturing continued until no contamination was detected. Then, a pure culture was prepared by isolating a tip of hyphae under the microscope. Later, the pure cultures were used for DNA extraction and preserved for future needs. Preservation was carried out by growing the single spore cultures on PDA plates with sterile filter paper disks. Filter paper disks were removed after mycelium developed over the disks and air dried before storage at -20 ºC.

3.3.4.2 Isolation of *Fusarium* sp. from the chaff

Approximately 0.5 g of chaff was surface sterilized for 1 min with 1% bleach, followed by 1 min washing with autoclaved distilled water. The chaff was held with a clean strainer during the sterilizing process. The same protocol described in the previous section was used to isolate the *Fusarium*-like colonies.

3.3.4.3 DNA extraction

The hypal tip cultures grown on PDA media were used for DNA extraction. The mycelium was harvested by scraping with a sterile scalpel into a sterile 1.5 mL Eppendorf microcentrifuge tube containing seven to eight sterile glass beads. Then mycelium was ground for 1 min in a Precellys tissue homogenizer after adding 600 µL of TES buffer (100 mM Tris, 10 mM EDTA, 2% sodium

dodecyl sulphate). Next, 140 µL of 5 M NaCl and 70 µL 10% cetyltrimethylammonium bromide (CTAB) was added to each tube and incubated at 65°C for 20 min followed by vortexing every 4 min. After incubation, 600 µL of phenol: chloroform: isoamyl alcohol (25:24:1 v/v) were added and mixed well until two layers disappeared. Next, the mixture was centrifuged at 9 000 g for 15 min. The clear supernatant was transferred into a new tube, and the previous step was repeated once again. Finally, DNA was precipitated by adding 80 µL 5 M NaCl and 1 mL of 100% ethanol, followed by centrifugation at 12 000 g for 5 min. After that, 200 µL of ice-cold 80% ethanol was added to wash the precipitated DNA and then centrifugate at 6 000 *g* for 5 min. Finally, the pellet was air-dried and dissolved in 400 µL of warm (37 °C) sterile distilled water. The DNA solution was stored at -20 °C for further use.

3.3.4.4 Identification of *Fusarium* sp.

PCR with specific primers (Table 3.2) was carried out to identify the *Fusarium* genus and species. A total of 25 µL reaction mix containing PCR buffer (1.5 mM MgCl2, 50 mM KCl, 10 mM Tris.HCl, pH 8.0), 0.2 mM of each dNTP, 0.4 µM of each primer, and 0.75 U Taq DNA polymerase and 20 ng of template DNA were prepared for each isolate (Amarasinghe et al., 2015). Amplification was completed with following PCR cycle; initial denaturation at 95 °C for 3 min; with 35 cycles of 30 s at 95 °C, 30 s at 55 °C, 1 min at 72°C; and a final extension of 72°C for 5 min. PCR products were run on a 1.5% agarose gel to check the amplification. The percentage of each species was calculated by dividing the number of isolates from the total number of isolates recovered from each province.

3.3.4.5 Identification of chemotype

Multiplex PCR markers were used to determine the chemotype of the *F. graminearum*. A PCR reaction was prepared with the same procedure as indicated in section 3.4 with two primer pairs 3DON (TGG CAA AGA CTG GTT CAC), 3NA (GTG CAC AGA ATA TAC GAG C), 3D15A (ACT GAC CCA AGC TGC CAT C), and 3D3A (CGC ATT GGC TAA CAC ATG) (Ward et al., 2002). Chemotype was identified by length polymorphism of amplified bands in 1% agarose gel where a 610 bp fragment indicates the presence of 15ADON chemotype, and a 243 bp fragment indicates the presence of 3ADON chemotype (Guo et al., 2008). The percentage for each of the

chemotypes was calculated by dividing the number of each chemotype from the total number of chemotypes.

Table 3.2 Primers utilized for *Fusarium* species identification

Fusarium Species		Sequence (5'-3')	Reference
Fusarium genus	R	ATGGGTAAGGARGACAAGAC	O'Donnell et al. (2004)
	F	GGARGTACCAGTSATCATGTT	
F. graminearum	R	CTCCGGATATGTTGCGTCAA	Demeke et al. (2005)
	F	GGTAGGTATCCGACATGGCAA	
F. culmorum	R	ATGGTGAACTCGTCGTGGC	Nicholson et al. (1998)
	F	CCCTTCTTACGCCAATCTCG	
F. avenaceum	R	AACATACCTTAATGTTGCCTCGG	Mishra et al., (2003)
	F	ATCCCCAACACCAAACCCGAG	
F. sporotrichioides	R	CTTGGTGTTGGGATCTGTGTGCAA	Kulik et al. (2004)
	F	ACAAATTACAACTCGGGCCCGAGA	
F. poae	R	CAAGCAAACAGGCTCTTCACC	Parry & Nicholson, (1996)
	F	TGTTCCACCTCAGTGACAGGTT	
F. proliferatum	R	CGGCCACCAGAGGATGTG	Jurado et al. (2005)
	F	CAACACGAATCGCTTCCTGAC	
F. pseudograminearum	R	CGGGGTAGTTTCACATTTCYG	Aoki & O'Donnell, (1999)
	F	GAGAATGTGATGASGACAATA	
F. cerealis	R	CTCAGTGTCCACCGCGTTGCGTAG	Nicholson et al. (2004)
	F	CTCAGTGTCCCATCAAATAGTCC	

3.3.4.6 Morphological identification with spore shapes

Sporulation was promoted in each selected isolate from different species by growing on Spezieller nahrstoffarmer Agar (SNA) media. Spores were visualized after one week of incubation at room temperature. A sterilized needle was used to mount spores on glycerol, and the spores were observed under the light microscope.

3.3.5 Characterization of *Fusarium* species and chemotypes in 2020 samples by total DNA extraction

Both grain and chaff samples collected from 2020 were subjected to total DNA extraction using the GeneJet plant DNA purification Mini kit (Thermo Fisher Scientific, USA, Cat. No. K0792). A total of 12 diseased seeds were collected and separated into two replicates from each sample. The collected seeds were ground into powder in liquid nitrogen and homogenized in lysis buffer A with glass beads. At the same time, 200 mg of chaff was divided into three replicates. Each replicate was homogenized with sterile metal beads in lysis buffer A. The rest of the extraction was carried out according to the user manual provided by the manufacturer. Three replicates (nearly 20 mg) from each chaff sample were used for DNA extraction. Before DNA extraction, chaff was roughly ground with liquid nitrogen and pulverized with metal beads in lysis buffer A. All eluted DNA samples were stored at -20 ºC.

3.3.5.1 SmartChip Real-Time PCR to identify *Fusarium* species and chemotype

The total DNA was extracted from the samples collected in 2020 and subjected to *Fusarium*-specific PCR assays to identify different *Fusarium* species present in each sample. All DNA samples were diluted to be under 10 ng/µL. The SmartChip Real-Time PCR System (Takara Bio Inc) was used to run assays simultaneously to identify *F. avenaceum, F. asiaticum, F. acuminatum, F. tricinctum, F. crookwellense, F. cerealis, F. culmorum, F. equiseti, F. graminearum, F. langsethiae, F. poae, F. pseudogramearum, F. tricinctum,* and *F. sporotrichioides*. Identification of chemotypes was also conducted with chemotype-specific PCR assays (3ADON, 15ADON and NIV). The same primers from previously validated studies were used (Appendix B). Each PCR assay was conducted in a 100 nL reaction in a SmartChip (Takara Bio Inc). The PCR mixture contained a final concentration of 1X LightCycler 480 SYBR Green I Master Mix (Roche Inc., USA), 250 nM of each forward and reverse primer and 0.5 - 2 ng/µl DNA template. Each reaction was dispensed to Smartchip using the SmartChip Multi-sample Nanodispenser (Taraka Bio Inc.). Next, the PCR cycle was completed using a SmartCycler (Takara Bio Inc) using the following protocol, initial denaturation at 95 °C for 173 s, 40 cycles of denaturation at 95 °C for 34 s, annealing at 60 °C for 74 s. The amplification specificity was determined using a melt curve analysis from 60 to 97 °C with an inclining rate of 0.4 °C per step. The final results were analyzed using SmartChip qPCR software (V2.7.0.1). Further, reactions with primer melting temperatures

(Tm) more than 2 °C above or below the expected primer Tm were ignored. Finally, the quantification cycle (Cq) values below 32 were considered as positive results. The percentage of positives for each species/chemotype from three provinces was calculated by dividing the number of positives from the total number of samples.

3.3.6 Quantification of *Fusarium graminearum* abundance in spring wheat stalks

A quantitative PCR (qPCR) assay was implemented to quantify the *Fusarium* load in the spring wheat stalks collected in 2019 and 2020 fields samples from Manitoba, Saskatchewan, and Alberta. A total of 55 samples were collected from all three provinces (21 from 2019 and 34 from 2020).

3.3.6.1 Sample preparation and DNA extraction

In studying *F. graminearum* abundance, the collected stalk samples were cut into three 6 cm sections (A, B and C) starting at the beginning of the peduncle (below spike) (Appendix B, **Error! R eference source not found.**). The stalk did not include the first nodes. The pieces were collected separately and cut into small pieces to facilitate the grinding process. The controls for qPCR were collected from wheat plants grown in the greenhouse (disease-free). They were processed in the same way as the samples from fields. After adding the lysis buffer, all samples were ground in a tissue pulverizer with metal beads. DNA extraction was done using the GeneJet plant DNA purification Mini kit (Thermo Fisher Scientific, USA, Cat. No. K0792).

3.3.6.2 qPCR assay development

Two qPCR probe-based assays were used to detect *F. graminearum* and wheat present in the sample. The ITS2 region was used to identify *F. graminearum* (ITS2.Fusarum.F AGCGTCATTTCAACCCTCAA, ITS2.sambuc.R TACTACGCTATGGAAGCTCGAC and ITS2.gram.probe AGCTG[+C][+A]GTCCTGCTGCACTC). The translation elongation factor 1-alpha gene was used to detect wheat in the sample. A pair of primers (forward primer: GGAGGTCTCTTCCTACCTGAA and reverse primer: GTTGGTGGACCTCTCAATCAT) were designed to be used with Hv. EF1a.probe (AAGGTCGGCTACAACCCTGACAAG) using the PrimerQuest tool from IDT (https://www.idtdna.com/pages/tools/primerquest).

3.3.6.3 Calculation of *F. graminearum* abundance

First, the assays were validated by creating standard curves with pure *F. graminearum* and wheat DNA. A pure *F. graminearum* culture and disease-free wheat leaves were used for this purpose. Then a dilution series (10-fold) was prepared with each DNA sample. The same qPCR program and primers were used to generate standard curves. Then the R^2 value and efficiency of the assays were checked.

All the DNA samples were diluted to 10 ng/µL before starting the assay. The qPCR assays were performed using the QuantStudio™ 7 pro-Real-Time PCR system (Applied Biosystems, ThermoFisher Scientific), using a two-step protocol with the thermocycling program of 3 min at 95°C, 10 min at 94°C, and 40 cycles of 15 s at 95°C and 60 s at 60°C. qPCR reactions (20 µl) consisted of 10 µl of PrimeTime™ Gene Expression Master Mix (Integrated DNA Technologies, Inc, USA, Cat. No. 1055772), 1.5 µl of 3 µM IDT probe, 1 µl of 10 µM forward and reverse primers, 4.5 µl of molecular grade water, 1.4 µl of the reference dye and 2 µl of sample DNA. All the samples, controls and no-template controls were run in duplicates to increase the accuracy. Cq values from both assays were recorded. The *Fusarium* abundance was expressed as a measure relative to the host plant DNA, hence calculated as below,

***F. graminearum* abundance =** $2 \wedge (Cq_{Ta} - Cq_{Fg})$,

where Cq_{Ta}: Cq is the value of assay for wheat and Cq_{Fg}: Cq is the value for *F. graminearum* assay.

Abundance data from 2019 and 2020 were pooled together and analyzed with ANOVA and tukey's test in the R package (version 4.1) to compare the mean differences in three sections of stalks and between provinces.

3.4 Results

3.4.1 DON levels in western Canadian producer fields

The DON levels in grains collected from spring wheat and winter wheat were measured in both years. Further, the DON levels were compared between grain and chaff from spring wheat for each year.

3.4.1.1 DON levels in spring wheat and winter wheat grain samples

For spring wheat, the analysis for DON revealed that levels in spring wheat in 2019 were 0.01 - 1.7 ppm, 0.01 - 8.5 ppm and 0.01 - 1.7 ppm for Manitoba, Saskatchewan, and Alberta samples, respectively. The highest DON level in 2019 was recorded from a Saskatchewan field that cultivated a moderately susceptible wheat variety (Appendix C). However, the 2020 growing season recorded much lower DON levels than 2019. Specifically, the highest DON level was recorded as 1.6 ppm in Manitoba, where moderately resistant spring wheat was grown (Figure 3.2A, Appendix D).

For winter wheat, in both years, the grains contained lower DON levels (<0.2 ppm) than spring wheat (Figure 3.2B). All samples from 2019 were not contaminated with DON as most values were near zero. The highest DON value observed was 0.5 ppm in a winter wheat sample from Saskatchewan. In 2020, DON accumulation in winter wheat grain was higher than the DON levels recorded in 2019 except in Alberta. In 2020, most of the winter wheat samples from Alberta were found as no DON in grain (Appendix D).

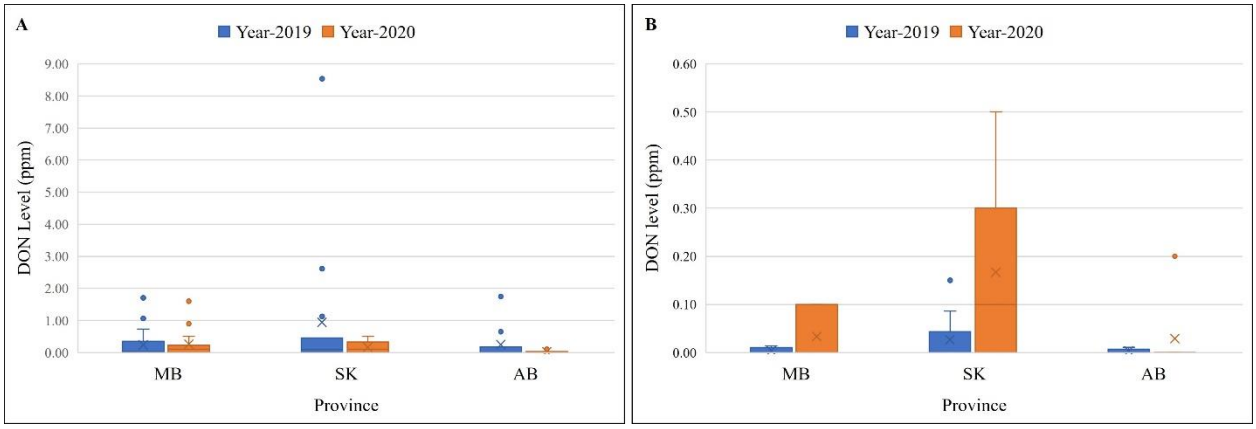

Figure 3.2 A comparison of DON content in grain samples collected from 2019 and 2020 spring wheat and winter wheat fields. The blue colour bars indicate 2019 results, and the orange colour bars indicate 2020 results. A: DON content in spring wheat grain (Y-axis 0 to 9 ppm) and B: DON content in winter wheat grain (Y-axis 0 to 0.6 ppm).

3.4.1.2 The comparison of DON levels between grain and chaff in spring wheat samples

In 2019 and 2020, a higher DON level was observed in the chaff than in grain collected from the same spring wheat samples from either province of Manitoba, Saskatchewan, or Alberta. However, the overall DON level in chaff and grain was lower in 2020. Manitoba showed the highest DON contamination for both grain and chaff samples, while the lowest DON content was observed in the samples from Alberta (Figure 3.3).

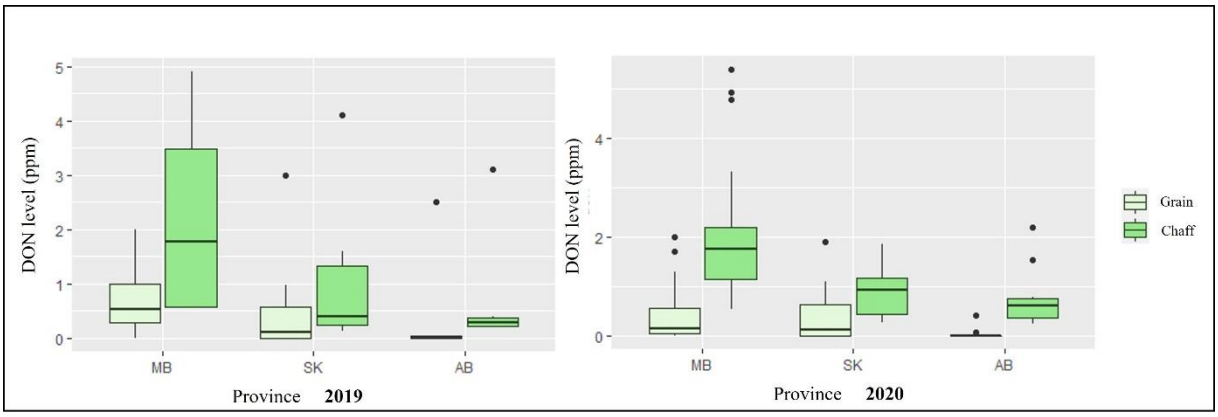

Figure 3.3 The box plot of DON content found in the grain and chaff of spring wheat samples collected from Manitoba (MB), Saskatchewan (SK) and Alberta (AB) in the growing seasons of 2019 and 2020.

ANOVA analysis was conducted for DON levels observed in spring wheat grain and chaff. The analysis was conducted for 2019 and 2020 data separately. As indicated in Table 3.3, the mean DON levels in chaff and grain were significantly different for the cases in both years of 2019 ($P < 0.01$) and, remarkably, 2020 ($P < 0.001$). The Levene test on both 2019 and 2020 data sets confirmed that the assumption of variance is valid for ANOVA ($P > 0.05$). Further, the results showed that DON level in chaff increased with the DON level in grain as the probability of interaction between DON level in grain and chaff was significant at $P < 0.01$ in both years.

Table 3.3 ANOVA results for the difference of DON level between spring wheat grain and chaff for all three provinces.

Year	Variable	df	F value	Pr (>F)
2019	Province	2	1.813	0.1769
	Sample type (grain/chaff)	1	3.264	0.0787**
	Province: Sample type	2	0.733	0.4872
2020	Province	2	7.435	0.00167**
	Sample type (grain/chaff)	1	36.187	6.8e-08***
	Province: Sample type	2	3.945	0.02367*

Significant at *P<0.1, ** P<0.01, ***P< 0.001

3.4.2 Inoculum availability in sampling fields from three provinces

The spore density values were calculated by dividing the mean number of spores by air volume passed through the spore trap. Then, the mean spore density values were used to compare the differences in inoculum availability during the anthesis to soft dough stage. In 2019, a higher spore influx was observed in the spring wheat fields of Saskatchewan and Manitoba than in the fields of Alberta (Figure 3.4A). For spring wheat, the mean spore densities were 233.3, 195.6, and 80.1 spores/m^3 for Saskatchewan, Manitoba, and Alberta, respectively. For the winter wheat fields, smaller values of spore density were observed in 2019 fields compared to the spring wheat fields. However, the highest mean spore density was recorded in Saskatchewan, similar to the case in the spring wheat fields (198 spores/m^3). In Manitoba, winter wheat fields only received a mean inoculum density of 72 spores/m^3, while the number is 75.4 spores/m^3 for Alberta fields. Interestingly, the inoculum availability in Alberta was less varied between the winter wheat and spring wheat flowering period (Figure 3.4A).

An experimental error occurred in spore traps of winter wheat fields from Manitoba and spring wheat fields from Saskatchewan, which resulted in a loss of spore density data in 2020. However, Manitoba spring wheat fields received a mean spore density of 203.3 spores/m^3, which was higher than in 2019. Compared to 2019, Alberta fields received higher mean spore density, where 144.7 spores/m^3 in spring wheat fields and 217.6 spores/m^3 in winter wheat fields (Figure 3.4B).

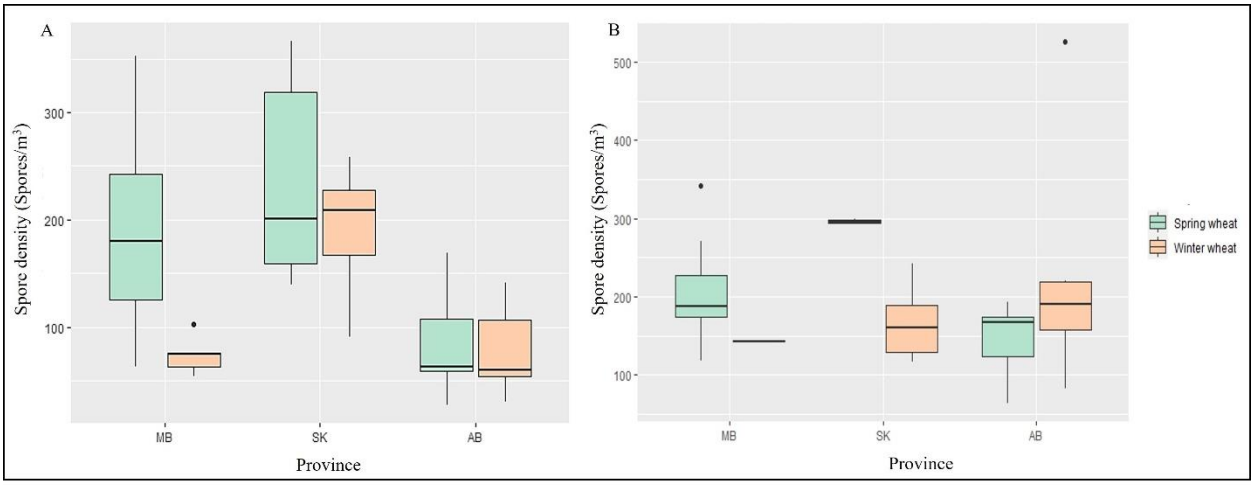

Figure 3.4 Box plots of mean spore density observed during the flowering/filling period of, A: 2019 and B: 2020 in farmers' fields of Manitoba (MB), Saskatchewan (SK) and Alberta (AB).

3.4.3 *Fusarium* species diversity and chemotypes

Fusarium species and chemotypes present in each field were surveyed by analyzing grain and chaff samples from each field. DNA markers were used for species identification from pure cultures (2019) and total DNA extractions from grain and chaff (2020).

3.4.3.1 Diversity of *Fusarium* in the levels of species and chemotype in spring and winter wheat grain samples from 2019 growing season

The percentage of *Fusarium* infected fields was calculated by dividing the number of fields with FHB contamination by the total number of fields in each province. Spring wheat samples from Saskatchewan and Manitoba fields were highly infected with *Fusarium*, and their percentages of FHB contaminated fields were 71% and 69%, respectively. In Alberta, only 40% of samples were

contaminated with FHB. However, winter wheat samples were less contaminated than spring wheat in all three provinces (Figure 3.5).

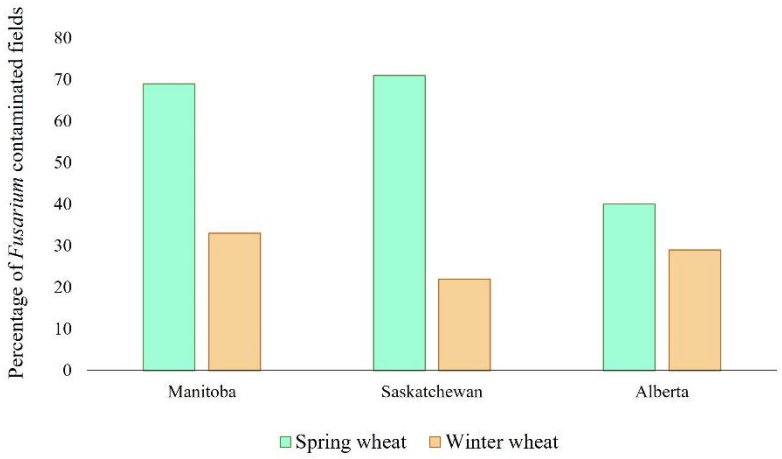

Figure 3.5 The percentage of *Fusarium* contaminated spring wheat and winter wheat samples collected from Manitoba, Saskatchewan, and Alberta producer fields in 2019. (The bar states one data point for each province)

Nine previously developed PCR assays were used to detect *Fusarium* spp., *F. graminearum, F. culmorum, F. avenaceum, F. sporotrichioides, F. poae, F. proliferatum, F. pseudograminearum* and *F. cerealis*. Through PCR identification on the recovered isolates from spring wheat grain, it was found that *F. graminearum* is the most frequently identified species in Manitoba and Saskatchewan. In Manitoba, 87% of isolates recovered from spring wheat grains were *F. graminearum*, and the other 5 % were *F. poae*, and 3% were *F. sporotrichioides*. The rest of the isolates were identified non-*Fusarium* species. In Saskatchewan, the population of isolates comprised 65% of *F. graminearum*, 21% of *F. sporotrichioides* and minor percentages of *F. avenaceum* and *F. culmorum*. In Alberta, only 27% of isolates were *F. graminearum*, while the proportion of *F. avenaceum* is 45% spring wheat grain. For winter wheat, only a few samples were contaminated with *F. graminearum* in Manitoba fields (Figure 3.6A).

The *F. graminearum* isolates recovered from three provinces included 3ADON and 15ADON chemotypes. Among these two chemotypes, most isolates were 3ADON chemotypes for all three provinces. Another *Fusarium* species, *F. culmorum,* was recovered from the three provinces and

were all found to produce 3ADON. The percentage of *Fusarium* isolates making 3ADON was 80% in Saskatchewan, the highest value among the three provinces, while the second highest was 70% in Manitoba. Further, most of the *F. graminearum* and all *F. culmorum* isolates recovered from Alberta produced 3ADON with a total percentage of 83%. In contrast, the percentage of 15ADON-producing isolates was lower in all three provinces compared to 3ADON isolates (Figure 3.6). Compared to the spring wheat grain, the percentage of DON-producing isolates was lower in winter wheat grain. Among them, 75% of Manitoba samples and 80% of Saskatchewan samples produced 3ADON. However, no DON-producing isolates were recovered from Alberta winter wheat samples (Figure 3.6B).

3.4.3.2 *Fusarium* species diversity and chemotypes in spring wheat grain and chaff samples from the 2019 growing season

The percentages of isolate recovered from either grain or chaff of spring wheat were compared. Compared to chaff, a higher percentage of *F. graminearum* isolates were recovered from grain samples. The highest percentage of *F. graminearum* over total *Fusarium* species was found in chaff samples from Manitoba (74%). Further, 50% of isolates recovered from Saskatchewan chaff samples were identified as *F. graminearum. Fusarium* species diversity found in grain and chaff was similar. For Alberta, the percentage of non-*F. graminearum* species isolated were high in both grain and chaff samples. At the same time, the percentage for *F. avenaceum* was higher in chaff than in grains in Alberta (Figure 3.7A). Taking all three provinces together, most of the isolates recovered from chaff were producing 3ADON. For example, in Manitoba, 64% of chemotype-producing isolates contained 3ADON, while, in Alberta, all the *F. graminearum* isolates recovered from chaff samples were 3ADON (Figure 3.7B).

The isolates identified by DNA markers were confirmed by comparing their spore morphology with a reference (Nelson et al., 1983). Figure 3.8 illustrated typical macroconidia shapes for different *Fusarium* species recovered from all samples, including grain and chaff.

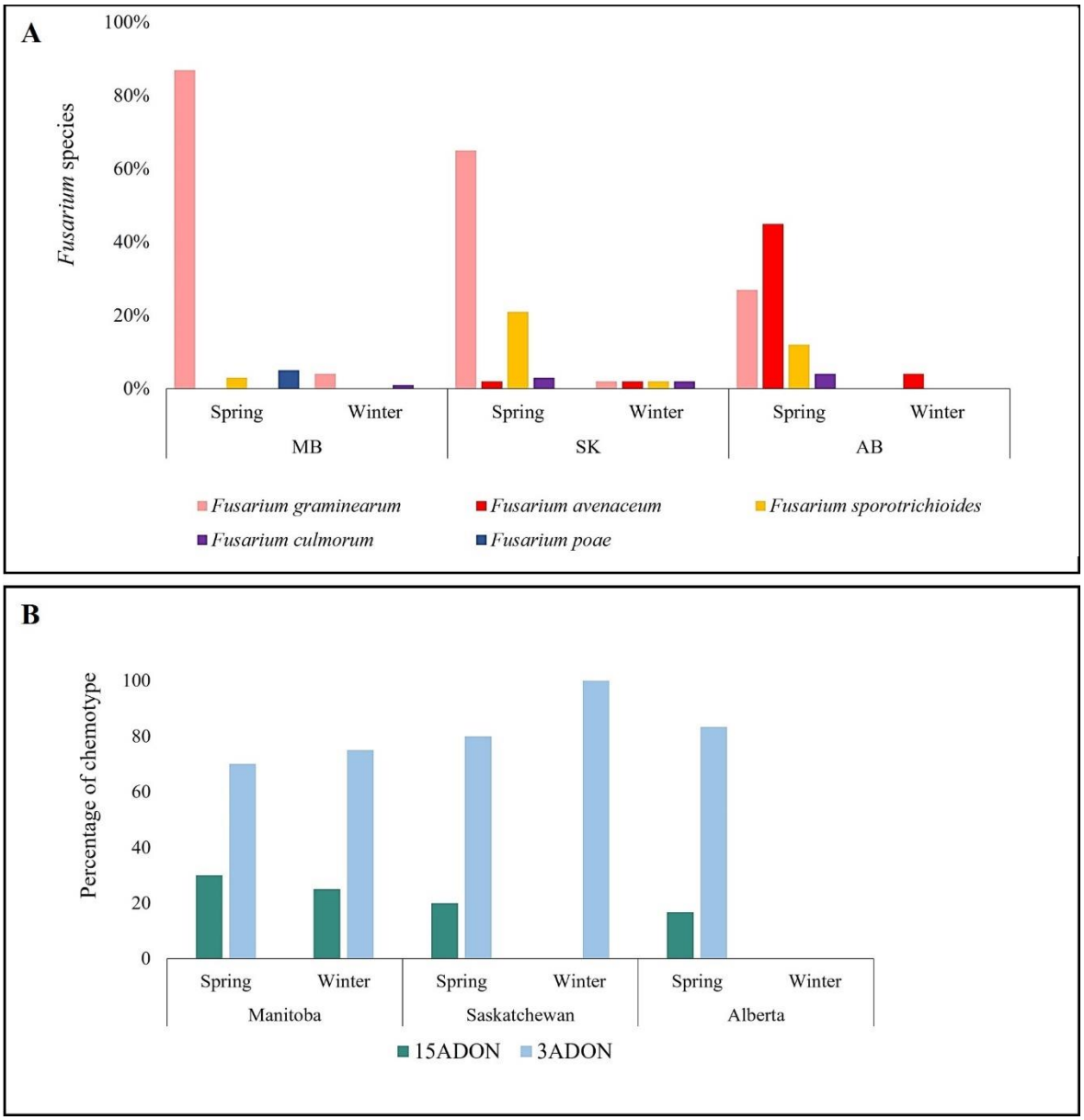

Figure 3.6 *Fusarium* species diversity and chemotypes observed in spring wheat and winter wheat samples of Manitoba, Saskatchewan and Alberta in 2019. A: *Fusarium* species as a percentage of the total number of isolates recovered from each province., B: Chemotypes as a percentage of total mycotoxin-producing isolates.

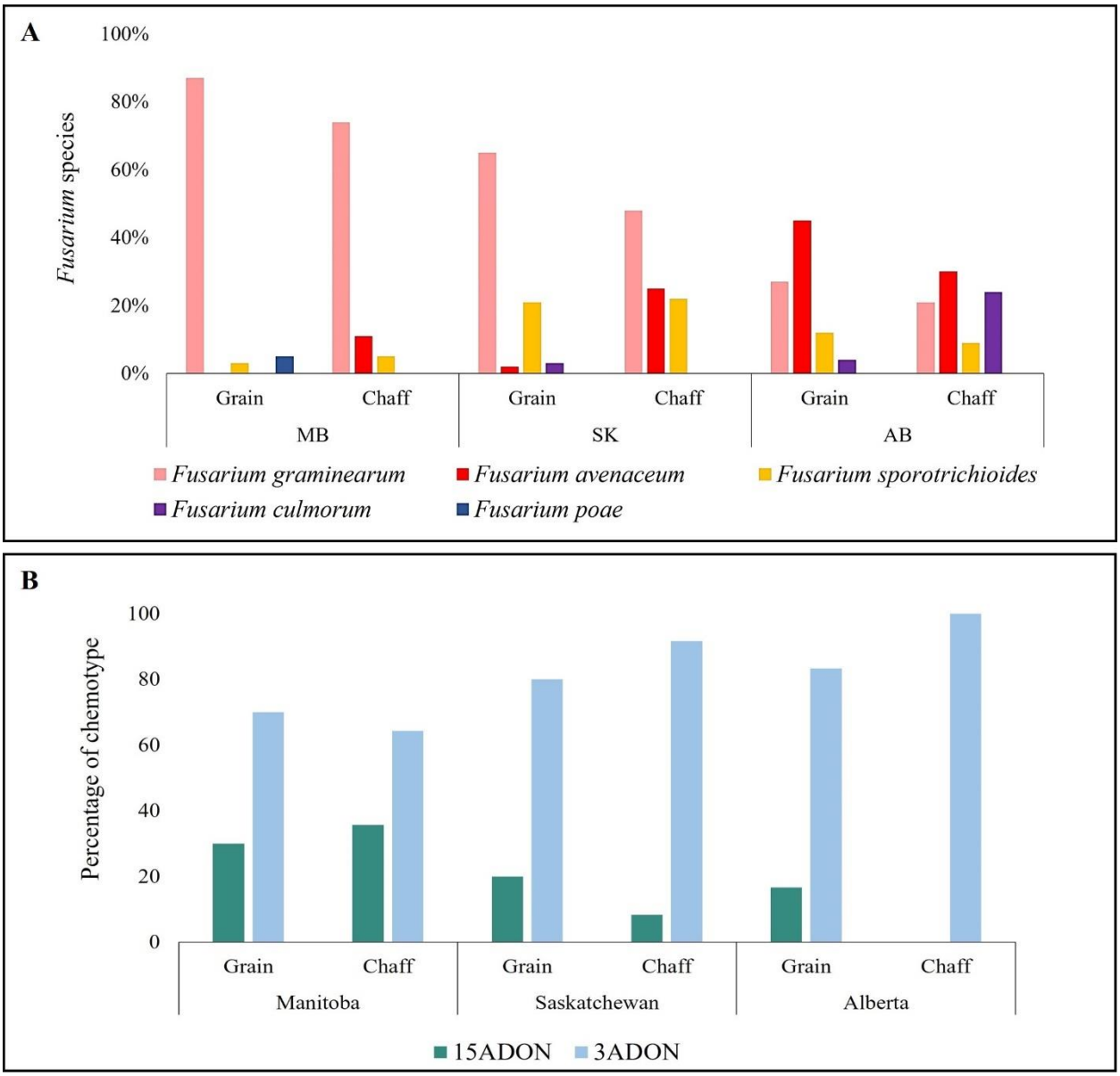

Figure 3.7 *Fusarium* species diversity and chemotypes observed in spring wheat grain and chaff samples of Manitoba, Saskatchewan, and Alberta in 2019. A: *Fusarium* species as a percentage of the total number of isolates recovered from each province, B: Chemotypes as a percentage of total mycotoxin producing isolates.

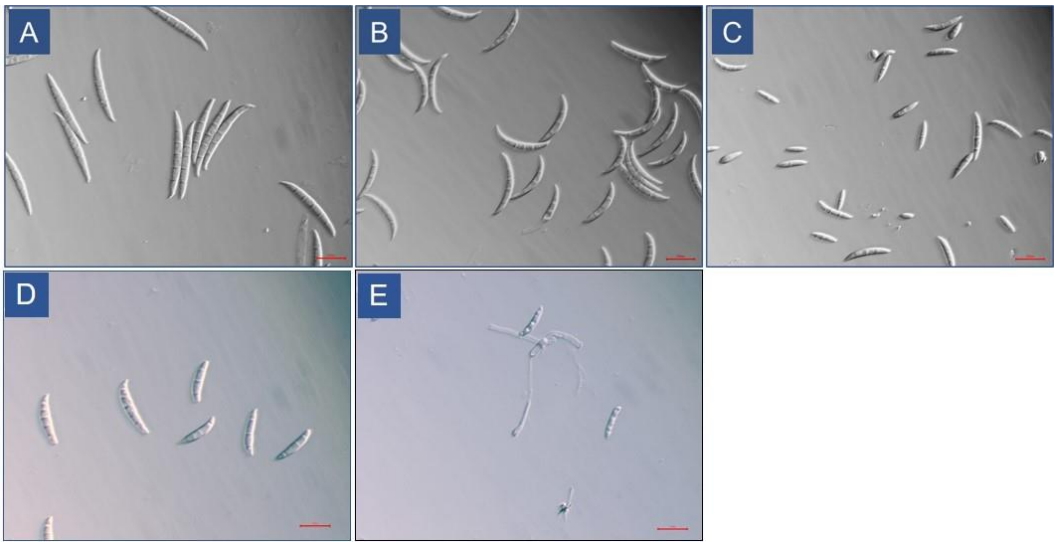

Figure 3.8 Morphology of macroconidia produced by identified *Fusarium* species in spring wheat and winter wheat samples from western Canada in 2019, A: *F. graminearum*, B: *F. avenaceum* and C: *F. sporotrichioides*, D: *F. culmorum* and E: *F. poae* (magnification ×400). Scale bar indicates 20 µm. (Laxco SeBaView 3.7).

3.4.3.3 *Fusarium* species diversity and chemotypes in spring wheat and winter wheat grain samples from 2020 growing season

Fusarium species and their chemotypes of grain samples collected in 2020 were identified by high throughput genotyping. For both spring and winter wheat, Manitoba samples were highly contaminated with *Fusarium* species, but the situation was less serious in Alberta samples. Other than *F. graminearum*, *F. poae* was more common from all three provinces in spring wheat and winter wheat samples. Specifically for spring wheat, the highest percentage (71%) of *F. graminearum* was found in Manitoba, while the percentages were 60% and 16% in Saskatchewan and Alberta, respectively. *F. culmorum* was only present in spring wheat grain samples from Manitoba (Figure 3.9A). For winter wheat, the presence of *F. graminearum* was higher in Saskatchewan (45%) compared to the other two provinces (36% for Manitoba and 7% for Alberta, respectively). For other *Fusarium* species, *F. poae* was present in all winter wheat grain samples except in Alberta. *F. avenaceum* was only found in winter wheat samples from Alberta.

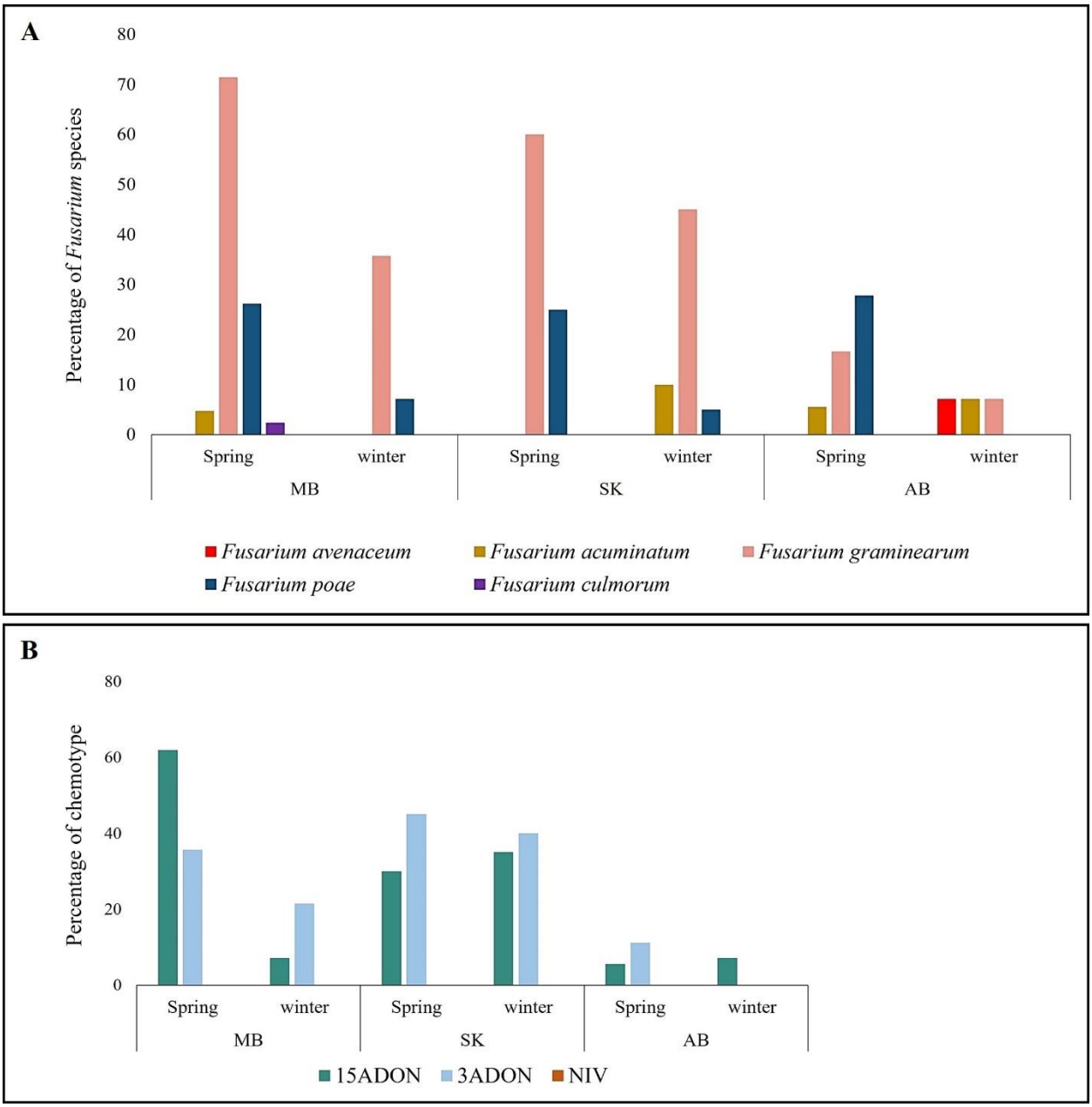

Figure 3.9 *Fusarium* species diversity and chemotypes observed in spring wheat and winter wheat samples of Manitoba, Saskatchewan, and Alberta in 2020. A: *Fusarium* species as a percentage of the total number of samples from each province. B: Chemotypes as a percentage of the total number of samples from each province.

With both spring and winter wheat samples, the PCR assays showed that the presence of DON (taking 3ADON, 15ADON and NIV together) in Alberta samples was very low compared to the other two provinces. However, most of the Manitoba and Saskatchewan samples contained 3ADON and 15ADON chemotypes. The highest percentage of 15ADON producing isolate was

found in Manitoba spring wheat (62%), while the number is 30% and 6% for Saskatchewan and Alberta samples. In comparison, most Saskatchewan spring wheat and winter wheat samples contained the 3ADON chemotype (45% and 40%, respectively). The NIV chemotype was not found in any grain sample (Figure 3.9B).

3.4.3.4 *Fusarium* species diversity and chemotypes in spring wheat grain and chaff samples from 2020 growing season

Total DNA extracted from spring wheat grain and chaff samples collected in 2020 were subjected to high-throughput genotyping. Quantitative assays were conducted to identify each *Fusarium* species. *F. graminearum* was the most frequent species found in both grain and chaff samples. 71% of grain samples and 81% of chaff samples from Manitoba were contaminated with *F. graminearum*, which was higher than the corresponding percentage in Saskatchewan and Alberta. Further, the percentage of *F. graminearum* contamination declined from Manitoba to Saskatchewan to Alberta. Other *Fusarium* species were more frequently observed in chaff samples compared to grain samples. For example, *F. poae* was found in 84% of chaff samples, while 26% of grain samples were positive for *F. poae* in Manitoba. This pattern was also observed for Saskatchewan and Alberta samples. Moreover, a more diverse *Fusarium* species were found in chaff samples than grain samples from all three provinces (Figure 3.10A).

The percentage of 3ADON producing isolates was higher in all chaff samples than the value for 15ADON producing isolates (70% vs. 58% from Manitoba, 42% vs. 25% from Saskatchewan and 23% vs. 7% from Alberta). However, grain samples from Manitoba contained the greatest 15ADON percentage in 2020 (62%). Further, the NIV chemotype was detected in 4.3% of chaff samples collected from Manitoba in 2020 (Figure 3.10B).

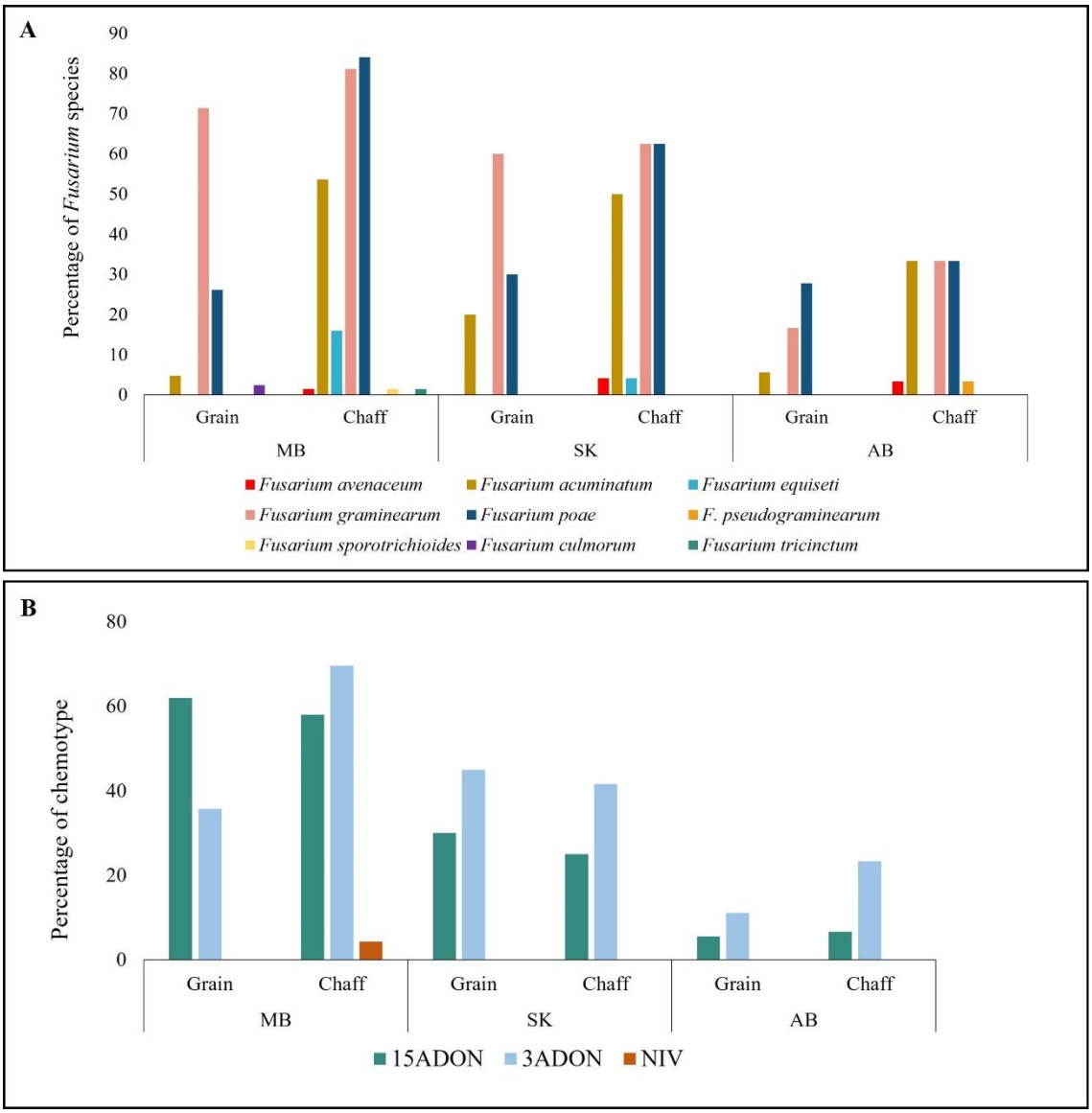

Figure 3.10 *Fusarium* species diversity and chemotypes observed in spring wheat grain and chaff samples of Manitoba, Saskatchewan, and Alberta in 2020 A: *Fusarium* species as a percentage of the total number of samples from each province. B: Chemotypes as a percentage of the number of samples from each province.

3.4.4 Quantification of *F. graminearum* in spring wheat stalks

The standard curves for both *F. graminearum* and wheat assays were constructed. Both assays showed more than 90% efficiency and R^2 value of 0.99. The results suggested that the assays would accurately infer the *F. graminearum* and wheat quantity in an unknown sample (Figure 3.11).

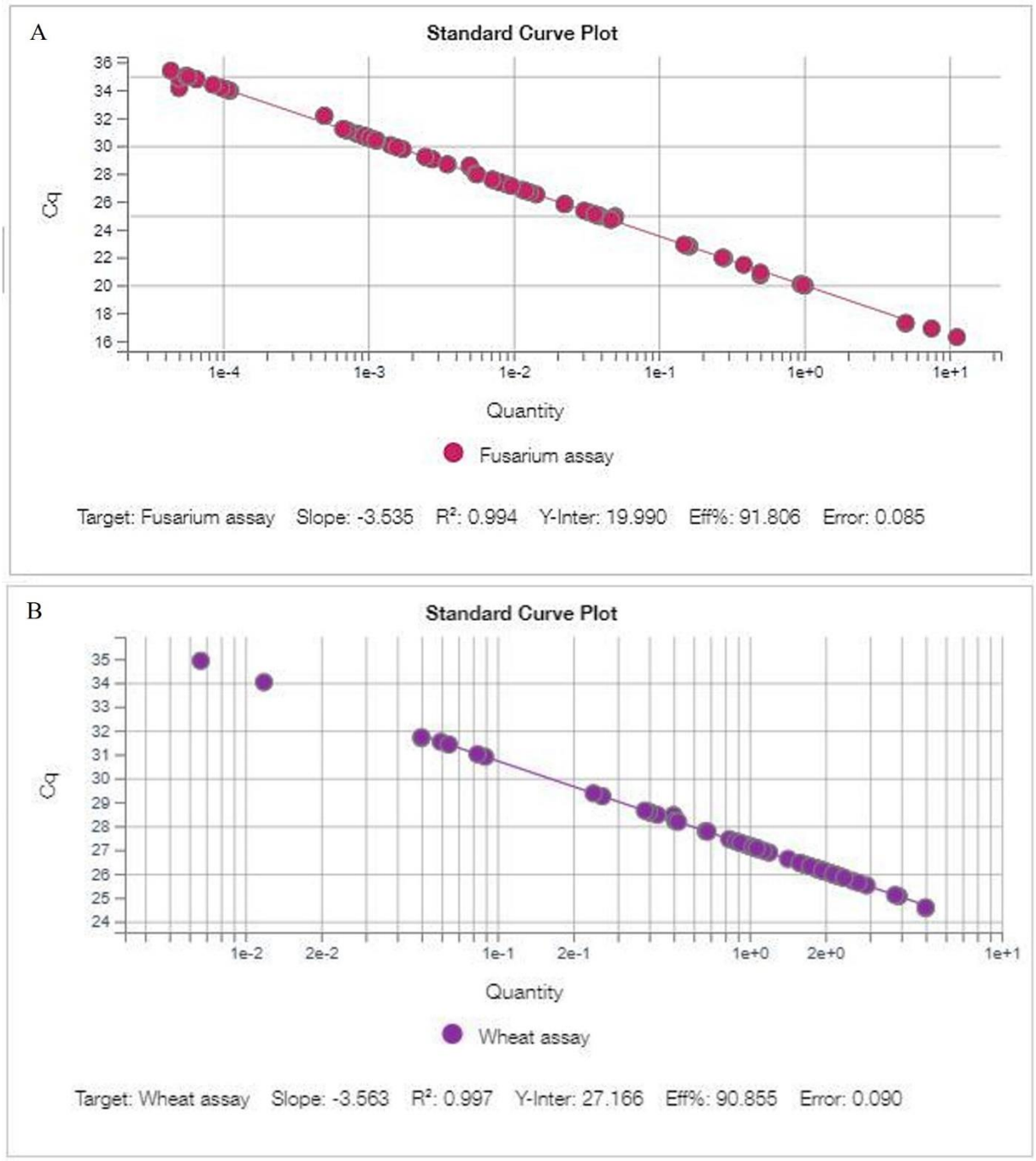

Figure 3.11 Standard curves for *F. graminearum* (A) and wheat (B) assays generated by QuantStudio™ 7 pro-Real-Time PCR system (Applied Biosystems, ThermoFisher Scientific).

The samples collected from 2019 and 2020 were subjected to qPCR, and results were analyzed together. The Cq values from qPCR were analyzed with statistical package R (version 4.1.2) to see differences in *F. graminearum* abundance (*Fg* abundance) according to the section of the stalk

and the province. The highest *Fg* abundance among the three provinces was recorded from Manitoba. The *Fg* abundance was reduced from section A (6 cm long stalk next to wheat heads) to section C (Figure 3.12). This interaction was more apparent in Manitoba samples than in other provinces (Figure 3.13).

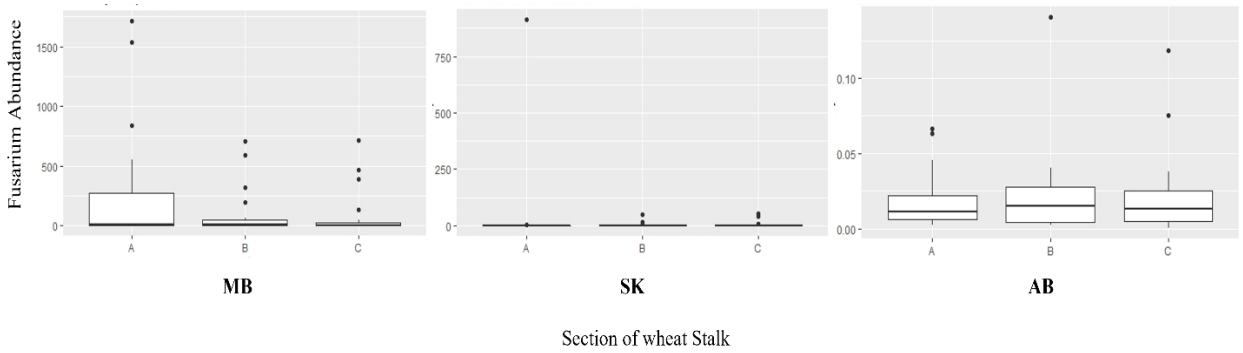

Figure 3.12 *F. graminearum* abundance found on spring wheat stalks in the 2019 growing season from three provinces, MB: Manitoba, SK: Saskatchewan and AB: Alberta. The three box plots for each province represent the three sections of stalk (A, B and C).

The two-way ANOVA test conducted on the results showed a significant difference in *Fg* abundance of stalk samples from three provinces ($P < 0.01$). However, there was no significant difference in *Fg* abundance between the three stalk sections ($P = 0.08$). Tukey's test (Tukey HSD) was conducted to compare the mean *Fg* abundance of stalk samples from three provinces. According to the results, there is evidence that the *Fg* abundance in Manitoba was significantly different from Alberta. At the same time, there is no evidence to say that the *Fg* abundance in Saskatchewan was significantly different from Alberta (Table 3.4).

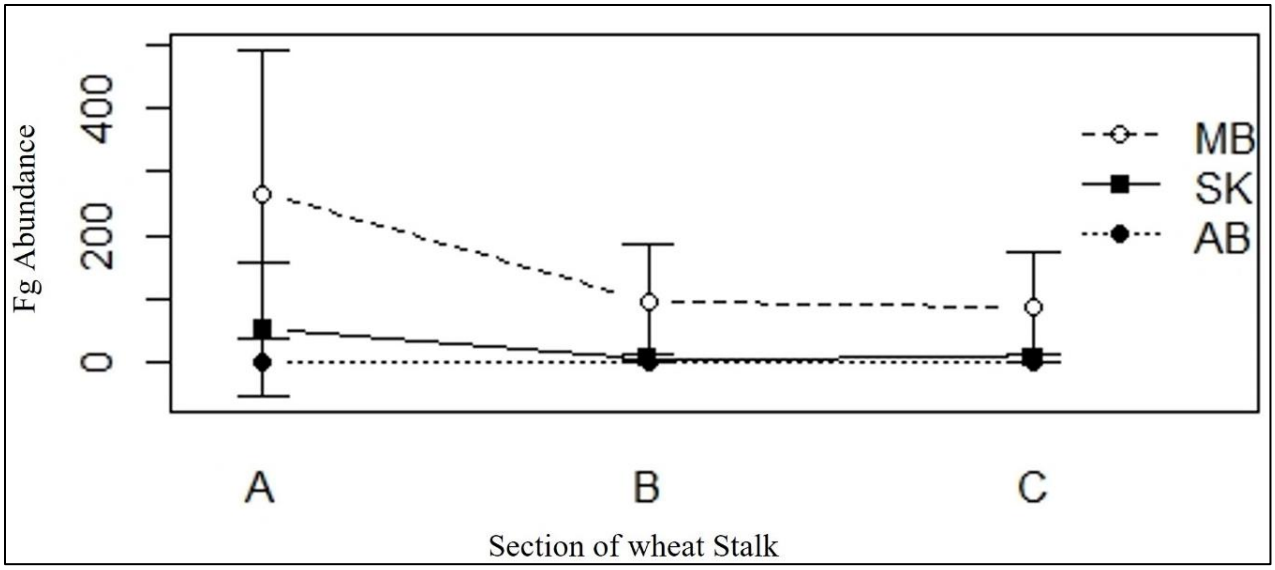

Figure 3.13 The interaction between *F. graminearum* abundance at three sections of the stalk (A, B and C) in three provinces.

Table 3.4 Comparison between mean *F. graminearum* abundance in stalks from three provinces

Province/P value	SK	AB
MB	0.0053*	0.0014*
SK		0.8793

* Significantly different at $P < 0.01$ MB: Manitoba, SK: Saskatchewan and AB: Alberta

3.5 Discussion

Fusarium head blight is the most destructive wheat disease in the Canadian prairies and is primarily caused by *Fusarium graminearum*. Molecular methods including PCR assays and high-throughput genotyping, were used to identify *Fusarium* species and chemotypes in spring wheat grain, chaff and winter wheat grain samples collected in western Canadian wheat fields in 2019/2020 and indicated that *F. graminearum* was the most frequent *Fusarium* species associated with the FHB disease. Further, the 3ADON producing *Fusarium* chemotypes are more prevalent in western Canada compared to 15ADON. Moreover, spring wheat chaff contained higher DON levels than grain in both years and greater *Fusarium* diversity than grain in 2020. Except for the fungicide application, all these participated spring wheat and winter wheat fields were managed according to standard agricultural practices. Therefore, the results represent the actual situation of FHB of western Canadian producer fields. In Alberta, recorded Fusarium damage was relatively lower compared to other two provinces.

According to the annual statistics on *Fusarium* damage of the Canadian Grain Commission, the mean percentage of CWRS wheat samples containing FDK was lower in Manitoba, Saskatchewan, and Alberta in 2019 and 2020 compared to 2016 data. In Manitoba, 31.5% of samples in 2020 and 21.8% in 2019 were recorded as *Fusarium* damaged. However, this value was 90.1% in 2016, showing milder FHB damage in tested seasons. The reported FDK percentage was similar in Saskatchewan, where 25.7% and 37.3% of damage were recorded in 2020 and 2019, respectively, lower than half of the damage recorded in 2016. In 2016, Alberta was recorded with a lower percentage of FDK (32.8%), and the ratios observed in 2020 and 2019 were 8% and 28.3%, respectively. In 2018 and 2017, samples from all three provinces showed lower FDK percentages than in 2020 and 2019 (Canadian Grain Commission, 2020). These data are essential in understanding the present situation of FHB in western Canada compared to past years. The results observed in this study aligned with the reported data. Further, the less FHB severity may also impact the percentages of *Fusarium* species observed in the study.

Contamination with mycotoxins in FHB infected fields is one of the main reasons causing wheat financial losses (Amarasinghe et al., 2016). DON is the primary mycotoxin associated with FHB

in Canada (McMullen et al., 1997). DON is also identified as a vomitoxin as it causes vomiting and dietary issues in humans and livestock. The DON level should be below 1 ppm in products for human consumption such as flour, bran, and germ, while the level should be less than 5-10 ppm in animal feed (US Food and Drug Administration, 2010). In this study, the DON levels were measured from spring wheat and winter wheat. In 2019, the highest DON level was recorded from Saskatchewan spring wheat field (8.5 ppm), and the highest recording from the other two provinces was 1.7 ppm. In 2020, DON contamination was lower than the previous year as the highest recorded DON level was 1.6 ppm from Manitoba (Figure 2.1). The observed DON level in spring wheat was always higher than in winter wheat in western Canada, indicating a lower FHB severity in winter wheat. This is because the winter wheat matures and reaches anthesis sooner than spring wheat. Thus, the crop may escape from the influx of *Fusarium* inoculum (Gilbert & Tekauz, 2000).

The spore density data from 2019 showed that the inoculum availability during the anthesis to soft dough stage was higher for spring wheat fields in all provinces than for winter wheat fields (Figure 3.4A). The reduced availability of spores in air supports the observation of lower DON accumulation in winter wheat (less than 0.5 ppm) in 2019. The mean spore densities recorded from spring wheat fields also explained the DON levels observed in spring wheat samples. For instance, the highest mean spore density was recorded from Saskatchewan (233.3 spores/m^3), where the DON accumulation was higher in 2019 (0.01 ppm to 8.5 ppm). Similarly, the lowest inoculum level was observed in Alberta (80.1 spores/m^3), where DON accumulation was lowest in 2019 (Figure 3.2A). Past studies confirmed that the inoculum availability during flowering highly correlates with the disease severity (Inch et al., 2005; Paul et al., 2004). Thus air-borne spore densities will be a good indicator for predicting FHB disease and mycotoxin content (Inch et al., 2005). However, the amount of inoculum may depend on several criteria, such as remaining infected crop debris in the field and environmental factors. For example, the likelihood of getting higher FHB severity increased when the previous crop was wheat or corn (Inch et al., 2005). Further, rainfall, high humidity, and wind may influence the number of spores in the environment (Sung & Cook, 1981). High humidity periods provide suitable conditions for spore dispersal and germination on wheat spikelets (Parry et al. 1995, Gilbert and Fernando 2004). In addition, Fernando et al. (1997) observed that the ascospores were dispersed by the wind as a gradient along the wind direction from the infected loci to neighbouring crops.

In this study, temperature (T), relative humidity (RH), and rainfall (R) data for each producer field were retrieved from the nearest weather stations to explain our observations. Data were collected for 4 days (4MA), 7 days (7MA), 10 days (10MA), 14 days pre-mid anthesis (14MA) and 3 days pre-mid anthesis to 3 days post-anthesis (3MA3PA). Data indicates that all spring wheat fields received a mean RH of more than 60% in both years. However, Manitoba and Saskatchewan received higher mean RH during 3MA3PA, which may facilitate the observed higher DON contamination in their samples (Appendix E). Further, the higher mean R3MA3PA may be attributed to higher spore availability observed in Manitoba and Saskatchewan spring wheat fields (Appendix E). A study published by Cowger et al. (2009) showed that the post-anthesis moisture level significantly affects FHB severity, FDK, and DON accumulation. Further, they showed that cultivar rating (resistant level of the cultivar) was not correlated with the development of FHB (Cowger et al., 2009).

The rainfall level received during 2020 was much lower than in 2019, which was unfavourable for FHB. Thus, the DON content in grain was lower in 2020 compared to 2019 (Appendix F). Further, previous studies can clearly explain results, which showed that the DON accumulation positively correlates with rainfall (Audenaert et al., 2009). Even though winter wheat fields received favourable rainfall conditions, the DON contamination was lower due to lower inoculum availability as the pathogen may not mature to produce sufficient inoculum (Figueroa et al., 2018). In both years, all fields from three provinces experienced milder temperatures during flowering week (15 - 25 °C) and may not affect the observed FHB contamination differences between the three provinces (Appendix F). Further, a previous study published by Beyer et al. (2004) stated that the mycelium growth of *F. graminearum* was not significantly affected by the temperature fluctuations during infection.

The wheat chaff is an essential source of animal feed. Therefore, lack of information about DON content in chaff may result in toxicosis in livestock (Seeling et al., 2006). Further, toxins may affect humans through the consumption of animal products. Thus, this study focused on how FHB affects DON concentration of chaff compared to its grain. The mean DON levels in grain and chaff were compared using spring wheat samples collected in 2019 and 2020 (Figure 3.3). The chaff from winter wheat was not considered for this analysis as their FHB infection level was very low

(Appendix B). Results showed that the chaff samples contained a significantly higher mean DON content than grain samples from all spring wheat fields in both years. The same effect was observed in previous studies conducted in China using experimental plots, where they observed high DON levels in wheat glumes, intermediate DON levels in stalks and low DON levels in grain (Ji et al., 2015). Further, a previous study conducted on barley showed that dehulling at harvest reduced the DON by 59%, dehulling at laboratory reduced DON in grain by 49% and pearling of grain reduced DON level by 86% (Clear et al., 1997). Thus, the results from the current study confirmed that removing chaff during processing may significantly reduce the DON impact on wheat grain.

Fusarium spores land on the glume or rachis to initiate the infection process. The growing mycelium must penetrate many physical barriers to reach the endosperm, including lemma, palea and ovary wall (Hope et al., 2005). Therefore, higher pathogen concentrations may present in the outer parts of wheat spikelets than in the grain. Further, the DON produced by *Fusarium* was found to travel from high DON concentration to low concentration via the phloem from the rachis, lemma, and grain to peduncle (Ji et al., 2015). Moreover, *Fusarium* spores injected into rachis tended to travel inside the plant and produce more inoculum longitudinally than transversely. Thus, the wheat residue may contain more DON and fungal biomass than the grain (Sinha & Savard, 1997). Results from the present study also confirmed these findings by showing the presence of *F. graminearum* in chaff and stalks of spring wheat samples. Moreover, leaving these contaminated residues on the soil surface may increase the amount of FHB inoculum in the following growing season (Sutton, 1982).

In the 2019 growing season, both grain and chaff samples were analyzed by culturing on PDA to isolate *Fusarium* spp. DNA was extracted from each isolate, and PCR was used to identify the species and chemotype. The species-specific primers designed to identify *Fusarium* spp. have been used by many studies (Demeke et al., 2005; O'Donnell et al., 2004; Parry et al., 1995). The development of molecular technologies in species identification has reduced the difficulties faced during phenotypic identification. PCR is an easy, affordable, and reproducible solution for species identification (Mishra et al., 2003). In this study, nine previously developed PCR assays were used to detect *Fusarium* spp., *F. graminearum, F. culmorum, F. avenaceum, F. sporotrichioides, F. poae, F. proliferatum, F. pseudograminearum* and *F. cerealis*. Most spring wheat samples (~70%)

from Manitoba and Saskatchewan were contaminated with *Fusarium* spp. Further, 40% of spring wheat samples from Alberta got infected with *Fusarium* spp. The results can also be explained by the higher mean spore densities observed in Manitoba and Saskatchewan spring wheat fields (233.3 and 195.6 spores/m^3, respectively) than Alberta (80.1 spores/m^3). However, less than half of the winter wheat samples were found to be colonized by detectable amounts of *Fusarium* spp. (Figure 3.5). Further, results showed that *F. graminearum* was the most prominent causal agent of FHB infection in western Canada, as recorded in many previous studies (Amarasinghe et al., 2016; Fernando et al., 2021; McMullen et al., 2012). The higher percentages of *F. graminearum* isolates were detected from spring wheat samples from Manitoba and Saskatchewan (87% and 65% of total isolates in each province). In contrast, most spring wheat samples from Alberta in 2019 were not contaminated with *F. graminearum*, where the *F. avenaceum* percentage was higher than the *F. graminearum* (Figure 3.6A).

Since 1948, FHB began to spread from Manitoba to Saskatchewan and then Alberta. A survey conducted from 1993 to 1998 delivered the evidence for westward movement of *F. graminearum* from southeastern Manitoba, replacing the other *Fusarium* species (Clear & Patrick, 2000). Clear and Patrick (2010) explained that this species shift might be occurring due to increased precipitation levels at anthesis and infected seeds supporting long-distance spore dispersal, which facilitate the movement of *F. graminearum*. The higher *F. graminearum* involvement in FHB has caused more significant economic losses (Panthi et al., 2014). However, disease severity in Alberta is still relatively low due to the lower frequency of *F. graminearum* present in the FHB pathogen population. For example, a study that isolated *Fusarium* species from cereals from Alberta 18 years ago showed the most common species were *F. avenaceum* and *F. culmorum,* followed by *F. pseudograminearum* (Turkington et al., 2011). In 2019, the highest percentage of *F. avenaceum* (45%) was recovered from spring wheat samples from Alberta. Further, *F. avenaceum* was the only species found in winter wheat from Alberta. However, only 27% of total isolates from spring wheat were identified as *F. graminearum* in Alberta (Figure 3.6A).

The chemotypes of isolates were identified by conducting multiplex PCR assays. The *Tri5* gene encodes the first biosynthetic step for DON production in the *Fusarium* species. Neighbouring *Tri* genes in the genome are also involved in the production of DON; thus the PCR primers were

developed to determine polymorphisms in *Tri* genes that contribute to chemotype differences (Desjardins, 2006). Most of the *F. graminearum* isolates from three provinces were of the 3ADON chemotype. During previous years of FHB surveys, much research explained a shift of chemotype of *F. graminearum* from 15ADON to 3ADON. The percentage of the 15ADON chemotype was significantly lower in Alberta, showing that the 3ADON is becoming the dominant chemotype in FHB disease epidemics (Figure 3.6B). Ward et al. (2008) stated that *F. graminearum* isolates recovered from western Canada from 1998 to 2004 showed a 14-fold increase in 3ADON chemotype frequency. Further, they observed that 3ADON populations were potentially more virulent than 15ADON populations as 3ADON chemotypes, have higher trichothecene production, fecundity, and growth rates. Guo et al., 2008 suggested that this genetic variation in *F. graminearum* population may occur with sexual recombination, population age and cropping systems. Further, they inferred that long-distance spore dispersal and seed shipments might support this genetic migration and chemotype shift in western Canada.

A limited number of studies described how FHB affects *Fusarium* species diversity within the wheat chaff. Thus in this study, *Fusarium* species and chemotypes in spring wheat chaff were compared with the results from their grain. In 2019, chaff collected from the same spring wheat samples as the grain showed a higher *F. graminearum* percentage of total isolates obtained from Manitoba and Saskatchewan. Most of the *F. graminearum* isolates recovered from chaff were also found to be 3ADON producers. In Manitoba, 64% of DON-producing isolates produced 3ADON, while all the *F. graminearum* isolates recovered from Alberta chaff samples were 3ADON producers (Figure 3.7). The *Fusarium* species diversity was similar in both grain and chaff in 2019 samples. However, the frequency of other *Fusarium* species such as *F. avenaceum* and *F. sporotrichioides* was higher in chaff than in grain (Figure 3.7A). Previous studies showed that DON-producing *Fusarium* species were more likely to be present in grain than in chaff. DON production increased pathogen virulence, helping the pathogen to penetrate tissues and colonize in deeper tissues (Tillmann et al., 2017). For example, *F. avenaceum* is a non-DON producer, and a higher percentage of *F. avenaceum* was recovered from chaff samples than the grain. Further, a study conducted on *F. avenaceum* infection and colonization showed that the germ tubes of *F. avenaceum* did not penetrate host tissues immediately but extended and branched on host surfaces.

Thus, the hyphal growth on abaxial surfaces of glume, lemma and palea was higher than fungal growth in grain (Kang et al., 2005).

Fusarium species isolation via whole sample agar plating and species-specific PCR has provided accurate species detection in infected crops (Demeke et al., 2005). However, culturing and isolating pure cultures is highly time-consuming. Thus, agar plating is not ideal for rapid *Fusarium* species identification. A robust and fast detection method is needed during large-scale surveys (Tittlemier et al., 2020). Therefore, direct DNA extraction from the grain/sample and PCR-based identification have been used to identify *Fusarium* species. This method allowed rapid and more sensitive species identification than plating the grain on PDA (Brandfass & Karlovsky, 2006; Demeke et al., 2005; Tittlemier et al., 2020). Thus, *Fusarium* species and chemotypes in grain and chaff samples collected from 2020 were identified by high-throughput genotyping using SmartChip Real-time PCR (Takara Bio Inc). High-throughput SmartChip technology allows analyzing more samples (5 184 reactions) at once without reducing sensitivity, accuracy and specificity. This system included a Smartchip MultiSample NanoDispenser that can accurately measure and precisely dispense the reagents and sample into 5 184 reaction wells in a short time. Thus, it provides the opportunity to run several assays simultaneously. Therefore, it will take two hours to identify *Fusarium* species and chemotypes present in the DNA sample. However, this culture-free method will not be suitable if further testing is needed for recovered *Fusarium* isolates or to maintain an isolates library for future reference.

The results from 2020 showed that *F. graminearum* was positive in the majority of spring wheat grain samples from Manitoba and Saskatchewan. In Manitoba, 71% of spring wheat samples were contaminated with *F. graminearum* while *F. poae*, *F. acuminatum* and *F. culmorum* were present less frequently. However, only 16% of spring wheat samples were positive for *F. graminearum* in Alberta. The results were similar to the previous year, except *F. poae* was more common in all samples and most frequently found from spring wheat samples from Alberta. When comparing the *Fusarium* species in spring and winter wheat, fewer winter wheat samples were positive for each *Fusarium* species, indicating a lower FHB severity in winter wheat grain. The analysis for 3ADON, 15ADON and NIV chemotypes showed that most samples were positive for 3ADON in spring wheat and winter wheat. The majority, 62%, of Manitoba spring wheat samples were

positive for 15ADON, which deviated from the previous year's result. However, when moving into Saskatchewan and Alberta, 3ADON became the more prominent chemotype, indicating that 3ADON is highly involved in disease spread (Ward et al., 2008). NIV chemotype was absent in grain samples (Figure 3.9).

In 2020, results clearly showed that spring wheat chaff contains higher *Fusarium* species diversity compared to its grain. The chaff samples from all three provinces were positive for many *Fusarium* species, including *F. graminearum*, *F. poae*, *F. acuminatum*, *F. avenaceum* and *F. pseudograminearum*. Another difference observed between grain and chaff was the higher percentages of non-DON producing species in chaff samples. This observation was also the same as in 2019, showing that DON producing *Fusarium* species are more likely to be present in grain than in chaff, which supports the conclusions made by Tillmann et al. (2017). Most of the chaff samples were positive for the 3ADON chemotype while the frequency of 15ADON was lower, which confirmed the shift of chemotypes in western Canada (Ward et al., 2008). Interestingly, 4.3% of spring wheat chaff samples from Manitoba contained the NIV chemotype. NIV chemotype is produced by trichothecene mycotoxin producing *Fusaria*, such as *F. graminearum* and *F. cerealis* (Amarasinghe et al., 2015; Goswami & Kistler, 2005; Wegulo, 2012). In Canada, NIV-producing *F. cerealis* species was first isolated from winter wheat heads (Amarasinghe et al., 2015). Even though NIV is less toxic to plants, it is more harmful to humans than DON. Thus, careful monitoring of NIV in Canadian wheat fields is necessary. The current study is an excellent example to state that NIV chemotype is present in Manitoba fields.

Quantitative PCR (qPCR) assays provide more understanding about the abundance of an organism in a given sample. Thus, qPCR assays can be used to compare the *Fusarium* load in sections of the plant. *F. graminearum* infects the wheat heads at their flowering stage. After invading through stomata, mycelia penetrate the spikelet tissues and propagate inside, destroying the host tissues. Later, the fungus starts to infect other nearby spikelets internally through the rachilla and rachis vascular system (Kheiri et al., 2019). This study detected the *F. graminearum* abundance in spring wheat stalks using qPCR assays. Three separate sections of wheat stalks were compared during the experiment (A: top, B: middle and C: bottom of 18 cm long stem). Probe-based qPCR has been used to increase sensitivity and accuracy. Further, *F. graminearum* abundance was measured by

quantifying *F. graminearum* DNA presence in the total DNA extracts relative to the quantity of wheat DNA present in the same sample. Results found *F. graminearum* in the stalk samples proving that *F. graminearum* spread from the point of infection (wheat spike) to stalks. However, no significant difference of abundance was recorded between the sections of stalks (Figure 3.13). *F. graminearum* abundance was significantly higher in Manitoba stalk samples than in Alberta.

In conclusion, this study provides insights into DON levels, and *Fusarium* species and chemotypes found in both spring wheat and winter wheat fields of western Canada. The DON contamination was generally low in both years 2019 and 2020. However, the highest mean DON level was recorded in Manitoba, followed by Saskatchewan. Comparatively, higher DON contamination was observed in spring wheat fields than in winter wheat fields. *F. graminearum* was found as the primary pathogen involved in FHB in western Canada. Further, results provided evidence for chemotype shift in FHB populations in western Canada as 3ADON was the most frequent chemotype in all analyzed samples. Moreover, the chaff collected from the same spring wheat heads showed a significantly higher DON content than the grain in both years, emphasizing a need for DON testing of chaff before using as a livestock feed. Further, chaff contained higher *Fusarium* species diversity in 2020, and a higher percentage of *F. graminearum* was found in both years. The analysis on *F. graminearum* abundance in spring wheat stalks revealed the *Fusarium* abundance was higher on the stem next to wheat heads than the stalk at the bottom. However, the difference in *Fusarium* abundance along the stalk was not significant. It is important to note chaff and stalks left on the field may act as primary inoculum in the following disease cycle.

Chapter Two

4.0 Generating *Leptosphaeria maculans* isolates carrying single avirulent (*Avr*) genes

4.1 Abstract

Blackleg is a disease in canola, caused by *Leptosphaeria maculans*, that is a significant constraint to yield and trade. Much research was conducted on the interaction and identification of blackleg resistance in canola. However, there is a considerable limitation in characterizing the resistant genes. A growing concern among blackleg researchers is that host resistance (*R*) genes are not correctly identified because different researchers used a non-standardized set of pathogen isolates. Further, the same *R*-gene determined by two independent labs, may be named differently as two separate genes. Another concern is a lack of an effective method to create a set of blackleg isolates carrying a single *Avr* gene to circumvent the above problem. Therefore, the objective of the research is to develop a method to generate universally acceptable isolates of *L. maculans* with single avirulent (*Avr*) genes that can be used to identify both existing and novel *R* genes. Mating between two *L. maculans* isolates may allow recombination in progeny, which may change their phenotype. However, results showed that selected *L. maculans* isolates produced fewer sexual fruiting bodies or pseudothecia than pycnidia. Further, the recombination events occurred with lesser frequency in laboratory settings, making it challenging to have mutated isolates available for study. On the other hand, clustered regularly interspaced short palindromic repeat (CRISPR)/Cas9 mediated gene editing was identified as a promising tool in mutating *Avr* genes. This study aimed to utilize CRISPR/Cas9 to create an isolate carrying only *AvrLepR1* by knocking off the *AvrLm5* gene of *L. maculans* isolate, *D3*. The CRISPR/Cas9 system was delivered to the *L. maculans* genome through the vector *sgAvrlm5_pKHT332* via *Agrobacterium* mediated transformation. The vector, *sgAvrlm5_pKHT332*, was created by combining a sgRNA designed to bind the *AvrLm5* gene in *D3* and a fragment of *pFC334* plasmid containing *Aspergillus nidulans tef1* promoter, Cas9 gene and *A. nidulans tef1* terminator via In-Fusion cloning. Antibiotic-resistant isolates were selected, and the mutants were identified by sequencing the target gene, *AvrLm5*. A total of 141 transformed isolates were tested for mutations. Transformants did not carry the expected mutation even though few displayed reduced pathogenicity on canola cultivar Westar.

4.2 Introduction

Canola is the most important oilseed crop grown in Canada. The Canadian canola industry can be severely damaged by the by blackleg disease which is primarily caused by *Leptosphaeria maculans* (West et al., 2001). Canola cultivars have developed a resistance against the fungal pathogen by expressing resistant gene products (*R* genes) in the presence of the pathogen's avirulence (*Avr*) genes. The interaction between the compatible *R* gene and the *Avr* gene results in a hypersensitive reaction on the site of infection, causing cell senescence to prevent the disease progression into the plant (Cook et al., 2015). A total of 18 *R* genes are identified in *Brassica* species, including *Rlm1* to 11, *LepR1* to *R5, RlmS, BLMR1* and *BLMR2.* At the same time, 14 *Avr* genes are identified in *L. maculans* including *AvrLm1*, *AvrLm2*, *AvrLm3*, *AvrLm5-9*/*AvrLmJ1*, *AvrLm4-7*, *AvrLm6, AvrLm11* and *AvrLepR1* to *3*, (Fernando et al., 2018; Liu et al., 2020b).

Genetic resistance is advantageous when the pathogen population contains the corresponding *Avr* genes in high frequencies. Unfortunately, *L. maculans* have a high evolutionary potential to overcome major *R* genes introduced into canola (Van de Wouw et al., 2014b). Some studies proved the ability of *L. maculans* to overcome *R* gene resistance and cause disease on resistant cultivars. For example, the epistatic suppression of *AvrLm3* recognition by *Rlm3* will be deactivated when the pathogen also contains *AvrLm4-7* (Plissonneau et al., 2016) and a similar suppression mechanism was also found in *AvrLm9* - *Rlm9* recognition due to the presence of *AvrLm4-7* (Ghanbarnia et al., 2018). Moreover, overuse of a single *R* gene may increase the risk of resistance breakdown. For instance, the *Rlm1* resistant varieties are less effective in resisting pathogens as the *AvrLm1* carrying isolates tend to decrease in the population (Rouxel et al., 2003; Van de Wouw et al., 2014b). Moreover, Zhang *et al*. (2016) showed the breakdown of *Rlm3* over time with the intensive usage of this gene. Therefore, the introduction of other *R* genes is required to address this rapid plant-pathogen arms race.

Although much research has been done on the interaction and identification of resistance, the research in characterizing the genes is limited significantly. A growing concern among blackleg researchers is that R-genes are incorrectly identified as not all groups use a standard set of well-characterized isolates. Another problem is that two different labs may determine the same R gene

and name them as two genes (Ghanbarnia et al., 2018; Plissonneau et al., 2016). Thus, two key research gaps are identified, 1) a lack of a standard set of isolates in identifying *Avr*/*Rlm* interactions and 2) a lack of an effective method to create a set of isolates carrying a single *Avr* gene to circumvent the first research gap. This study aimed to develop a procedure to generate a universally acceptable isolate set of *L. maculans* isolates, each of which carries only a single *Avr* gene. Such an isolate set will be beneficial in screening for existing and novel *R* genes with higher accuracy and precision. Furthermore, novel isolates carrying a single *Avr* gene will be beneficial for identifying mechanisms of pathogenicity. Most importantly, single-gene isolates will be advantageous for breeders as they allow rapid selection of resistant genes.

First, mating between two compatible *L. maculans* isolates is utilized to generate a single *Avr* gene isolate. *L. maculans* is an ascomycetes fungus that produces pseudothecia during the sexual stage of its lifecycle. The pseudothecia consist of asci, each of which consists of eight ascospores. The ascospores are produced by meiosis followed by mitotic division (Gall et al., 1994). Meiotic segregation may produce a haploid progeny, which may differ from parental isolates. Sexual reproduction only occurs between isolates with the compatible mating type (Petrie & Lewis, 1985). Thus, checking their mating type before sexual recombination is mandatory in laboratory experiments. *L. maculans* has two idiomorphs of a single mating type locus (*MAT*) *MAT 1_1* and *MAT 1_2*. The mating type is identified by completing multiplex PCR using specific *MAT* primers (Cozijnsen & Howlett, 2003). The mating is performed under controlled environmental conditions in a Petri-dish containing nutrient media. If the sexual outcrossing occurs successfully, different combinations of *Avr* genes will appear in new isolates. For example, genes may be stacked or lost in a single ascus (Eckert et al., 2005).

The experiment contained four main steps: 1) selecting a set of isolates with proper *Avr* and *avr* gene combinations, 2) checking the mating type of the isolates, 3) performing the mating between a pair of compatible isolates using the standard methods, and 4) identifying the *Avr* genes present in the progeny. *Avr* genes of the progeny can be identified using specific PCR markers for each *Avr* gene (Fernando et al., 2018). The phenotype was detected by inoculating the isolates on canola seedlings and evaluating disease (or resistance) post-inoculation (Rimmer & Van Den Berg, 1992; Williams & Delwiche, 1980).

The second experiment involving site-directed mutagenesis via CRISPR/Cas9 gene editing. The clustered regularly interspaced short palindromic repeats (CRISPR)/Cas9 system has been recognized as a revolutionary technique with its unprecedented performance in genome editing. The applicability of CRISPR/Cas9 in plant disease research has proven to be successful in many studies, including plants, bacteria, and fungi (Barrangou et al., 2007; Cong & Zhang, 2015; Darma et al., 2019). The availability of the genome sequence of *L. maculans* has led to a rise in CRISPR/Cas9 genome editing (Rouxel et al., 2011). Recent studies that used CRISPR/Cas9 genome editing in *L. maculans* showed its potential in rapid and precise gene editing to create target mutations. For example, CRISPR/Cas9 tools were successfully implemented to identify genes of *L. maculans* that involve pathogenicity (Darma et al., 2019; Liu et al., 2020a; Urquhart & Idnurm, 2019; Zou et al., 2020) and fungicide resistance (Idnurm et al., 2017b).

This research aims to utilize CRISPR/Cas9 gene editing to create an isolate carrying only *AvrLepR1* by knocking out the *AvrLm5* gene of *L. maculans* isolate, *D3*. The *D3* isolate was identified to have two *Avr* genes, *AvrLm5* and *AvrLepR1*. The CRISPR/Cas9 system was delivered to the *L. maculans* genome through the vector *sgAvrlm5_pKHT332* via *Agrobacterium* mediated transformation. The vector, *sgAvrlm5_pKHT332*, was created by combining a sgRNA designed to bind the *AvrLm5* gene of *D3*, a section of *pFC334* plasmid containing *Aspergillus nidulans tef1* promoter, Cas9 gene, and *A. nidulans tef1* terminator via In-Fusion cloning. Antibiotic-resistant isolates were selected, and the desired mutants were identified by sequencing the respective portion of the target gene. The selected mutants were not edited at the *AvrLm5* gene sequence; however, a few of them expressed reduced virulence on the Westar cultivar, suggesting that the transformation affected their pathogenicity.

4.3 Materials and methods

4.3.1 Mating between two isolates to get recombinant progeny

L. maculans isolate pairs were selected from the Fernando lab collection. Each pair of isolates was inoculated on the same Petri-dish to generate pseudothecia, following the protocol below.

4.3.1.1 Selection of isolates with proper *Avr* and *avr* gene combinations

A set of recently isolated *L. maculans* isolates from Manitoba fields were selected (personal communication, Dr. Fernando), which carry few *Avr* genes were considered (Table 4.1). The pairs were selected for mating according to the mating type and rate of growth.

4.3.1.2 Detection of mating type and the growth rate

Selected isolates were cultured in V8 juice media (200 mL of V8 juice, 800 mL water, 15 g agar, 0.75 g $CaCO_3$, and 0.0035% (w/v) streptomycin sulphate) and incubated under continuous fluorescent light at room temperature (25 °C). The pycnidiospores used for DNA isolation were harvested by scraping the plate with 400 µL of sterile water. DNA extraction was performed according to the protocol explained in Liban et al. (2016). The extracted DNA solution was stored at -20 ºC for future use.

The mating type was determined by conducting multiplex PCR using three primers *MAT1.1-F* (CTC GAT GCA ATG TAC TTG G), *MAT1.2-F* (AGC CGG CGG TGA AGT TGA AGC CG) and *MAT-R* (TGG CGA ATT AAG GGA TTG CTG) (Cozijinsen and Howlett, 2003). Amplified bands were detected on 1% agarose gel after electrophoresis. All selected isolates were cultured on cleared V8 media (prepared with filtered V8 using a sterile mira cloth) for one week at 22 ºC with a 12 h photoperiod. The culture diameter was measured using a standard ruler. The mean diameter of vegetative growth of each isolate was compared before proceeding.

4.3.1.3 Mating between compatible isolates

Two selected isolates with compatible mating types and similar growth rates were selected for crossing. The crossing procedure was carried out according to the method reported by Van de Wouw *et al*. (2019). Briefly, two agar plugs from selected isolates were placed 5 mm apart on cleared V8 media. The mycelia were grown for one week at 22 ºC with a 12 h photoperiod. During this period, two mycelia grew and mingled at the intersection. After that, each plate was layered with 1% water agar (cooled to 45 ºC) to cover the mycelia entirely. The cultures were incubated at 14 ºC with a 12 h black light photoperiod for 4 to 8 weeks until pseudothecia appeared and matured (Van de Wouw et al., 2019). Mature pseudothecia were harvested by a sterile needle and placed in a drop of β-glucuronidase to allow asci ejection. Next, each pseudothecium was placed

over water agar and allowed germination overnight at 24 ºC (Gall et al., 1994). Finally, the germinated ascus was cultured on V8 media and incubated under continuous fluorescent light at room temperature (25 °C) to obtain pycnidia for DNA extraction.

4.3.1.4 Identification of genotype of progeny isolates

DNA extraction and PCR assays were used to identify genotypes of *Avr* genes in the progeny. A modified CTAB DNA extraction protocol was used (Liban et al., 2016). In short, pycnidia and mycelium grown on V8 were harvested by scraping after adding sterile distilled water. Next, the collected sample was centrifuged at 12 000 rpm for 2 minutes. Then, the supernatant was removed before adding 400 µl of preheated (65 ºC) CTAB extraction buffer. The sample was homogenized using the tissue pulverizer after adding ceramic beads. The mixture was incubated in the water bath at 65 ºC for 30 minutes. Next, 400 µl of phenol: chloroform: Isoamyl alcohol (25:24:1) mixture was added and centrifuged at 12 000 rpm for 10 minutes. Next, the supernatant was carefully transferred to a new microcentrifuge tube. The above protein purification step was repeated. Then, DNA was precipitated by adding the same volume of 100% ethanol and 80 µl of NaCl. Finally, the precipitate was washed with 70% alcohol and centrifuged briefly. The remaining DNA pellet was air-dried for a few minutes before dissolving it in sterile water.

PCR was used to identify the *Avr* genes with specific primers (Table 4.2) in a Takara thermocycler, which was programmed as follow: initial denaturation at 95 °C for 3 min, 30 cycles of 95 °C for 30 sec, 50 °C for 30 sec and 72 °C for 1 min, finally at 72 °C for 5 min for the extension. Next, the amplified fragments were visualized in 1% agarose gel electrophoresis.

Table 4.1 Candidate *L. maculans* isolates selected from the collections of Fernando Lab at the University of Manitoba

	Name	Avirulence Genes										Source
		AvrLm1	*AvrLm2*	*AvrLm3*	*AvrLm4*	*AvrLm5*	*AvrLm6*	*AvrLm7*	*AvrLm9*	*AvrLepR1*	*AvrLepR2*	*AvrLmS*	
1	1-1	a	A	a	A	a	A	A	a	A	a	a	
2	3-1	A	a	a	A	a	A	A	a	a	a	?	
3	5-1	a	A	a	A	a	A	A	a	a	a	a	
4	8-1	A	a	a	A	a	A	A	a	A	a	?	
5	21-2	a	A	a	A	a	A	A	a	a	a	a	
6	25-1	a	A	a	A	a	A	A	a	a	a	a	
7	30-3	a	A	a	A	a	A	A	a	a	a	a	
8	41-2	a	A	a	A	a	A	A	a	a	a	A	Dr. Dilantha Fernando
9	43-1	a	A	a	A	a	A	A	a	a	a	a	
10	DM65	a	A	a	a	a	A	A	a	a	a	a	
11	DM77	a	A	a	a	a	A	A	a	a	a	a	
12	DM78	A	a	a	A	a	A	A	a	a	a	?	
13	DM79	a	A	a	a	a	A	A	a	a	a	A	
14	DM81	a	a	a	A	a	A	A	a	a	a	A	
15	DM85	a	A	a	a	a	A	A	a	a	a	A	
16	DM96	a	A	A	a	a	A	a	A	a	a	A	
17	DM118	a	A	A	a	a	A	a	A	a	a	A	
18	DS105	a	a	a	a	A	A	A	a	a	a	a	
18	D3	a	a	a	a	A	a	a	a	A	a	a	
19	D8	a	a	a	a	A	a	A	a	A	a	a	Zhang et al., 2016
20	D13	a	a	a	A	a	A	A	a	a	a	a	
21	S7	A	a	a	a	a	a	A	a	A	a*	A*	

'A' indicates avirulent allele, and 'a' indicates virulent allele

**AvrLepR2* and *AvrLmS* are now identified as the same gene by Neik et al., 2022 (In press).

Table 4.2 Primers used to identify *Avr* genes of *L. maculans* by PCR

Primer	sequence (5'-3')	Reference
AvrLm1-F	CTATTTAGGCTAAGCGTATTCATAAG	(Gout et al., 2006)
AvrLm1-R	GCGCTGTAGGCTTCATTGTAC	
AvrLm2-F	CGTCATCAATGCGTTCGG	(Ghanbarnia et al., 2015)
AvrLm2-R	CTGGATCGTTTGCATGGA	
AvrLm3-F	GAGAGAACTAGTCTGTTAAATGCCTGCTGT	(Plissonneau et al., 2016)
AvrLm3-R	GAGAGACTCGAGCGCGCTTATGTTAGAATC	
AvrLm4-7-outerF	GTAACAAAGTAACGAAGGGCTTAATT	(Zou et al., 2018a)
AvrLm4-7-outerR	GAAAACTCACCTCCGTATCTTTAGTC	
AvrLm4-7-innerF	TCTAAACCAGTCTCCTGCCC	
AvrLm4-7-innerR	TAG CTCAGC ACCTGG AGTTATATATC	
AvrLm5-9-F	ACAACCACTCTTCTTCACAGT	(Liu et al., 2020b)
AvrLm5-9-R	TGGTTTGGGTAAAGTTGTCCT	
85C-F	TCCTTCGCTTAGTGATTACCCAATTGAACA	
85C-R	CGTTCTTTGTTCTGTAGTGTAACGTCGCG	
AvrLm6-F	TCAATTTGTCTGTTCAAGTTATGGA	(Fudal et al., 2007)
AvrLm6-R	CCAGTTTTGAACCGTAGTGGTAGCA	
AvrLm11-F	TGCGTTTCTTGCTTCCTATATTT	(Balesdent et al., 2013)
AvrLm11-R	CAAGTTGGATCTTTCTCATTCG	

4.3.1.5 Identification of the phenotype of progeny isolates of blackleg

The *Avr* genes which cannot be identified with PCR were characterized by phenotyping via cotyledon inoculation assay. A set of different lines of *B. napus* (Table 4.3) were inoculated on cotyledons with spore suspension (2×10^7 spores/mL) of each isolate on the seventh day after seeding. The seedlings were grown in a controlled growth chamber for 14 days at 21 °C in daytime and 16 °C at night. The cotyledons were maintained by removing the true leaves and fertilizing them. After 14 days of inoculation, disease severity was rated according to the size of lesions on cotyledons vs. the lesions on Westar as control (sensitive variety).

Table 4.3 Set of canola varieties used for phenotyping the blackleg isolates

Brassica species	Cultivar/line	Host resistance genotype
B. napus	Westar	Susceptible line to blackleg
B. napus	MT29	*Rlm1, Rlm9*
B. napus	Topaz Rlm2	*Rlm2*
B. napus	02-22-2-1	*Rlm3*
B. napus	Jet Neuf	*Rlm4*
B. juncea	Forge	*Rlm6*
B. napus	01-23-2-1	*Rlm7*
B. napus	*Goéland*	*Rlm9*
B. napus	1065	*LepR1*
B. napus	1135	*LepR2*
B. napus	Surpass 400	*LepR3, RlmS*

4.3.2 CRISPR/Cas9 mediated gene editing to create a *L. maculans* isolate carrying a single avirulent gene - *AvrLepR1*

L. maculans isolate, *D3* (provided by Dr. Van de Wouw, University of Melbourne, Australia), was selected for genome editing by CRISPR/Cas9. The *Avr* gene profile of *D3* was confirmed before the transformation.

4.3.2.1 Genotypic and phenotypic characterization of *L. maculans* isolate

The *D3* isolate was known to carry *AvrLm5* and *AvrLepR1*. For seven days, the isolate was grown on V8 media under fluorescent light at room temperature (25 °C). A single pycnidiospore was subcultured in a new plate to obtain a pure culture of *D3*. The pycnidia and mycelium were scraped and collected into an microcentrifuge tube after adding 3 mL sterile distilled water. The collected spores were used for DNA extraction and inoculum preparation.

A modified CTAB DNA extraction protocol was used to extract genomic DNA (Liban et al., 2016). Specific PCR markers confirmed the presence/absence of avirulent genes for *AvrLm1*, *AvrLm2*, *AvrLm3*, *AvrLm4-7*, *AvrLm5*, *Avrlm5-9* and *AvrLm11*. The PCR reaction mixture (25 µL) contained 10-50 ng genomic DNA, 25 pmol of forward and reverse primers and 2 X Froggabio Master mix (FroggaBio Scientific Solutions, cat.no. FBTAQM). PCR was performed in a Takara thermocycler with a program of initial denaturation at 95 °C for 3 min, 30 cycles of 95 °C for 30 sec, 50 °C for 30 sec and 72 °C for 1 min, and finally at 72 °C for 5 min for the extension.

The cotyledon inoculation test was used to confirm the phenotype of avirulent genes in the greenhouse. A set of different lines of *B. napus* (Table 4.3) were inoculated with *D3* spore suspension (2×10^7 spores/mL) at the seven-day cotyledon stage. The procedure was the same as section 4.3.1.5.

4.3.2.2 Generating mutant isolates

CRISPR/Cas9 mediated gene editing was utilized to generate a mutant *D3* isolate carrying only *AvrLepR1*. The CRISPR/Cas9 system was delivered to *D3* by *pKHT332* vector via *Agrobacterium*-mediated transformation. The CRISPR/Cas9 construct was prepared by *Aspergillus nidulans tef1* promoter, Cas9 gene and *Aspergillus nidulans tef1* terminator from the *pFC334* plasmid inserted into the *pKHT332* plasmid via In-Fusion cloning (Nødvig et al., 2015).

4.3.2.3 CRISPR/Cas9 vector for directed mutagenesis of *D3*

The coding sequence of *AvrLm5* was retrieved from GenBank, NCBI (ID number KF853561.1). The sgRNA required to target *AvrLm5* was generated by submitting the above sequence to CRISPR RGEN tools (http://www.rgenome.net/). The sgRNA was selected based on the criteria of both its position on the *AvrLm5* gene and the number of off-target sites (the lower, the better) in the *L. maculans* genome. The possible off-targets were detected by searching the selected sgRNA sequence against the *L. maculans* genome using the NCBI BLASTn tool (https://blast.ncbi.nlm.nih.gov/Blast). Next, the new sgRNA was integrated into *gdA* promoter and *trpC* terminator by amplifying *pFC334* with primers designed by the Takara primer designing tool (at https://www.takarabio.com/learning-centers/cloning/primer-design-and-other-tools) (Table 4.4). The amplification was performed with PrimeSTAR® GXL DNA polymerase (Takara Bio, Cat. No. R050B). The resulting two fragments were purified by Nucleospin PCR and the gel clean-up kit (Takara Bio, Cat. No. 740609.250). Finally, the CRISPR/Cas9 vector for *D3* was created by combining the above two fragments with linearized *pKHT332* (digested with the restriction enzyme, *pst1*) using 5x In-Fusion HD enzyme premix (In-Fusion HD cloning, Takara Bio - clone tech) (Nødvig et al. 2015, Zou et al., 2020). This vector was named as *sgAvrlm5_pKHT332*. Then, the vector was transferred into Stellar Competent cells (Takara Bio, Cat. No. 636766) using heat-shock transformation at 42 °C according to manufacture instructions. Successfully transformed colonies were collected by culturing on LB agar supplemented with 50 µg/mL of kanamycin.

Later, colony PCR was performed with Lmp70_F1 and Lmp70_R2 primers to validate the presence of CRISPR vectors on selected colonies (Table 4.4). Further, the PCR products were sequenced and those with100% accuracy were selected.

Table 4.4 Primers used for vector designing and identifying *Avrlm5* gene

Primer	Sequence (5'to3')	Length (bp)
Lmp70-F1	GAAATGTTGAATACTCATACGCGTAAGCTCCCTAATTGGCCC	42
Lmp70-R1	GCTCTAAAACCCTTTACGGACATATAACGAGTGGACGAGCTTACT CGTTTCGTCC	55
Lmp70-F2	TCCGTAAAGGGTTTTAGAGCTAGAAATAGC	30
Lmp70-R2	CTCAGCGGAAACAGCTATGCGTCCCATTCGCCATGCCG	38
Avrlm5F	GTATGCGCGTCTATCGACAA	20
Avrlm5R	CGCCATATAATAGCCCTCCA	20

4.3.2.4 *Agrobacterium*-mediated transformation

The vector plasmid was extracted using NucleoSpin Plasmid DNA extraction kit (Macherey-Nagel GmbH & Co.) and electroporated into AGL-1 *Agrobacterium* electrocompetent cells (GOLDBIO technology, USA, Cat. No CC-208-TR) according to the protocol of the manufacturer. Successfully transformed *Agrobacterium* colonies were collected by culturing LB agar supplemented with 30 µg/mL of carbenicillin and 50 µg/mL of kanamycin. The vector transformation into the *D3 L. maculans* isolate was carried out using the protocol reported by Gardiner & Howlett (2004). First, the *D3* isolate was cultured in V8 agar at 22 °C under fluorescent lights for at least five days to induce sporulation. Next, a liquid LB culture (7.5 mL in a 50 mL tube) was inoculated with a single transformed *Agrobacterium* colony and cultured at a 28 °C using a shaker incubator. After culturing overnight, the colony concentration (measured OD at 660 nm) was adjusted by diluting in sterile induction media (IM: MM salts; KH_2PO, K.HPO, NaCl, $MgSO_4.7H_2O$, $FeSO_4.7H_2O$, $(NH)_2SO$, 0.5% glycerol, 500 µM glucose) and 10 µM acetosyringone (AS; at 200 µM final concentration) to obtain OD 660nm-0.15 in 20 mL (17-18 mL IM, 200 µM glucose, 400 µM AS, 800 µM MES, plus around 1 mL overnight culture). The IM culture was incubated in 250 mL conical flasks in a 28 °C orbital shaker for about 6 hours or until OD at 660 nm is close to 0.6.

For transformation, *L. maculans* spores were prepared by adding 7 mL of sterile distilled water to 7-day old culture to loosen the spores. The spore suspension was filtered through a sterile mira cloth with a clean funnel. The number of spores in the solution was adjusted to at least $1x10^7$ spores/mL by diluting and counting the spores with a hemocytometer. The *Agrobacterium* and *L. maculans* were co-cultured by mixing 4.5 mL of log-phase *Agrobacterium* cells with 2.25 mL of spores of *L. maculans*, then concentrating the mixture to 900 µl with centrifugation at 8 000 rpm for 5min. 400 uL of the mixture was plated into 15 cm Petri-dishes containing 25 mL of IM agar +AS. Co-cultures were incubated at 22 °C for 48 hours in the dark. After 48 hours, plates were overlaid with 25 mL of 10% V8 agar (10% V8 juice and 2% agar, 100 µg/mL hygromycin and 400 µg/mL cefotaxime). The plates were sealed again and allowed to grow in a growth cabinet at 22 °C under fluorescent light. *L. maculans* colonies were observed after 10 days. Next, colonies were sub-cultured onto new V8 with the same antibiotics for another round of selection. All isolates were screened with antibiotics (100 µg/mL hygromycin) at least twice before storing isolate on filter paper discs.

4.3.2.5 Detection of CRISPR/Cas9 efficiency and pathogenicity of transformed isolates

Candidate *D3* mutant colonies (*D3M*) were subjected to DNA extraction with the CTAB method described in section 2.1. The PCR was performed for each isolate with reaction mixture (50 µL) containing 10-50 ng genomic DNA, 25 pmol of *AvrLm5F* and *AvrLm5R* primers (Table 4) and 2 X Froggabio Master mix (FroggaBio Scientific Solutions, cat.no. FBTAQM). PCR was performed using a Takara thermocycler with a program of initial denaturation at 95 °C for 3 min, 30 cycles of 95 °C for 30 s, 50 °C for 30 sec and 72 °C for 1 min, finally at 72 °C for 5 min for the extension. PCR fragments were sequenced to see any deletions or insertion at the CRISPR/Cas9 edited site (Research Institute of Oncology and Hematology DNA sequencing, University of Manitoba). The forward and reverse sequences were aligned with the control (wild-*D3*) and *AvrLm5* sequence available at NCBI using multiple sequence alignment in DNASTAR Lasergene software (MegAlign Pro, Clustal W).

All isolates were grown in V8 media, which was supplemented with hygromycin. The growth rate of each isolate was noted by measuring culture diameter after seven days. Each plate was scraped to get a pycnidia solution after adding 1.5 mL of sterile water. Then, each isolate was screened for

their phenotype on Westar by cotyledon inoculation assay to compare their pathogenicity. Isolates with reduced pathogenicity on Westar were selected for further testing. The lesions on canola cotyledon were cut and cultured on V8 media with hygromycin (100 µg/mL). After five days, single pycnidia were picked and re-cultured on new plates to obtain single spore cultures. The reproducibility of pathogenicity reduction was detected by conducting the canola cotyledon inoculation assay with the above isolates. The morphology of hyphae was compared by preparing slide cultures from each isolate. The slide cultures were prepared by inoculating a slab of V8 on the microscopic slide. After inoculation, a coverslip was placed on the V8 slab and sealed in a Petri-dish. Microscopic photographs of the fine hyphae grown on the coverslip were taken 5 days and 11 days post-inoculation after staining with lactophenol blue.

4.4 Results

4.4.1 Mating between two compatible isolates

Sexual reproduction only occurs between isolates with compatible mating types. Thus, the mating types of selected isolates were checked before crossing. Further, the growth rates of selected isolates were evaluated by measuring culture diameter, and isolates were grouped according to their vegetative growth per week (Table 4.5). The mating was performed only within similar growth rate groups to prevent the early maturation of one parent.

D13 x DM78, DM85 x DS103, S7 x 30_3, D3 x D13, DM77 x 3_1, and DM77 x 43_1 pairs were selected for mating. Seven weeks after mating, the pseudothecia were observed at the intersection of two agar plugs (Figure 4.1A). Pseudothecia were larger, round and darker in colour than pycnidia. Pseudothecia were harvested under a dissecting microscope using a sterile needle. Each pseudothecium was separately crushed on 2% water agar media with a drop of β-glucuronidase (Figure 4.1B). Crushed pseudothecia were detected under a light microscope to verify the presence of ascospores (Figure 4.2).

Table 4.5 Grouping selected blackleg isolates according to their mean growth per week on V8 and mating type

Isolate ID	Mating type	Average growth per week (Mean diameter-cm)
DM85	1	5.0 cm - 6.0 cm
30_3	1	
DS103	2	
S7	2	
DM79	2	
DM78	1	4.5cm - 5.0 cm
8_1	1	
D13	2	
3_1	1	4.0cm - 4.5cm
41_2	1	
DM81	1	
43_1	1	
D8	2	
DM77	2	
D3	1	3.5cm - 4.0cm
1_1	1	
5_2	2	
DM96	2	

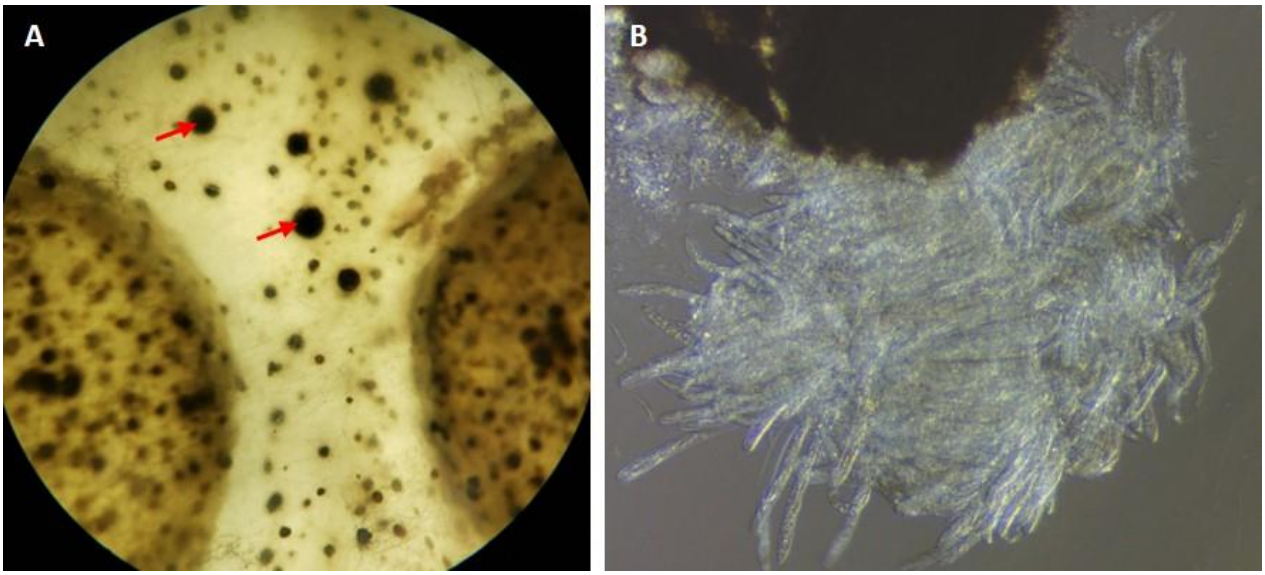

Figure 4.1 Results of mating between two compatible blackleg isolates A: Pseudothecia (shown in red arrows) produced between the agar plugs of parent isolates (D13 × DM78). Pseudothecia are larger, dark in colour and globular than the asexual spore-bearing structures or pycnidia (×10 magnification). B: A crushed pseudothecia (×400 magnification).

The germinated ascospores were harvested by extracting a single hyphal tip. Each mating combination resulted in a varied number of pseudothecia. A smaller number of pseudothecia production was observed in crosses between parents with a high average growth rate per week (Table 4.6). For example, both parents in the DM85 x DS103 cross had an average growth hyphae rate of 5.0 - 6.0 cm per week on V8 media, and the cross between them showed one to zero production of pseudothecia. Similarly, crosses between S7 and 30_3 isolates with the highest mean growth rate per week resulted in four pseudothecia.

On the other hand, the mating of isolate DM77 to either 3_1 or 43_1 produced the highest number of F_1 pseudothecia (20 and 25, respectively). Parents of these two crosses had moderate growth rates per week (4.0 - 4.5 cm per week). The mating pairs usually showed a negative correlation between growth rate and the number of harvested pseudothecia (Table 4.6).

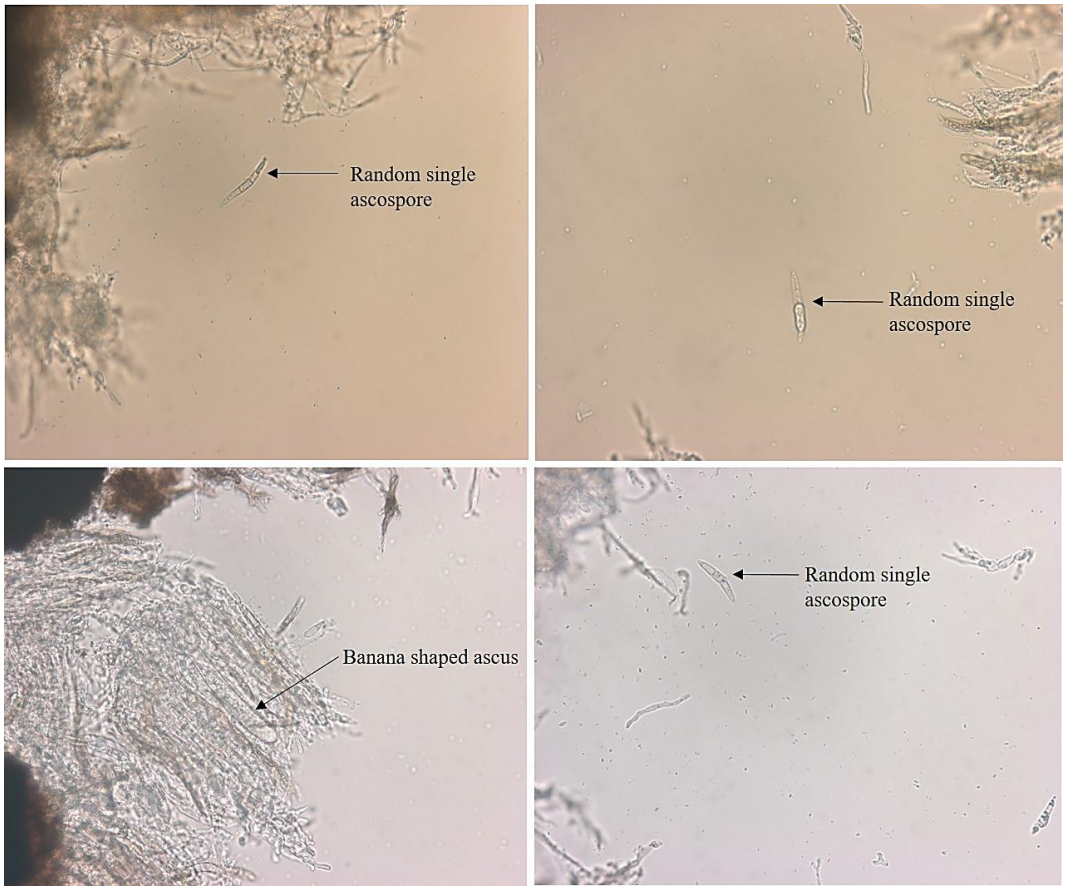

Figure 4.2 Visualizing ascospores and asci produced by crosses between blackleg isolates under the light microscope (×400 magnification).

The isolates obtained from germinating pseudothecia were genotyped by PCR. The genotypes of progeny isolates were compared with genotypes of their parent isolates by visualizing PCR bands. For example, Figure 4.3 shows the results of D13 x DM78. The gene combinations found in the progeny of other crosses are summarized in Table 4.6. The presence of *AvrLepR1*, *AvrLmS* were confirmed by cotyledon inoculation assay at greenhouse using canola cultivar 1065 (*LepR1*) and Surpass 400 (*RlmS*/*LepR2*). The results showed that progeny and parent isolates contained the same *Avr* gene profiles.

Table 4.6 Number of pseudothecia and their *Avr* gene combinations resulted from crosses between selected blackleg isolates

Cross	Number of pseudothecia	*Avr* gene combination
D13 x DM78	10	*AvrLm4,6,7* and *AvrLm1,4,6,7*
DM85 x DS103	1	*AvrLm2,6,7, AvrLmS* and *AvrLm5,6,7*
S7 x 30_3	4	*AvrLm1,7, LepR1*, *AvrLmS* and *AvrLm2,4,6,7*
D3 x D13	5	*AvrLm5, LepR1* and *AvrLm4,6,7*
DM77 x 3_1	20	*AvrLm2,6,7* and *AvrLm1,4,6,7*
DM77 x 43_1	25	*AvrLm2,6,7* and *AvrLm2,4,6,7, S*

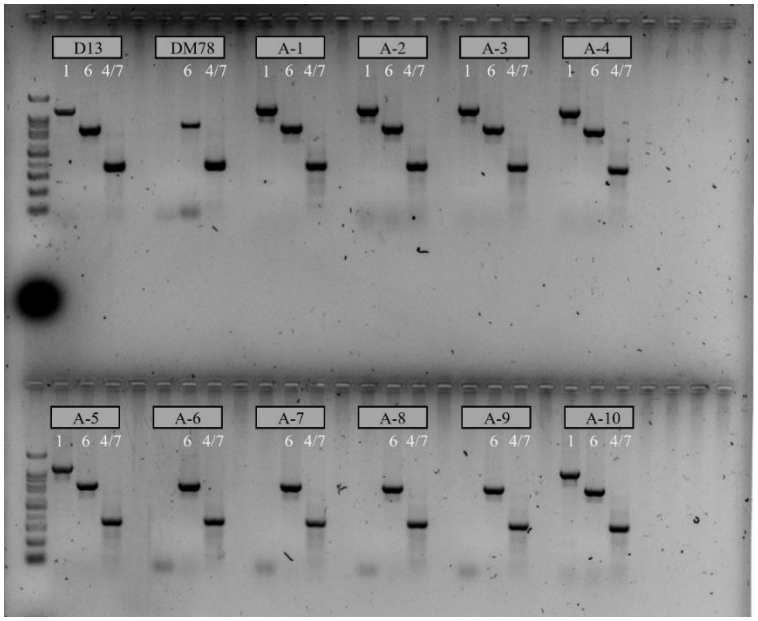

Figure 4.3 Image of agarose gel electrophoresis of genotyping results of the cross between *L. maculans* isolates D13 and DM78. D13 contained *AvrLm1*, *6* and *4/7*, while DM78 contained *AvrLm6* and *4/7*. The progeny isolates obtained from the cross between the above two blackleg isolates resulted in the same *Avr* gene combinations.

4.4.2 CRISPR/Cas9 mediated gene editing to create an *L. maculans* isolate with *AvrLepR1*

4.4.2.1 Genotype confirmation for *D3* isolate

The genotyping and phenotyping test confirmed that the *D3* isolate does not contain any known *Avr* gene other than *AvrLm5* and *AvrLepR1*. PCR assays were conducted to identify *Avr* genes of *AvrLm1*, *2*, *3*, *4-7*, *5*, *6*, *5-9* and *10*. Results confirmed that PCR for *AvrLm5* produced a positive amplification. The *AvrLepR1* was not tested with PCR because of the lack of specific PCR primers. Further, a cotyledon inoculation assay was conducted on differential lines carrying resistant genes *Rlm1*, *2*, *3*, *4*, *6*, *7*, *9*, and *LepR1*, *R2*, *R3* to identify the avirulent genes in the *D3* isolate. Results confirmed that the *D3* isolate contained *AvrLepR1* as it showed a compatible reaction (no disease) when inoculated on cultivar 1065, which carries the resistant gene for *LepR1*. All other lines had an average disease rating of 7 to 9, which means a susceptible reaction and lack of the corresponding compatible *Avr* gene (Figure 4.4).

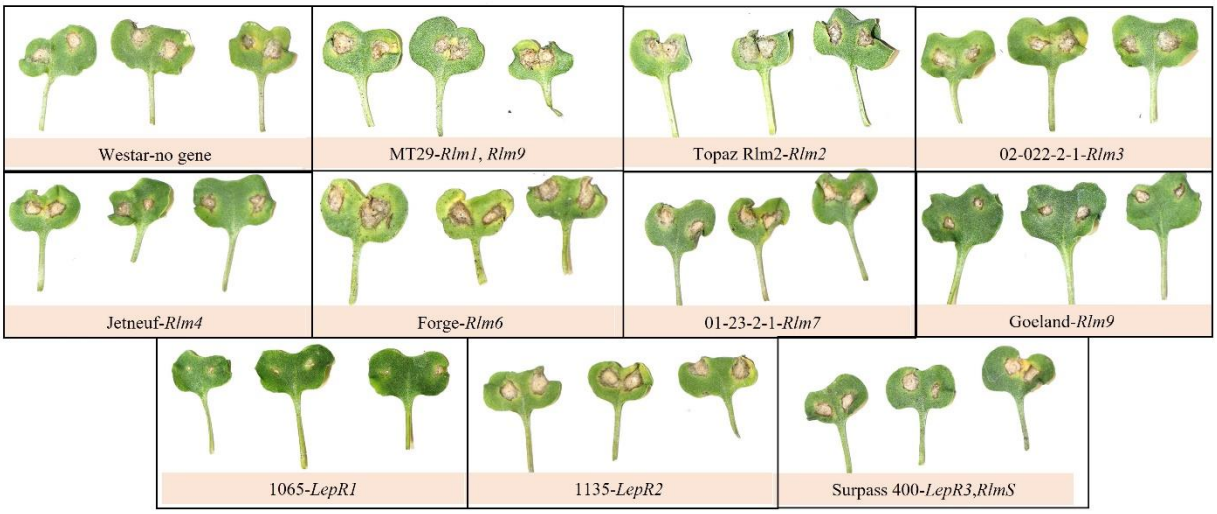

Figure 4.4 The canola cotyledon inoculation test was conducted to confirm the phenotype of the blackleg isolate, *D3*. The resistance in the variety 1065 showed that *D3* contained the *AvrLepR1* gene. In addition, the *AvrLm5* gene was confirmed by genotyping.

4.4.2.2 Generating mutant isolates using CRISPR/Cas9

The selected sgRNA had a 22 bp sequence (CATTCGTATATGCCGTAAAAGG), which binds the *D3* genome at the 192nd base position of the *AvrLm5* gene. The BLASTn results showed that selected sgRNA did not have any off-target in the *L. maculans* genome. The primers Lmp70-F1, Lmp70-R1, Lmp70-F2 and Lmp70-R2 were used to amplify the *pFC334* plasmid to incorporate *gpdA* promoter and *trpC* terminator from the *pFC334* plasmid with sgRNA sequence. In-Fusion cloning obtained two PCR fragments containing the *gpdA* sequence in fragment 1 and sgRNA, *trpC* in fragment 2. The results of In-Fusion cloning PCR were confirmed by running electrophoresis on an agarose gel to confirm the presence of two bands. The result indicated successful amplification of two fragments (Figure 4.5). The gel purification was carried out to take out two fragments before ligation. The two fragments were ligated with *pKHT332* plasmid, which was linearized by digesting at *pstI* site (Figure 4.6).

The resulting vector named *sgAvrlm5_pKHT332* was transferred into Stellar Competent cells. Successfully transformed colonies contained kanamycin resistance (Figure 4.9A). Next, colony PCR validated the presence of *sgAvrlm5_pKHT332* vectors in selected colonies (Figure 4.7). The plasmid DNA was extracted to confirm the presence of two fragments in Stellar cell colonies by PCR followed by sequencing. Further, the sequenced PCR products were a 100% sequence identity match to the sgRNA, *gpdA* promoter and *trpC* terminator sequences from the *pFC334* plasmid.

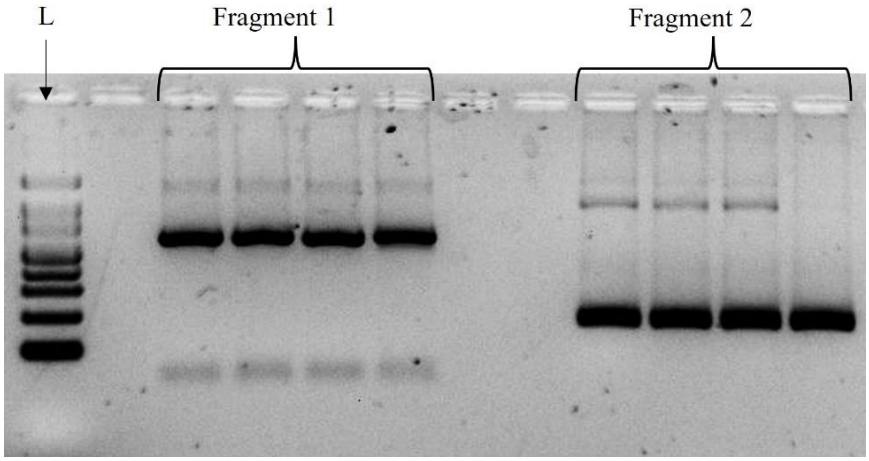

Figure 4.5 Gel image of fragment 1 and 2 produced by In-Fusion cloning. Two bands were separately purified by Nucleospin PCR and the gel clean-up kit (Takara Bio, Cat. No. 740609.250) and combined to linearized *pKHT332* to create CRISPR/Cas9 vector for *D3*.

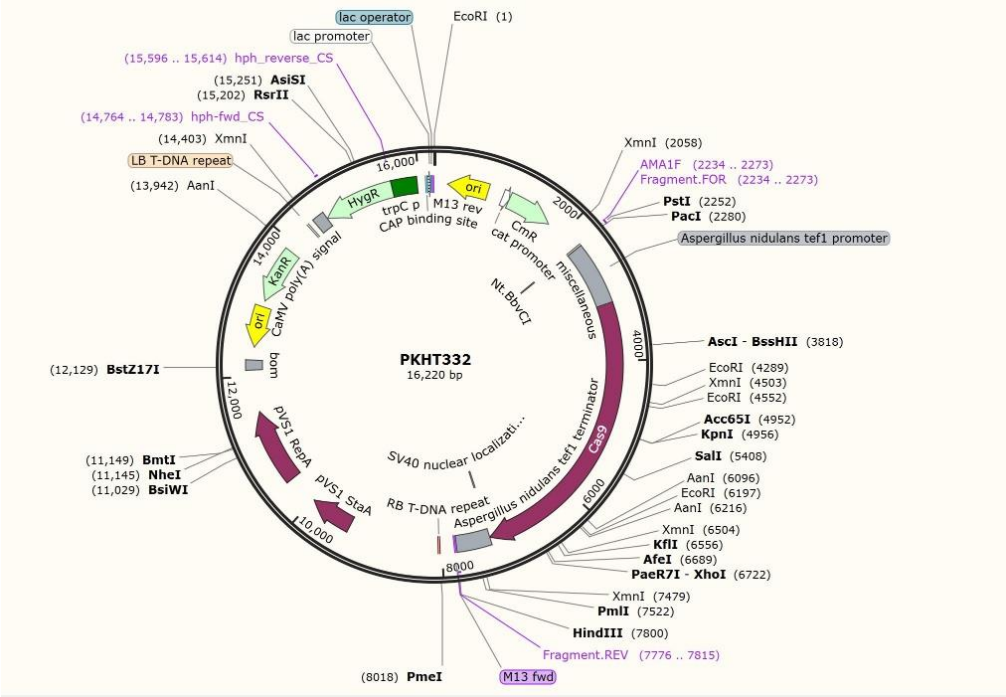

Figure 4.6 Image of *PKHT332* plasmid, which was used to transform the CRISPR/Cas9 system into blackleg isolate, *D3*. The sgRNA targeted to bind *Avrlm5* was inserted at the *PstI* site by restriction digestion and In-Fusion cloning.

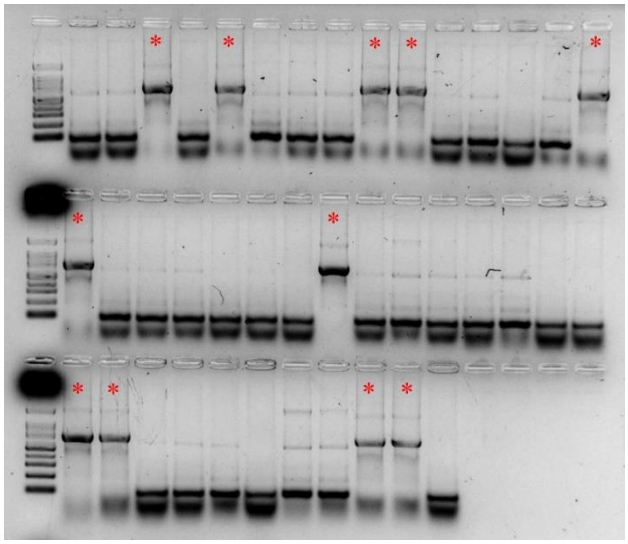

Figure 4.7 Gel image of colony PCR performed with Lmp70_F1 and Lmp70_R2 primers to validate the presence of CRISPR vectors on selected colonies. Red stars indicate the positive amplification from successfully transformed colonies. The identity of the PCR products was confirmed by sequencing.

The *sgAvrlm5_pKHT332* vector was transformed into *D3* via *Agrobacterium* mediated transformation. The successfully transformed isolates were resistant to hygromycin (Figure 4.9B). In addition, a primer pair was designed to target the *AvrLm5* gene to determine any gene editing at the sgRNA binding site (

Figure **4.8**).

```
PRIMER PICKING RESULTS FOR AvrLm5I

No mispriming library specified
Using 1-based sequence positions
OLIGO            start  len      tm     gc%   any   3'  seq
LEFT PRIMER        130   20   59.86   50.00  6.00  2.00 gtatgcgcgtctatcgacaa
RIGHT PRIMER       293   20   59.91   50.00  5.00  0.00 cgccatataatagccctcca
SEQUENCE SIZE: 426
INCLUDED REGION SIZE: 426

PRODUCT SIZE: 164, PAIR ANY COMPL: 5.00, PAIR 3' COMPL: 0.00
TARGETS (start, len)*: 192,23

    1 atgctctatttcctaatctacttaaaactccttctcttcaccatctgtgcacttgcacac


   61 gactgccatcaggtcaccgtttctcgagacgttacactacagaacaaagaacggcacgac


  121 tgcaaccaagtatgcgcgtctatcgacaaagaaaccgaaaacaaactcaacacggacatt
              >>>>>>>>>>>>>>>>>>>>

  181 ataccacgtctcactcgttatatgtccgtaaagggcaattctataatcgcacgagtacaa
                **********************

  241 caaagcaattccgatcctaagtgcagctgcacttggagggctattatatggcgggtgtat
                                      <<<<<<<<<<<<<<<<<<<<

  301 aaggcatacgatgaaaactccctcaacgtcgctctacacgtttcacaccctaaccaacag


  361 ataggggaaaacccggattggagcttagttatctctaatcctaatgttcattgtctaaag


  421 cattag


KEYS (in order of precedence):
****** target
>>>>>> left primer
<<<<<< right primer
```

Figure 4.8 Image of Primer 3 output for the selected primer pair to amply the *AvrLm5* gene in *D3*. The primer pair will specifically amplify the fragment of the *AvrLm5* gene, including the sgRNA binding site (sgRNA binding site is underlined with *** in the figure).

A total of 141 transformed isolates (named *D3M*) were selected from the *Agrobacterium* transformations. Each isolate was sub-cultured two times with single spores for each time to purify isolates and verify their antibiotic resistance (Figure 4.9C). The diameter of single spore cultures was measured after seven days to compare growth rates among isolates (Figure 4.10). Most *D3M* isolates showed a reduced growth rate than wild-type *D3*. Nevertheless, a few isolates showed greater growth rate than the wild-type.

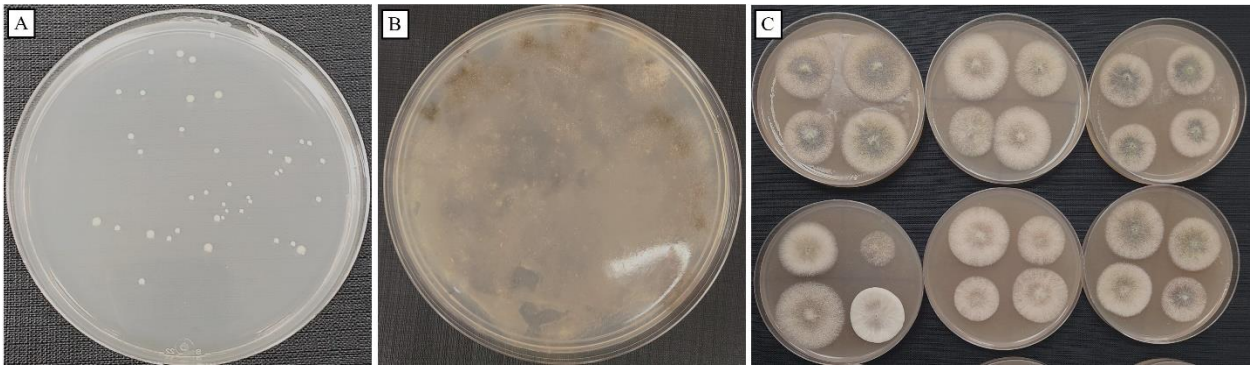

Figure 4.9 Images of A: screening of Stellar cell colonies which may contain the CRISPR/Cas9 plasmid based on kanamycin resistance, B: co-culturing plate of *Agrobacterium* carrying CRISPR/Cas9 vector with blackleg isolate *D3*. The black fungal growth was observed 10 days after overlaying the V8 with hygromycin. C: Plated hygromycin resistance transformed blackleg isolates (*D3M*).

Westar cotyledons were inoculated with pycnidiospore suspensions for each *D3M* isolate to rate their lesion size. Results showed that the 81 *D3M* isolates showed the same phenotype (susceptible reaction) as the wild-type *D3*. Others showed relatively lower pathogenicity on Westar. Seven isolates from 141 *D3M* showed reduced pathogenicity as a resistant reaction was observed on susceptible Westar (Figure 4.11). Figure 4.12 summarizes the results in the cotyledon inoculation assay of a few isolates. Specifically, Westar showed a resistant response to both *D3M111* and *D3M112*.

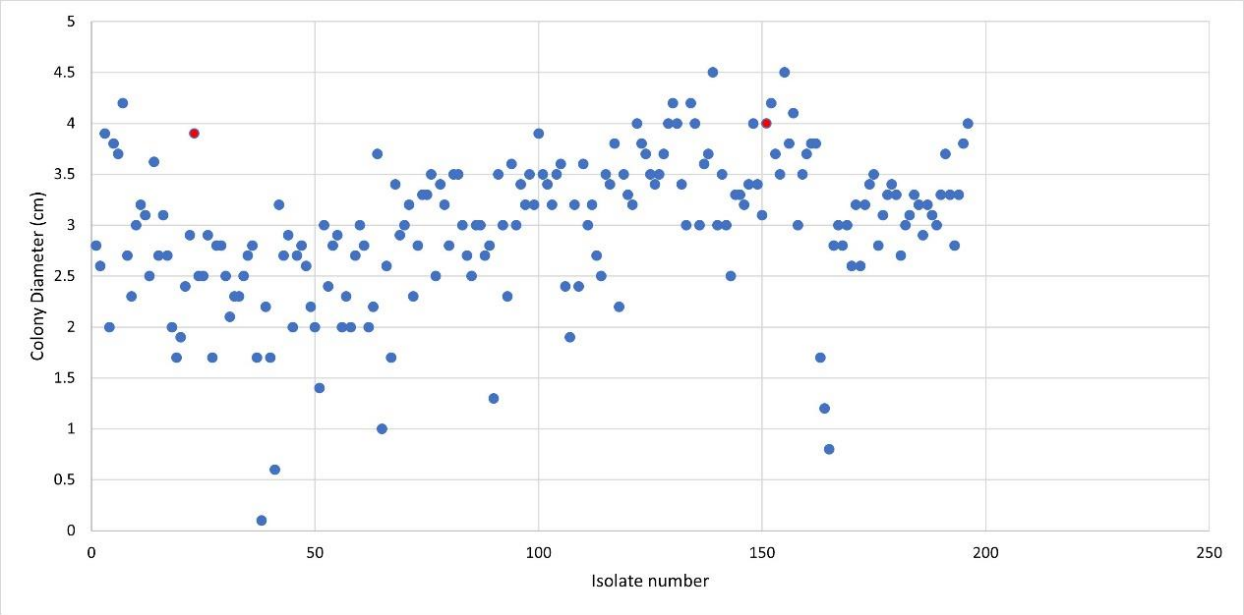

Figure 4.10 Scatter plot of colony diameters of transformed blackleg isolates (*D3M*). The diameter was measured from seven days single spore *D3M* isolates. The red colour dots showed the wild-type *D3*, and blue dots represent *D3M* isolates.

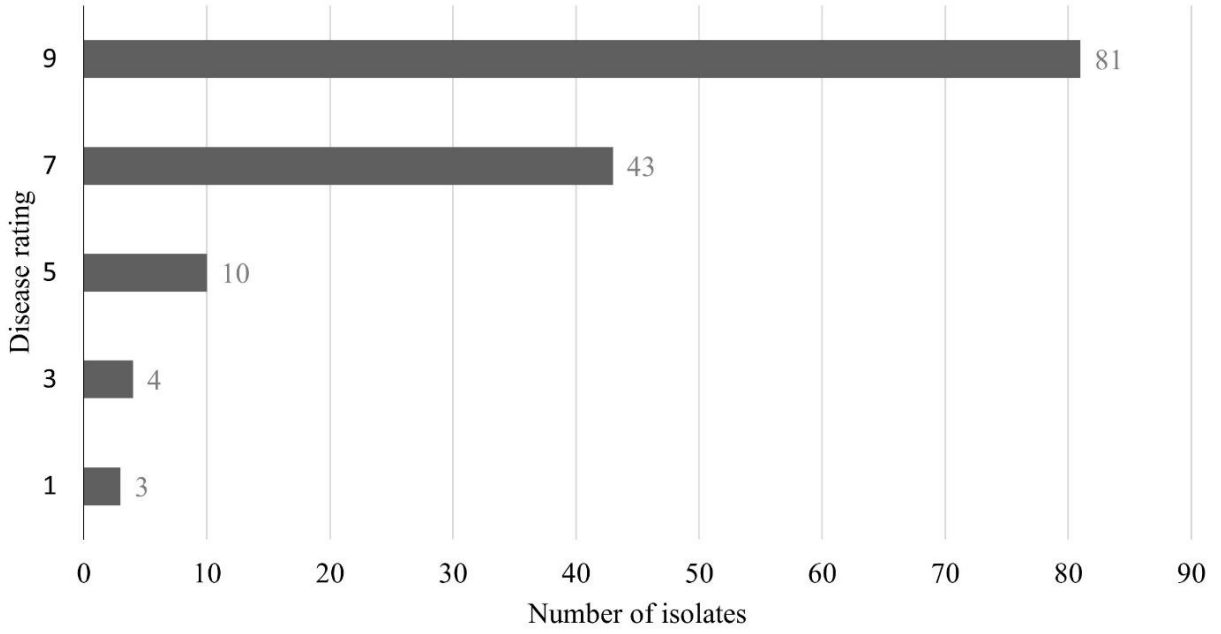

Figure 4.11 Disease rating of canola cotyledon inoculation assay with the blackleg pathogen (*D3M* mutant isolates) recovered from *Agrobacterium* transformation of *sgAvrlm5_pKHT332* vector.

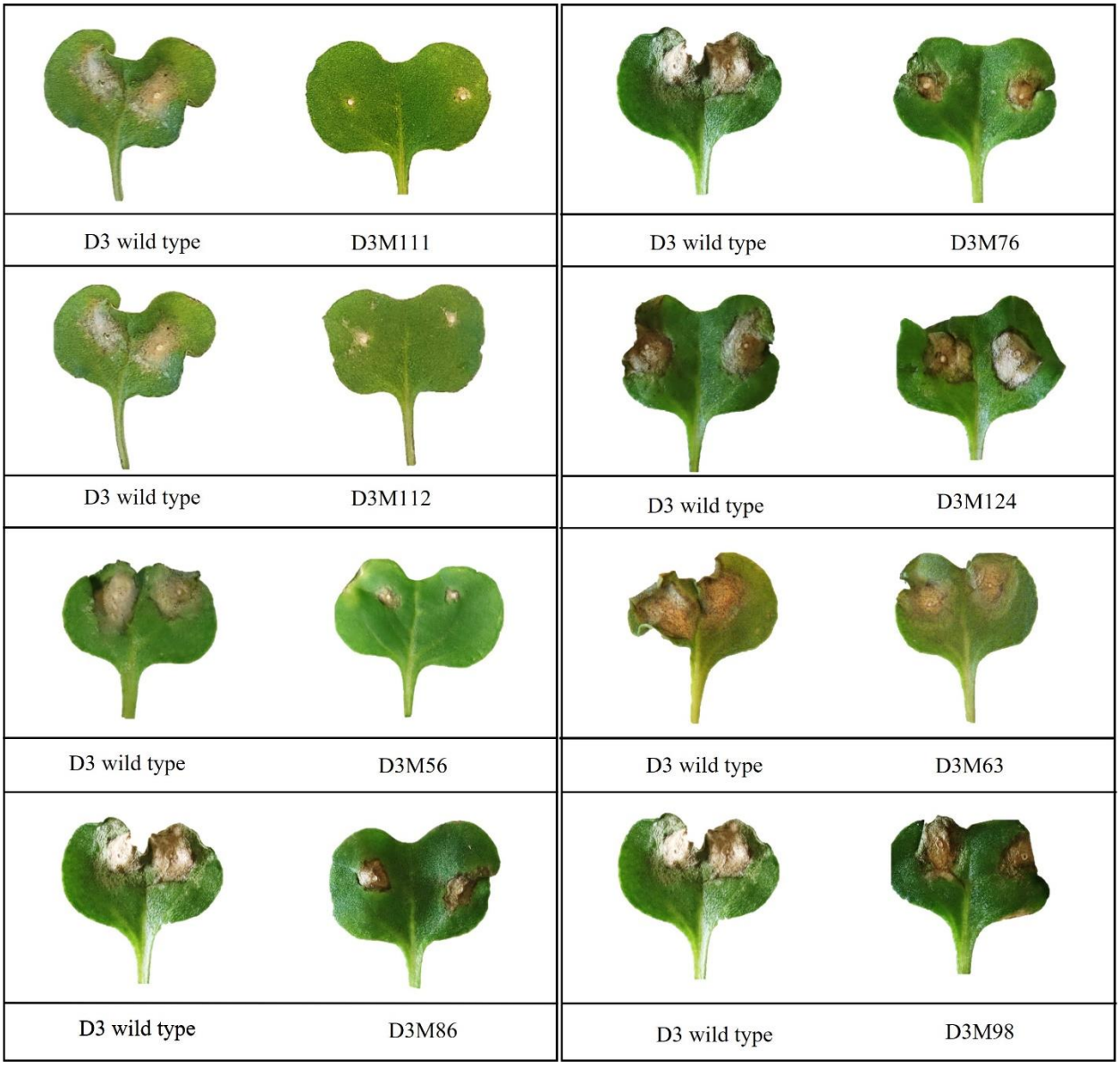

Figure 4.12 Images of canola cotyledon inoculation assay with the blackleg pathogen on Westar (11 days post-inoculation). The lesion size caused by inoculating *D3M* isolates was compared with the lesions caused by inoculating *D3* wild-type.

All the *D3M* isolates were subjected to DNA extraction followed by PCR with previously designed *AvrLm5* primers (Figure 4.8). The PCR products were confirmed by gel electrophoresis (Figure 4.13). Finally, the purified PCR products were sequenced and aligned with DNA STAR software with multiple alignment procedures. However, none of the *D3M* isolates showed any genetic variation within CRISPR/Cas9 target area.

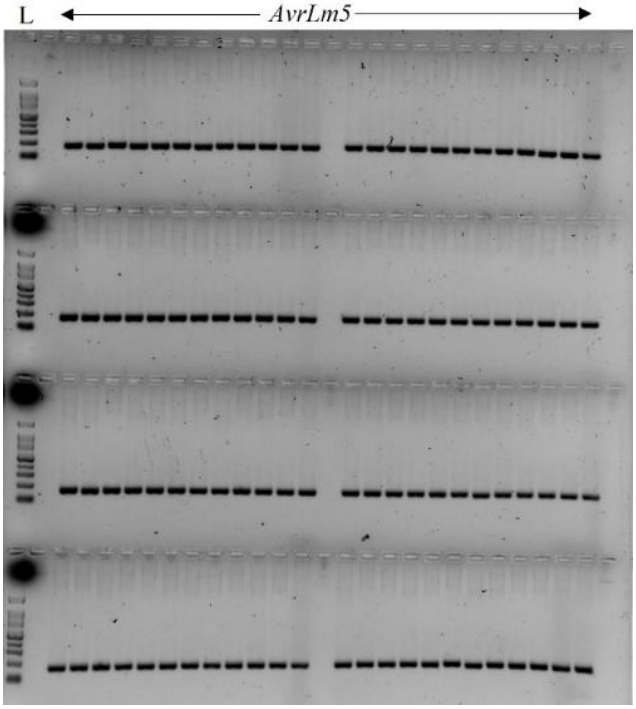

Figure 4.13 Gel image of PCR conducted for plasmid DNA extracts from transformants with *AvrLm5* primers. The PCR products were purified and sequenced to detect mutations at the CRISPR/Cas9 editing site

4.4.2.3 Comparing differences in pathogenicity and morphology of CRISPR/Cas9 transformants

The phenotypes of isolates *D3M111* and *D3M112* were further studied to confirm their reduced ability to cause disease on Westar. Figure 4.14 showed that after 11- and 14-days post-inoculation (dpi), the cotyledons remained healthy, and a compatible reaction occurred near the infection site resulting in necrosis. Thus, both *D3M111* and *D3M112* isolates lost their ability to cause disease when compared to the wild-type *D3* isolate.

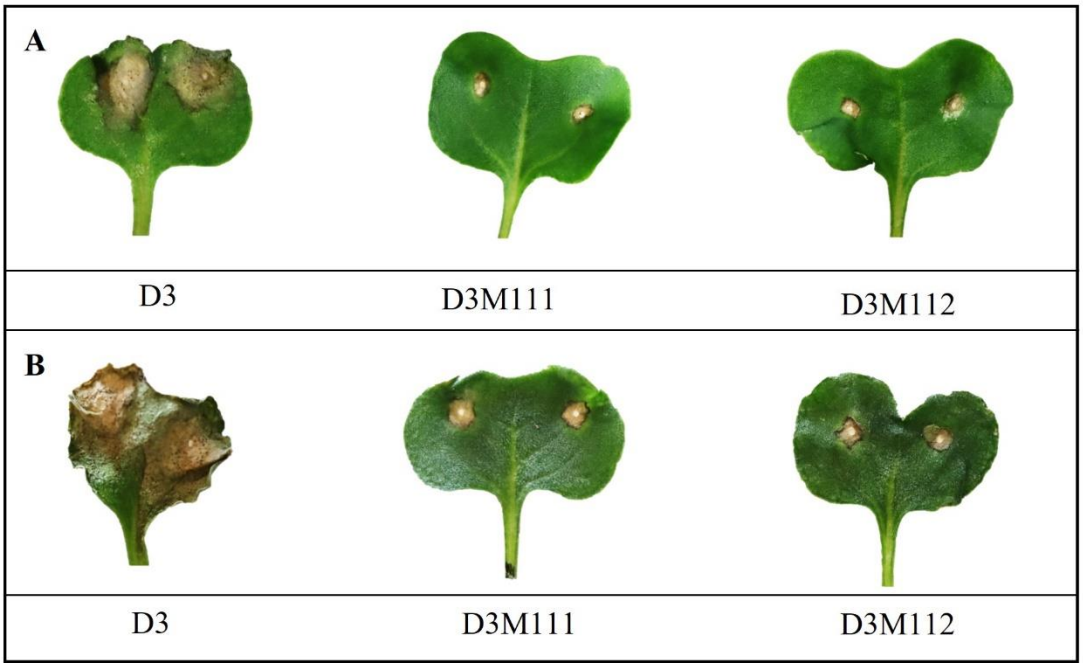

Figure 4.14 Images of canola cotyledon inoculation assays of transformed blackleg isolates, *D3M111* and *D3M112* to confirm their pathogenicity loss on Westar. A: Results of 11 days post-inoculation, B: results after 14 days post-inoculation. The wild-type blackleg isolate *D3* caused a susceptible reaction (disease rating score 9), and mutants caused a resistant response (disease rating score 1 to 3).

The lesions caused by *D3M86* (an intermediately resistant isolate to Westar), *D3M111* and *D3M112* were cultured on V8 to generate *D3M86_L*, *D3M111_L* and *D3M112_L* isolates. They were re-inoculated on Westar to rate the disease. Westar showed moderate resistance to *D3M86*. The isolates from lesions showed the same results as the transformed isolates. However, *D3111_L* and *D3112_L* isolates showed slightly larger lesions than the *D3M111* and *D3M112* (Figure 4.15).

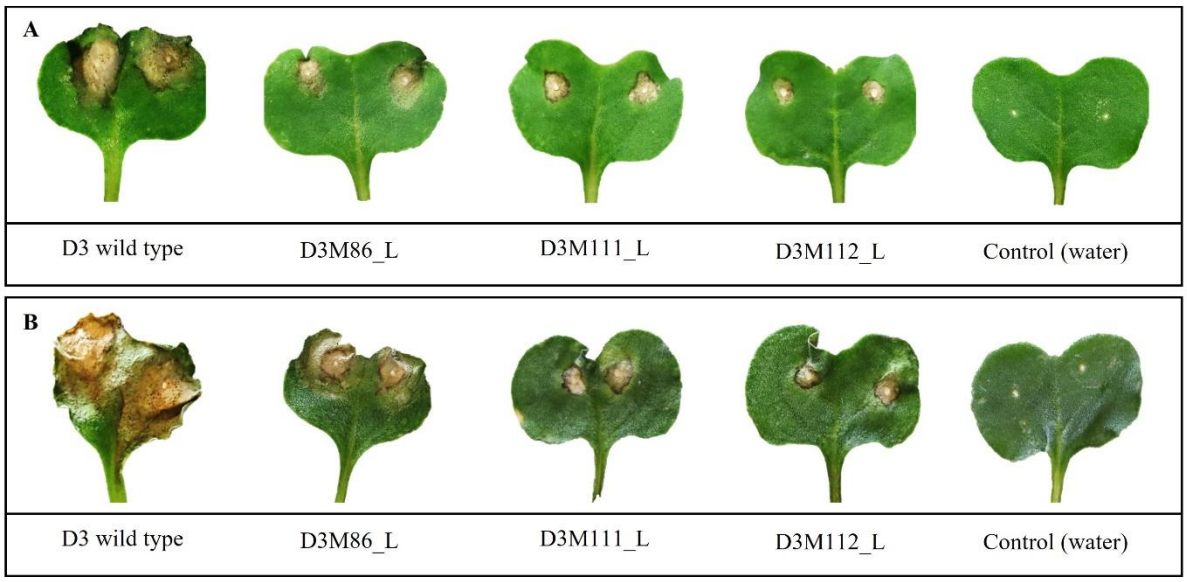

Figure 4.15 Comparison between lesion sizes on canola cotyledons (Westar) caused by inoculating wild-type blackleg isolate *D3* and transformed blackleg isolates recovered from lesions (*D3M_L*) of the previous inoculation on Westar. A: results after 11 days post-inoculation on Westar, B: results after 14 days post-inoculation.

Slide cultures were prepared from *D3M86_L*, *D3M111_L* and *D3M112_L* to compare the hyphae and spores of each isolate. Microscope images showed that the *D3* wild-type isolate and *D3M86_L* produced well-branched and dense mycelia, while *D3M111_L* and *D3M112_L* showed relatively less branches and a low mycelia coverage. However, the number of spores produced by *D3M111_L* and *D3M112_L* was higher than wild-type (Figure 4.16). The same results were observed in 11-day old cultures (Figure 4.17).

Cotyledon inoculation on *B. juncea* showed a resistance reaction of *B. juncea* to all isolates, including *D3* wild-type, *D3M86_L*, *D3M111_L* and *D3M112_L* (Figure 4.18). Thus, any isolates did not overcome the resistant genes in *B. juncea* (cultivar-Arid). Thus, the new isolates would not carry new genes that are different than D3.

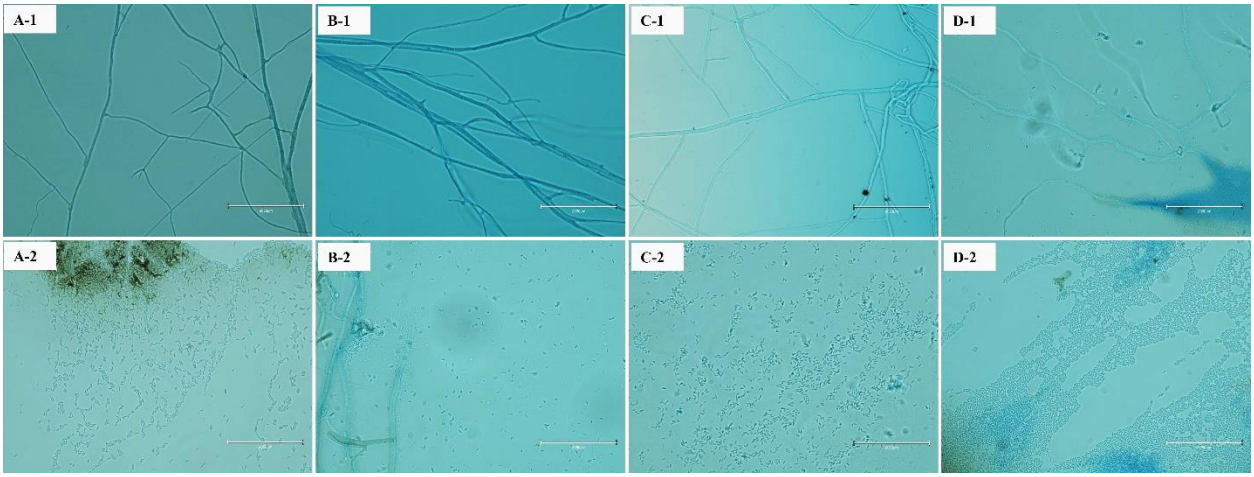

Figure 4.16 Microscopic images of hyphae (1) and spores (2) of blackleg isolates A: wild-type *D3*, B: *D3M86_L*, C: *D3M111_L* and D: *D2M112_L* after 5 days on V8 media and stained with lactophenol (magnification ×100 and scale bar illustrate 2050 µm).

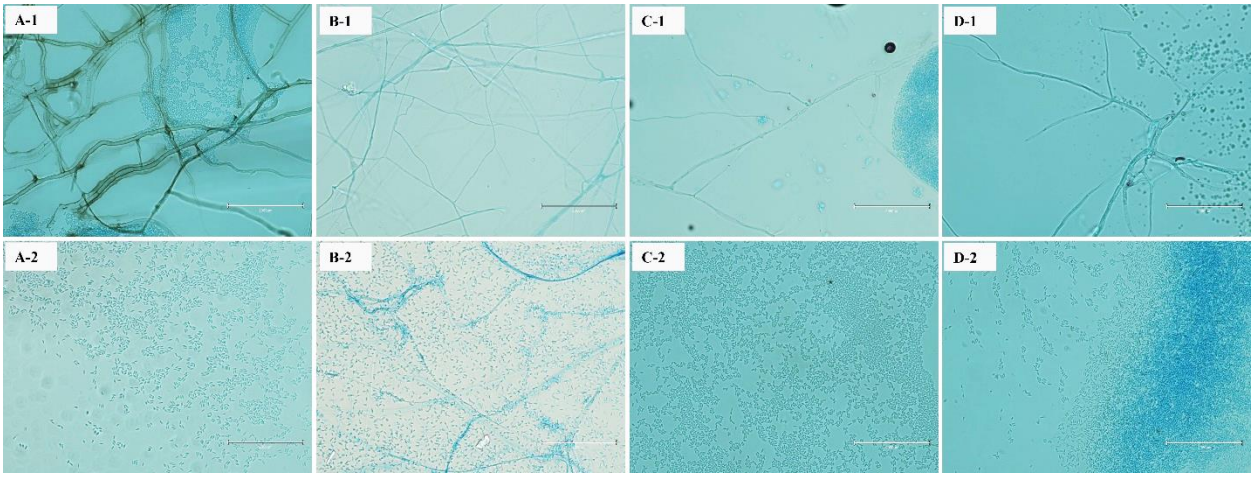

Figure 4.17 Microscopic images of hyphae (1) and spores (2) of blackleg isolates A: wild-type *D3*, B: *D3M86_L*, C: *D3M111_L* and D: *D2M112_L* after 11 days on V8 media and stained with lactophenol (magnification ×100 and scale bar illustrate 2050 µm).

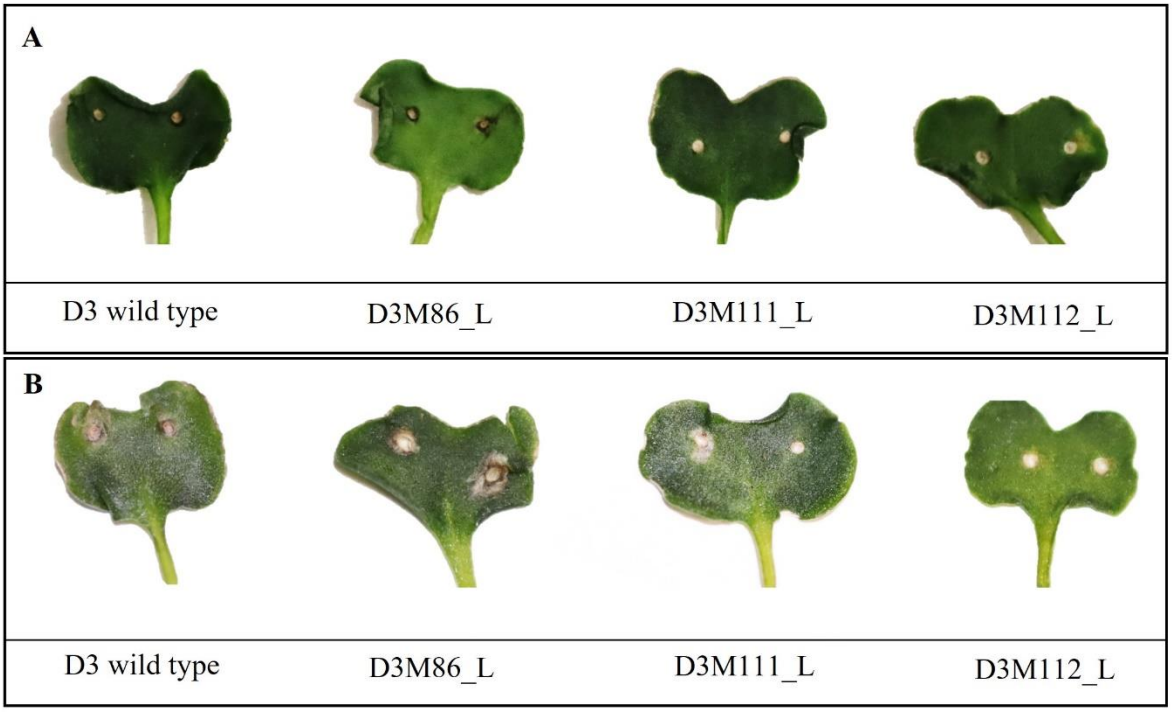

Figure 4.18 Images of canola cotyledon inoculation assay with wild-type *D3*, *D3M86_L*, *D3M111_L* and D: *D2M112_L* on *B. juncea*. A: Lesions after 11 days post-inoculation. B: Lesions after 14 days post-inoculation.

4.5 Discussion

4.5.1 Mating between two compatible isolates

The blackleg pathogen *L. maculans* is an ascomycete fungus that reproduce sexually and asexually (Zhang & Fernando, 2018). Meiotic segregation associated with sexual reproduction may cause genetic variations in progeny (Balesdent et al., 2013). Thus, mating between two compatible blackleg isolates was performed in a laboratory setting, and the progeny was screened for loss of *Avr* genes. However, results showed that mating between *L. maculans* isolates was less effective in getting isolates carrying a single *Avr* gene due to fewer pseudothecia production.

A single isolate of *L. maculans* usually contains two or more *Avr* genes. For example, Fernando et al., 2018 did a six-year study (2010 to 2015) to determine *Avr* gene profiles of *L. maculans* isolates present in commercial canola fields in Manitoba. Their results described three frequent races of *L. maculans*, and each of them contains *Avr* gene sets of *AvrLm-2-4-5-6-7-11* or *AvrLm-2-4-5-6-7-11-S*, or *Avr-1-4-5-6-7-11*-(*S*). However, for this study, isolates with two or three *Avr* genes were selected to reduce the complexity of possible *Avr* gene combinations and increase the possibility of getting a single *Avr* gene isolate.

Sexual reproduction or mating occurs between heterothallic fungi with opposite mating types (Van de Wouw et al., 2016). The two mating type idiomorphs of *L. maculans* are *MAT1-1* and *MAT1-2*. The *MAT1-1* gene is 1368 bp long and encodes a protein with 441 amino acids while, the *MAT1-2* gene is 1 246 bp long and produces a protein with 397 amino acids (Cozijnsen & Howlett, 2003). Further, the mating type distribution of the *L. maculans* populations reflects the ability of sexual reproduction (Fernando et al., 2018). For example, many studies reported that *L. maculans* populations in western Canada mainly produce pycnidia due to lack of sexual recombination (Dilmaghani et al., 2009; Ghanbarnia et al., 2011; Guo et al., 2005). However, Zou et al. (2018b) observed that the ratio of allele frequency between two mating types in western Canada is 1:1. Furthermore, Zou et al. (2018b) showed that both mating types of isolates were equally abundant, and there was no genetic restriction in the occurrence of sexual reproduction in western Canada (Zou et al., 2018b). Similar studies conducted in Australia and France showed that their *L. maculans* populations are equally abundant in both mating types. In contrast, sexual reproduction

is common in those regions (Barrins et al., 2004; Gout et al., 2006). Thus, Fernando et al. (2018) suggested that environmental conditions significantly affect sexual reproduction in *L. maculans* populations. In addition, the mating between *L. maculans* isolates has been utilized in previous studies for tetrad analysis of selected genes (Gall et al., 1994), repeat-induced point mutations (Van de Wouw et al., 2019), and genetic mapping (Cozijnsen et al., 2000).

In this study, sexual recombination during ascospore production was attempted to get an *L. maculans* isolate with a single *Avr* gene. Pseudothecia are the sexual fruiting bodies of *L. maculans,* producing asci. Each ascus contains eight ascospores produced by meiosis, followed by mitotic division. Thus, the ascospores are haploid. Therefore, cultures generated from ascospores are haploid, and their phenotype is directly influenced by their genotype (Gall et al., 1994). Sexual recombination is an essential factor in the pathogen's life cycle that supports the pathogen to evolve to overcome host resistance (Eckert et al., 2005). However, sexual recombination frequency was low in western Canada compared to *L. maculans* populations in Australia and France, because those environmental and agronomical factors are less favourable to sexual reproduction in Canada. For example, the cold winter climate and short cropping seasons promoted high rates of asexual reproduction in western Canadian populations (Dilmaghani et al., 2012).

Sexual recombination during meiosis may produce a progeny that deviates from their parents. For example, Australian field studies observed chromosomal length polymorphism in progeny populations due to sexual recombination (Leclair et al., 1996; Plummer & Howlett, 1993, 1995). The chromosomal length polymorphism may occur through crossing over during meiosis. These changes in chromosomal length were probably resulting in the gain or loss of non-essential sequences (Plummer & Howlett, 1993). Plummer and Howlett (1995) showed that chromosome length polymorphism might differ at any meiosis event, and it may differ by length up to 450 kbp.

The current study hypothesized that sexual recombination during mating would result in a loss of the *Avr* gene in the progeny population. However, results showed that progeny isolates contained similar *Avr* profiles as their parent isolates. Thus, this method was not able to fulfill the study's objective. The drawback experienced during the experiment was the lower production of pseudothecia in laboratory conditions. In addition, the random nature of recombination and lack

of knowledge about *L. maculans Avr* gene segregation increased the difficulty of achieving the objective. Further, previous studies, including Cozijnsen et al. (2000), showed a high level of repetitive sequences within the *L. maculans* genome generated by length polymorphism during meiosis. However, they did not observe any evidence of translocation in the performed crosses of *L. maculans* (Cozijnsen et al., 2000). Therefore, the probability of gene loss during the sexual recombination was random and rare, making this technique unsuitable for generating target mutations in *Avr* gene profiles of *L. maculans* isolates.

4.5.2 CRISPR/Cas9 mediated gene editing of *AvrLm5* in *L. maculans* isolate *D3*

CRISPR/Cas9 genome editing is a rapid and precise gene editing technique used to create target mutations. It has replaced old gene editing techniques, such as gene editing via homologous recombination, which are inefficient in fungi (Zou et al., 2020). Recently, CRISPR/Cas9 tools were successfully implemented in different aspects of gene editing in *L. maculans*. For example, Darma et al. (2019) and Liu et al. (2020a) used CRISPR/Cas9 gene editing to identify pathogenicity-related genes in *L. maculans*. In addition, Idnurm et al. (2017b) a discovered fungicide a resistant gene in *L. maculans* using CRISPR/Cas9 gene editing techniques. Moreover, Zou et al. (2020) created a virulent mutant isolate of *L. maculans* by knocking down the avirulent gene, *AvrLm7*.

In this study, CRISPR/Cas9 gene editing was used to mutate the *AvrLm5* gene from *L. maculans* isolate *D3*. The CRISPR/Cas9 system includes two main components: a single-stranded guide RNA (sgRNA) and a Cas9 endonuclease. The sgRNA was custom-built for the target nucleotide sequence, guiding the Cas endonuclease to the target site (Jinek et al., 2012). In this study, sgRNA was designed to target the *AvrLm5* gene. The sgRNA expression cassette was developed with In-Fusion cloning techniques, which is an alternative to restriction enzyme and ligase-based cloning procedures (Frandsen et al., 2012). In-Fusion system could connect two overlapping DNA pieces by designing In-Fusion primers to create 15 base pair overlap during PCR. The two primers were designed by incorporating the mutation (additional DNA sequence) and amplifying the gene of interest. The resulting PCR fragments contained the gene of interest with added mutations (Zhu et al., 2007). In this study, the sgRNA was added to a segment of the *pFC334* plasmid using this In-

Fusion cloning technique. This technique provides the advantages of a simple experimental design, compatibility with any DNA sequence and less time-consuming than other cloning techniques (Frandsen et al., 2008; Zhu et al., 2007). Thus, different studies widely use this technique to clone the desired DNA sequence into vectors. For example, Zou et al. (2020) used In-Fusion cloning to create a CRISPR vector for *Agrobacterium* mediated transformation of *L. maculans*. Further, vectors constructed with In-Fusion cloning were used to introduce genes responsible for the biosynthesis of fungal metabolites into the *Aspergillus oryzae* genome (Tagami et al., 2015).

The *D3* isolate was confirmed to carry *AvrLm5* and *AvrLepR1* (Figure 4.4). Hence knocking out the *AvrLm5* gene will create an isolate that only carries *AvrLepR1*. The presence of the *AvrLepR1* gene can only identified by phenotyping via cotyledon inoculation assay due to the unavailability of molecular markers. Thus, an isolate that only carries *AvrLepR1* is advantageous for phenotyping purposes. Similarly, it will help characterize the molecular aspects of the pathogenicity of the *AvrLepR1* gene. However, the results showed that the selected isolates were not mutated at the *AvrLm5* locus. Unfortunately, the developed CRISPR/Cas9 sgRNA system failed to target the *AvrLm5* gene. Failure to create mutations may be due to difficulties that occurred in Cas9 translation, insufficient nuclear transformation or problems in sgRNA expression (Blaise et al., 2007). Further studies are needed to troubleshoot each problem.

Compared to wild-type *D3* isolate, some transformed isolates (*D3M*) showed differences in their growth rates and pathogenicity when inoculated on canola cultivar Westar. Most *D3M* isolates showed a lower growth rate on the V8 medium than their wild-type (Figure 4.10). Further, during inoculation assays, some *D3M* isolates behaved differently from wild-type *D3*. The *D3* isolate was virulent on Westar, causing lesions on the scale of 9 as Westar does not have any known *R* gene. However, only 83 isolates from 141 transformants showed the same pathogenicity as *D3*, while others encountered a moderate resistance on Westar at 11 dpi (Figure 4.11 and Figure 4.12). Among the less pathogenic *D3M* isolates, *D3M111* and *D3M112* showed significantly different phenotypes causing no disease on Westar (Figure 4.14 and Figure 4.15). Further, reduced pathogenicity of *D3111* and *D3112* were reproducible as spores on the lesions (*D3M111_L* and *D3M112_L*) showed similar pathogenicity defects on Westar cotyledons at 11 and 14 dpi (Figure 4.15).

Agrobacterium mediated transformation was used to deliver the *sgAvrlm5_pKHT332* vector to the *D3* isolate. *A. tumefaciens* is a plant pathogenic bacterium that can transfer its phytopathogenic transferred DNA (T-DNA) into the host genome. The T-DNA is located on the *Ti* plasmid (tumour-inducing plasmid), which also contains virulence genes. That virulence DNA was replaced with desired DNA without damaging the T region (genes related to transferring DNA to another cell) to utilize the plasmid carrier of target DNA into the plant and fungal cells (Michielse et al., 2005). *Agrobacterium* mediated transformation is widely used and identified as an accurate gene transformation method in plants and fungi. The study published in 2004 claims the first successful *Agrobacterium* mediated transformation of *L. maculans* to knockout the genes encoding an ATP binding cassette transporter and a two-component histidine kinase gene (Gardiner & Howlett, 2004; Idnurm et al., 2017a). Further, *Agrobacterium* mediated transformation was used to create random mutagenesis in genes to identify their characteristics. For example, Elliott and Howlett (2006) reported insertional mutagenesis occurred by *Agrobacterium* mediated transformation in *L. maculans*. The insertion of T DNA caused overexpression of an alcohol dehydrogenase class 4 (ADH4)-like gene and a 3-ketoacyl-CoA thiolase gene resulting in reduced pathogenicity in the mutant isolate (Elliott & Howlett, 2006).

Blaise et al. (2007) conducted a detailed study with a library of *Agrobacterium*-mediated transformants containing 3 000 *L. maculans* isolates to observe the accuracy, the number of insertions in the genome, and patterns of T-DNA insertion in the host genome. Their results showed that T-DNA mostly integrated as a single copy within the gene-rich regions of the *L. maculans* genome. Further, 3.8% of transformants showed reproducible pathogenicity defects when inoculated on canola cotyledons with different phenotypes (Blaise et al., 2007). These observations help explain the current study results where the transformed isolates showed different phenotypes when inoculated on Westar cotyledons (Figure 4.11 and Figure 4.12). Therefore, the random insertion of T-DNA from *Agrobacterium* may be disturbing a pathogenicity-related genes in D3M111 and D3M112. Further studies will be needed to examine the T DNA insertion sites and identify the interrupted gene.

In addition, CRISPR off-targets effects may cause undesired gene editing anywhere at the genome sequence. Even though the CRISPR system is developed to target a specific location, many studies described non-desired results after editing. The Cas9 protein may be randomly integrated into the host genome, causing unwanted mutations. For example, Kuscu et al. (2014) observed the binding of deactivated Cas9 genome-wide in cultured HEK293T cells. They have utilized chromatin immunoprecipitation and high-throughput ChIP-seq sequencing to map those binding sites (Kuscu et al., 2014; Wang & Coleman, 2019). Further, the overexpression of Cas9 and sgRNA may induce the random integration of Cas9 in the host genome and the non-specific binding of sgRNA. In addition, loss of ability to identify the target site by Cas9/sgRNA complex and mismatches at the binding site may cause off-target effects during gene editing (Song et al., 2019). The methods, including whole-genome sequencing, GUIDE-seq and ChIP-seq, may provide more details of the genotype changes (Blaise et al., 2007; Song et al., 2019; Zou et al., 2020).

Slide culturing and microscopic photographing were used to compare the morphology between wild-type *D3* and the transformants *D3M111_L* and *D3M112_L*. The results showed that the *D3* isolate has higher hyphal growth and more branching than *D3M111_L* and *D3M112_L*. However, *D3M111_L* and *D3M112_L* produced higher conidia than the *D3* isolate (Figures 4.16, 4.17). These morphological differences may cause pathogenicity changes in those isolates. Similar results had been shown by Zou et al. (2020). In their study, a virulent uMavr7 isolate in which the *AvrLm7* gene was knocked out with CRISPR/Cas9 gene editing showed similar morphological changes after transformation, including higher production of conidia (Zou et al., 2020). Further, more experiments are needed to detect the exact cause of the pathogenicity difference.

The cotyledon inoculation on *B. juncea* showed that the wild-type, *D3M86_L*, *D3M111_L*, and *D3M112_L* isolates were avirulent on *B. juncea*. *B. juncea* has greater blackleg resistance than *B. napus* (Elliott et al., 2015; Pang & Halloran, 1996), including cotyledon and adult plant resistance (Van de Wouw et al., 2014a). Further, studies found that *B. juncea* cultivars carried known resistance genes, including *Rlm5*, *Rlm6*, *LMJR2* and unidentified resistant genes (Elliott et al., 2015). Thus, in this study, the *B. juncea* cultivar was used to identify the phenotype of transformed isolates. The results showed that the transformed isolates have the same phenotype as their wild type which is avirulent to *B. juncea*.

In conclusion, mating between two isolates was not suitable for generating an isolate with a single *Avr* gene as the pseudothecia production was limited in some isolates, while single ascospore extraction was complex and laborious. On the other hand, CRISPR/Cas9 gene editing is a promising method for knock-out *Avr* genes, as previous studies successfully conducted it. For example, Zou et., (2020) mutated the *AvrLm7* gene in *L. maculans*. Thus, even though this study was unable to mutate *AvrLm5*, future studies can address the limitations. For example, reconstructing sgRNA with higher binding efficiency or utilizing multiple sgRNAs to target same gene. Potential blackleg pathogenicity-related genes can be identified by studying the isolates with pathogenicity defects from this study. Further, those resistant isolates can be used to identify and study quantitative resistance in canola.

5.0 General discussion

5.1 Species diversity of Fusarium head blight and deoxynivalenol (DON) levels in western Canadian wheat fields

Fusarium head blight is a persistent problem for western Canadian wheat farmers, which causes severe yield losses and mycotoxin contamination. The severity of FHB disease depends on the availability of inoculum and conducive environmental conditions from the flowering to the soft dough stage of the wheat crop. Therefore, farmers have difficulty managing the disease using conventional disease management tools. Integrated disease management combined with FHB forecasting models is the best way of FHB management. Thus, much research aims to find the correlation of disease with environmental factors and generate models to predict FHB severity and DON accumulation with weather parameters such as temperature, rainfall, and relative humidity. Once the model is prepared, it can be validated using previously collected data. Thus, this research collected data from farmers' fields in western Canada during the 2019 and 2020 growing seasons. The data included spore density, mean temperature, relative humidity, mean rainfall between mid-anthesis to soft dough stage, DON level, *Fusarium* species diversity and chemotypes.

Results showed that most fields experienced relatively mild FHB damage in both seasons. However, samples from Manitoba and Saskatchewan fields were more highly contaminated with DON than Alberta. In addition, Manitoba and Saskatchewan fields contained higher mean spore densities during the infection window, proving the correlation between inoculum availability and DON contamination. Further, both provinces received conducive environmental conditions for the pathogen, including temperature (between 15 to 25°C) and high relative humidity (between 80 to 90%). Most of the *Fusarium* species discovered from grain samples were identified as *F. graminearum*. Moreover, 3ADON producing *Fusarium* samples were observed in higher frequency than those producing 15ADON.

Comparing both DON level and *Fusarium* species diversity between spring wheat grain and chaff showed that chaff contained a higher DON accumulation and a higher *Fusarium* species diversity. Thus, results indicate the importance of measuring DON level in chaff before adding it to livestock

feed. Higher DON levels may cause problems in livestock health upon consumption, and toxins may indirectly flow into humans by consuming livestock products such as milk and meat. In addition, farmers must be careful when leaving the chaff on the field as it may act as a source of inoculum during the next growing season. Further, *F. graminearum* abundance observed in spring wheat stalks also supports the above statement. Even though there was no significant difference between the *F. graminearum* abundance in the tested sections of stalks, results clearly showed a higher *F. graminearum* abundance in Manitoba and Saskatchewan samples. In addition, a more toxic NIV chemotype was recorded from one chaff sample from Manitoba fields, indicating the presence of NIV producing *Fusarium* species which was rarely found in past pathogen populations in western Canada.

5.2 Generating *L. maculans* isolates carrying single avirulent (*Avr*) genes

Plant diseases are causing a significant negative impact on the canola industry in Canada. Among diseases, blackleg of canola accounts for a more substantial fraction of annual yield loss. The blackleg disease is caused by the fungal pathogen *L. maculans.* The disease management of blackleg is mainly dependent on the resistant cultivars, *R* gene rotation, and crop rotation. The resistant cultivars contain *R* genes that can recognize the pathogen's *Avr* genes and prevent the disease progression. However, *R* genes can only recognize its compatible *Avr* genes. Thus, *R* genes will not provide a lasting solution for blackleg as the selection pressure created by *R* genes will increase the evolution of novel *L. maculans* isolates with different or mutated *Avr* genes.

Breeding for resistant canola varieties must be accelerated to secure the future of the canola industry. Screening for *R* genes involves phenotyping with a canola cotyledon inoculation assay. Thus, a standard set of pathogen isolates will be needed for rapid and accurate identification. Further, *R* genes are not always correctly named as not all research laboratories use a universal set of well-characterized isolates. The hurdle to overcome is the unavailability of an effective method to create a set of isolates carrying a single *Avr* gene. Therefore, this research targeted the possibility of generating a standard set of *L. maculans* isolates utilizing two techniques, 1) mating between two compatible isolates and 2) site-directed mutagenesis by CRISPR/Cas9 gene editing.

In this study, the concept of sexual recombination during ascospore production was used to test the possibility of getting an *L. maculans* isolate with a single *Avr* gene. Sexual recombination during meiosis may produce a progeny that deviates from their parent population in their *Avr* profiles. However, results showed that progeny isolates from this study contained similar *Avr* profiles as their parent isolates. Thus, this method was not able to fulfill the study's objective. The significant drawback experienced during the experiment was the low production of pseudothecia in laboratory conditions. In addition, the lack of knowledge about *L. maculans Avr* gene segregation increased the difficulty of achieving the objective.

CRISPR/Cas9 gene editing was used to mutate the *AvrLm5* gene from *L. maculans* isolate *D3*. The *D3* isolate carries only two *Avr* genes, *AvrLm5* and *AvrLepR1*. Thus, knocking out the *AvrLm5* gene will create an isolate that only carries *AvrLepR1*. Unfortunately, the developed CRISPR/Cas9 sgRNA system could not mutate the *AvrLm5* gene successfully. However, the transformed isolates (*D3M*) showed differences in their growth rates and pathogenicity when inoculated on the canola cultivar Westar when compared to the wild-type *D3* isolate. Two isolates, *D3M111* and *D3M112,* showed no disease on Westar, indicating loss of pathogenicity. Future studies are needed to investigate the shift of pathogenicity and morphological changes observed on *D3M111* and *D3M112*.

6.0 References

AAFC. (2020a). *Canada : Outlook for Principal Field Crops Canada*. 1–10. https://agriculture.canada.ca/en/canadas-agriculture-sectors/crops/reports-and-statistics-data-canadian-principal-field-crops/canada-outlook-principal-field-crops-2021-08-20%0Ahttps://www.agr.gc.ca/eng/crops/reports-and-statistics-data-for-canadian-princi

AAFC. (2020b). *Overview of the Canadian Agriculture and Agri-Food Sector*. Agriculture and Agri-Food Canada. https://agriculture.canada.ca/en/canadas-agriculture-sectors/overview-canadas-agriculture-and-agri-food-sector#s2

Aboukhaddour, R., Fetch, T., McCallum, B. D., Harding, M. W., Beres, B. L., & Graf, R. J. (2020). Wheat diseases on the prairies: A Canadian story. *Plant Pathology*, *69*(3), 418–432. https://doi.org/10.1111/ppa.13147

Amarasinghe, C. C., Sharanowski, B., & Fernando, W. G. D. (2019). Molecular phylogenetic relationships, trichothecene chemotype diversity and aggressiveness of strains in a global collection of *Fusarium graminearum* species. *Toxins*, *11*(5), 263. https://doi.org/10.3390/toxins11050263

Amarasinghe, C. C., Simsek, S., Brûlé-Babel, A., & Fernando, W. G. D. (2016). Analysis of deoxynivalenol and deoxynivalenol-3-glucosides content in Canadian spring wheat cultivars inoculated with *Fusarium graminearum*. *Food Additives and Contaminants - Part A Chemistry, Analysis, Control, Exposure and Risk Assessment*, *33*(7), 1254–1264. https://doi.org/10.1080/19440049.2016.1198050

Amarasinghe, C. C., Tamburic-Ilincic, L., Gilbert, J., Brûlé-Babel, A. L., & Fernando, W. G. D. (2013). Evaluation of different fungicides for control of Fusarium head blight in wheat inoculated with 3ADON and 15ADON chemotypes of *Fusarium graminearum* in Canada. *Canadian Journal of Plant Pathology*, *35*(2), 200–208. https://doi.org/10.1080/07060661.2013.773942

Amarasinghe, C. C., Tittlemier, S. A., & Fernando, W. G. D. (2015). Nivalenol-producing *Fusarium cerealis* associated with Fusarium head blight in winter wheat in Manitoba, Canada. *Plant Pathology*, *64*(4), 988–995. https://doi.org/10.1111/ppa.12329

Anderson, J. A. (2001). Variety Development and Uniform Nurseries : Progress in FHB Resistance in Hard Spring Wheat Resistant Varieties of Wheat. *National Fusarium Head Blight Forum*, *2001*, 225–293.

Aoki, T., & O'Donnell, K. (1999). Morphological and molecular characterization of *Fusarium pseudograminearum* sp. nov., formerly recognized as the Group 1 population of *F. graminearum*.*Mycologia*, *91*(4), 597–609. https://doi.org/10.1080/00275514.1999.12061058

Arie, T. (2019). *Fusarium* diseases of cultivated plants, control, diagnosis, and molecular and genetic studies. *Journal of Pesticide Science*, *44*(4), 275–281. https://doi.org/10.1584/JPESTICS.J19-03

Audenaert, K., van Broeck, R., van Bekaert, B., de Witte, F., Heremans, B., Messens, K., Höfte, M., & Haesaert, G. (2009). Fusarium head blight (FHB) in Flanders: Population diversity, inter-species associations and DON contamination in commercial winter wheat varieties. *European Journal of Plant Pathology*, *125*(3), 445–458. https://doi.org/10.1007/s10658-009-9494-3

Bai, G. H., Desjardins, A. E., & Plattner, R. D. (2002). Deoxynivalenol-nonproducing *Fusarium graminearum* causes initial infection, but does not cause disease spread in wheat spikes. *Mycopathologia*, *153*(2), 91–98. https://doi.org/10.1023/A:1014419323550

Bai, G., & Shaner, G. (2004). Management and resistance in wheat and barley to Fusarium head blight. In *Annual Review of Phytopathology* (Vol. 42, pp. 135–161). https://doi.org/10.1146/annurev.phyto.42.040803.140340

Bai Guihua, & Shaner, G. (1994). Scab of wheat: Prospects for control. In *Plant Disease* (Vol. 78, Issue 8, pp. 760–766). https://doi.org/10.1094/pd-78-0760

Balesdent, M. H., Fudal, I., Ollivier, B., Bally, P., Grandaubert, J., Eber, F., Chèvre, A. M., Leflon, M., & Rouxel, T. (2013). The dispensable chromosome of *Leptosphaeria maculans* shelters an effector gene conferring avirulence towards *Brassica rapa*. *New Phytologist*, *198*(3), 887–898. https://doi.org/10.1111/nph.12178

Barrangou, R., Fremaux, C., Deveau, H., Richards, M., Boyaval, P., Moineau, S., Romero, D. A., & Horvath, P. (2007). CRISPR provides acquired resistance against viruses in prokaryotes. *Science*, *315*(5819), 1709–1712. https://doi.org/10.1126/science.1138140

Barrins, J. M., Ades, P. K., Salisbury, P. A., & Howlett, B. J. (2004). Genetic diversity of Australian isolates of *Leptosphaeria maculans*, the fungus that causes blackleg of canola (*Brassica napus*). *Australasian Plant Pathology*, *33*(4), 529–536. https://doi.org/10.1071/AP04061

Bell, J. M. (1982). From Rapeseed to Canola: A Brief History of Research for Superior Meal and Edible Oil. *Poultry Science*, *61*(4), 613–622. https://doi.org/10.3382/ps.0610613

Beyer, M., Röding, S., Ludewig, A., & Verreet, J. A. (2004). Germination and survival of *Fusarium graminearum* macroconidia as affected by environmental factors. In *Journal of Phytopathology* (Vol. 152, Issue 2). https://doi.org/10.1111/j.1439-0434.2003.00807.x

Blaise, F., Rémy, E., Meyer, M., Zhou, L., Narcy, J. P., Roux, J., Balesdent, M. H., & Rouxel, T. (2007). A critical assessment of *Agrobacterium tumefaciens*-mediated transformation as a tool for pathogenicity gene discovery in the phytopathogenic fungus *Leptosphaeria maculans*. *Fungal Genetics and Biology*, *44*(2), 123–138. https://doi.org/10.1016/j.fgb.2006.07.006

Boenisch, M. J., & Schäfer, W. (2011). *Fusarium graminearum* forms mycotoxin producing infection structures on wheat. *BMC Plant Biology*, *11*, 110. https://doi.org/10.1186/1471-2229-11-110

Bottalico, A., & Perrone, G. (2002). Toxigenic *Fusarium* species and mycotoxins associated with head blight in small-grain cereals in Europe. In *Mycotoxins in Plant Disease* (Vol. 108, pp. 611–624). Springer, Dordrecht. https://doi.org/10.1007/978-94-010-0001-7_2

Brandfass, C., & Karlovsky, P. (2006). Simultaneous detection of *Fusarium culmorum* and *F. graminearum* in plant material by duplex PCR with melting curve analysis. *BMC Microbiology*, *6*(1), 1–10. https://doi.org/10.1186/1471-2180-6-4

Brar, G. S., Fetch, T., McCallum, B. D., Hucl, P. J., & Kutcher, H. R. (2019). Virulence dynamice and breeding for resistance to stripe, stem, and leaf rust in Canada since 2000. *Plant Disease*, *103*(12), 2981–2995. https://doi.org/10.1094/PDIS-04-19-0866-FE

Brun, H., Chèvre, A. M., Fitt, B., Powers, S., Besnard, A. L., Ermel, M., Huteau, V., Marquer, B., Eber, F., Renard, M., & Andrivon, D. (2010). Quantitative resistance increases the durability of qualitative resistance to *Leptosphaeria maculans* in *Brassica napus*. *New Phytologist*, *185*(1), 285–299. https://doi.org/10.1111/j.1469-8137.2009.03049.x

Buerstmayr, M., Steiner, B., & Buerstmayr, H. (2020). Breeding for Fusarium head blight resistance in wheat—Progress and challenges. *Plant Breeding*, *139*(3), 429–454. https://doi.org/10.1111/pbr.12797

Campbell, A. B. (2015). *Wheat*. The Canadian Encyclopedia. https://www.thecanadianencyclopedia.ca/en/article/wheat

Canadian Cereals. (2020). *Canadian Wheat Types - 2020 Crop & Grading | CEREALS CANADA*. https://canadiancereals.ca/2020-wheat-crop/#section-quality

Canadian Grain Commission. (2020). *Frequency and severity of Fusarium damaged kernels (FDK) in Harvest Sample Program: Red spring wheat samples*. https://www.grainscanada.gc.ca/en/grain-research/export-quality/cereals/wheat/western/annual-fusarium-damage/canada-western-red-spring/

Canola Council of Canada. (2021). *Canola: a sustainable source of healthy oil and premium protein*. https://www.canolacouncil.org/about-canola/

Champeil, A., Doré, T., & Fourbet, J. F. (2004). Fusarium head blight: Epidemiological origin of the effects of cultural practices on head blight attacks and the production of mycotoxins by *Fusarium* in wheat grains. *Plant Science, 166*(6), 1389–1415. https://doi.org/10.1016/j.plantsci.2004.02.004

Chylinski, K., Makarova, K. S., Charpentier, E., & Koonin, E. V. (2014). Classification and evolution of type II CRISPR-Cas systems. *Nucleic Acids Research, 42*(10), 6091–6105. https://doi.org/10.1093/NAR/GKU241

Clear, R. M., & Patrick, S. K. (2000). Fusarium head blight pathogens isolated from *Fusarium*-damaged kernels of wheat in western Canada, 1993 to 1998. *Canadian Journal of Plant Pathology*, *22*(1), 51–60. https://doi.org/10.1080/07060660009501161

Clear, R. M., Patrick, S. K., Nowicki, T., Gaba, D., Edney, M., & Babb, J. C. (1997). The effect of hull removal and pearling on Fusarium species and trichothecenes in hulless barley. *Canadian Journal of Plant Science, 77*(1), 161–166. https://doi.org/10.4141/P96-014

Clear, Randy M., & Patrick, S. (2010). *Fusarium head blight in western Canada*. Canadian Grain Commission. https://grainscanada.gc.ca/en/grain-research/scientific-reports/fhb-western/fhb-2.html

Coleman, J. J. (2016). The *Fusarium solani* species complex: Ubiquitous pathogens of agricultural importance. *Molecular Plant Pathology*, *17*(2), 146–158. https://doi.org/10.1111/mpp.12289

Cong, L., & Zhang, F. (2015). Genome engineering using CRISPR-Cas9 system. *Methods in Molecular Biology, 1239*, 197–217. https://doi.org/10.1007/978-1-4939-1862-1_10

Cook, D. E., Mesarich, C. H., & Thomma, B. P. H. J. (2015). Understanding Plant Immunity as a Surveillance System to Detect Invasion. In *Annual Review of Phytopathology* (Vol. 53, pp.

541–563). Annual Reviews. https://doi.org/10.1146/annurev-phyto-080614-120114

Cowger, C., Patton-Özkurt, J., Brown-Guedira, G., & Perugini, L. (2009). Post-anthesis moisture increased Fusarium head blight and deoxynivalenol levels in North Carolina winter wheat. *Phytopathology*, *99*(4), 320–327. https://doi.org/10.1094/PHYTO-99-4-0320

Cozijnsen, A. J., & Howlett, B. J. (2003). Characterisation of the mating-type locus of the plant pathogenic ascomycete *Leptosphaeria maculans*. *Current Genetics*, *43*(5), 351–357. https://doi.org/10.1007/s00294-003-0391-6

Cozijnsen, A. J., Popa, K. M., Purwantara, A., Rolls, B. D., & Howlett, B. J. (2000). Genome analysis of the plant pathogenic ascomycete *Leptosphaeria maculans*; mapping mating type and host specificity loci. *Molecular Plant Pathology*, *1*(5), 293–302. https://doi.org/10.1046/j.1364-3703.2000.00033.x

Darma, R., Lutz, A., Elliott, C. E., & Idnurm, A. (2019). Identification of a gene cluster for the synthesis of the plant hormone abscisic acid in the plant pathogen *Leptosphaeria maculans*. *Fungal Genetics and Biology*, *130*, 62–71. https://doi.org/10.1016/j.fgb.2019.04.015

De Wolf, E. D., Madden, L. V., & Lipps, P. E. (2003). Risk assessment models for wheat Fusarium head blight epidemics based on within-season weather data. *Phytopathology*, *93*(4), 428–435. https://doi.org/10.1094/PHYTO.2003.93.4.428

Delourme, R., Pilet-Nayel, M. L., Archipiano, M., Horvais, R., Tanguy, X., Rouxel, T., Brun, H., Renard, M., & Balesdent, M. H. (2004). A cluster of major specific resistance genes to *Leptosphaeria maculans* in *Brassica napus*. *Phytopathology*, *94*(6), 578–583. https://doi.org/10.1094/PHYTO.2004.94.6.578

Demeke, T., Clear, R. M., Patrick, S. K., & Gaba, D. (2005). Species-specific PCR-based assays for the detection of *Fusarium* species and a comparison with the whole seed agar plate method and trichothecene analysis. *International Journal of Food Microbiology*, *103*(3), 271–284. https://doi.org/10.1016/j.ijfoodmicro.2004.12.026

Desjardins, A. (2006). *Fusarium mycotoxins: chemistry, genetics, and biology.* American Phytopathological Society (APS) Press. https://www.cabdirect.org/cabdirect/abstract/20063036927

Dexter, J. E., Marchylo, B. A., Clear, R. M., & Clarke, J. M. (1997). Effect of Fusarium head blight on semolina milling and pasta-making quality of durum wheat. *Cereal Chemistry*, *74*(5), 519–525. https://doi.org/10.1094/CCHEM.1997.74.5.519

Dexter, J. E., Preston, K. R., Woodbeck, N. J., Popper, L., Schafer, W., & Freund, W. (2006). Canadian Wheat. In *Future of Flour a Compendium of Flour Improvement*. www.grainscanada.gc.ca.

Dilmaghani, A., Balesdent, M. H., Didier, J. P., Wu, C., Davey, J., Barbetti, M. J., Li, H., Moreno-Rico, O., Phillips, D., Despeghel, J. P., Vincenot, L., Gout, L., & Rouxel, T. (2009). The *Leptosphaeria maculans - Leptosphaeria biglobosa* species complex in the American continent. *Plant Pathology*, *58*(6), 1044–1058. https://doi.org/10.1111/j.1365-3059.2009.02149.x

Dilmaghani, A., Gladieux, P., Gout, L., Giraud, T., Brunner, P. C., Stachowiak, A., Balesdent, M. H., & Rouxel, T. (2012). Migration patterns and changes in population biology associated with the worldwide spread of the oilseed rape pathogen *Leptosphaeria maculans*. *Molecular Ecology*, *21*(10), 2519–2533. https://doi.org/10.1111/j.1365-294X.2012.05535.x

Dresselhaus, T., & Hückelhoven, R. (2018). Biotic and abiotic stress responses in crop plants. In *Agronomy* (Vol. 8, Issue 11, p. 267). Multidisciplinary Digital Publishing Institute. https://doi.org/10.3390/agronomy8110267

Eckert, M., Gout, L., Rouxel, T., Blaise, F., Jedryczka, M., Fitt, B., & Balesdent, M. H. (2005). Identification and characterization of polymorphic minisatellites in the phytopathogenic ascomycete *Leptosphaeria maculans*. *Current Genetics*, *47*(1), 37–48. https://doi.org/10.1007/s00294-004-0539-z

Elliott, C. E., & Howlett, B. J. (2006). Overexpression of a 3-ketoacyl-CoA thiolase in *Leptosphaeria maculans* causes reduced pathogenicity on *Brassica napus*. *Molecular Plant-Microbe Interactions*, *19*(6), 588–596. https://doi.org/10.1094/MPMI-19-0588

Elliott, V. L., Norton, R. M., Khangura, R. K., Salisbury, P. A., & Marcroft, S. J. (2015). Incidence and severity of blackleg caused by *Leptosphaeria* spp. in *juncea* canola (Brassica juncea L.) in Australia. *Australasian Plant Pathology*, *44*(2), 149–159. https://doi.org/10.1007/s13313-014-0337-0

FAO. (2021). *Codex Alimentarius International Food Standards*. https://www.fao.org/fao-who-codexalimentarius/roster/detail/en/c/297672/

FAOSTAT. (2019). *FAOSTAT*. http://www.fao.org/faostat/en/#data/QCL

Fernandez, M. R., Pearse, P., Holzgang, G., Hughes, G., & Clear, R. (2001). Fusarium head blight in Saskatchewan (1998-2000). *Harvest.Usask.Ca*, *In soil and crop workshop*, 429.

https://harvest.usask.ca/bitstream/handle/10388/9889/M.R. Fernandez et al., 2001.pdf?sequence=1

Fernando, W. G. D., Oghenekaro, A. O., Tucker, J. R., & Badea, A. (2021). Building on a foundation: advances in epidemiology, resistance breeding, and forecasting research for reducing the impact of Fusarium head blight in wheat and barley. *Canadian Journal of Plant Pathology*, *43*(4), 495–526. https://doi.org/10.1080/07060661.2020.1861102

Fernando, W. G. D., Paulitz, T. C., Seaman, W. L., Dutilleul, P., & Miller, J. D. (1997). Head blight gradients caused by *Gibberella zeae* from area sources of inoculum in wheat field plots. *Phytopathology*, *87*(4), 414–421. https://doi.org/10.1094/PHYTO.1997.87.4.414

Fernando, W. G. D., Zhang, X., & Amarasinghe, C. C. (2016). Detection of *Leptosphaeria maculans* and *Leptosphaeria biglobosa* causing blackleg disease in canola from Canadian canola seed lots and dockage. *Plants*, *5*(1), 3–15. https://doi.org/10.3390/plants5010012

Fernando, W. G. D., Zhang, X., Selin, C., Zou, Z., Liban, S. H., McLaren, D. L., Kubinec, A., Parks, P. S., Harunur Rashid, M., Padmathilake, K. R. E., Rong, L., Yang, C., Gnanesh, B. N., & Huang, S. (2018). A six-year investigation of the dynamics of avirulence allele profiles, blackleg incidence, and mating type alleles of *Leptosphaeria maculans* populations associated with canola crops in Manitoba, Canada. *Plant Disease*, *102*(4), 790–798. https://doi.org/10.1094/PDIS-05-17-0630-RE

Figueroa, M., Hammond-Kosack, K. E., & Solomon, P. S. (2018). A review of wheat diseases—a field perspective. In *Molecular Plant Pathology*, *19*(6), pp. 1523–1536. https://doi.org/10.1111/mpp.12618

Fitt, B. D. L., Brun, H., Barbetti, M. J., & Rimmer, S. R. (2006). World-wide importance of phoma stem canker (*Leptosphaeria maculans* and L. biglobosa) on oilseed rape (*Brassica napus*). *European Journal of Plant Pathology*, 114, pp. 3–15. https://doi.org/10.1007/1-4020-4525-5_1

Flor, H. H. (1971). Current status of the gene for gene concept. *Annual Review of Phytopathology*, *9*, 275–296.

Foroud, N. A., & Eudes, F. (2009). Trichothecenes in cereal grains. *International Journal of Molecular Sciences*, *10*(1), 147–173. https://doi.org/10.3390/ijms10010147

Frandsen, Rasmus J.N., Andersson, J. A., Kristensen, M. B., & Giese, H. (2008). Efficient four fragment cloning for the construction of vectors for targeted gene replacement in

filamentous fungi. *BMC Molecular Biology*, *9*(1), 1–11. https://doi.org/10.1186/1471-2199-9-70

Frandsen, R. J. N., Frandsen, M., & Giese, H. (2012). Targeted gene replacement in fungal pathogens via *Agrobacterium tumefaciens*-mediated transformation. *Methods in Molecular Biology*, *835*, 17–45. https://doi.org/10.1007/978-1-61779-501-5_2

Fudal, I., Ross, S., Gout, L., Blaise, F., Kuhn, M. L., Eckert, M. R., Cattolico, L., Bernard-Samain, S., Balesdent, M. H., & Rouxel, T. (2007). Heterochromatin-like regions as ecological niches for avirulence genes in the *Leptosphaeria maculans* genome: Map-based cloning of *AvrLm6*. *Molecular Plant-Microbe Interactions*, *20*(4), 459–470. https://doi.org/10.1094/MPMI-20-4-0459

Gall, C., Balesdent, M. H., Robin, P., & Rouxel, T. (1994). Tetrad analysis of acid phosphatase, soluble protein patterns, and mating type in *Leptosphaeria maculans*. *Phytopathology*, *84*(11), 1299–1305. https://doi.org/10.1094/Phyto-84-1299

Gardiner, D. M., & Howlett, B. J. (2004). Negative selection using thymidine kinase increases the efficiency of recovery of transformants with targeted genes in the filamentous fungus *Leptosphaeria maculans*. *Current Genetics*, *45*(4), 249–255. https://doi.org/10.1007/s00294-004-0488-6

Gasiunas, G., Barrangou, R., Horvath, P., & Siksnys, V. (2012). Cas9-crRNA ribonucleoprotein complex mediates specific DNA cleavage for adaptive immunity in bacteria. *Proceedings of the National Academy of Sciences of the United States of America*, *109*(39), E2579–E2586. https://doi.org/10.1073/pnas.1208507109

GeoforCXC. (2021). *Wheat Farming in Canada*. https://www.geoforcxc.com/economic-activities/wheat-farming-in-canada/

Gervais, J., Plissonneau, C., Linglin, J., Meyer, M., Labadie, K., Cruaud, C., Fudal, I., Rouxel, T., & Balesdent, M. H. (2017). Different waves of effector genes with contrasted genomic location are expressed by *Leptosphaeria maculans* during cotyledon and stem colonization of oilseed rape. *Molecular Plant Pathology*, *18*(8), 1113–1126. https://doi.org/10.1111/mpp.12464

Ghanbarnia, K., Fernando, W. G. D., & Crow, G. (2011). Comparison of disease severity and incidence at different growth stages of naturally infected canola plants under field conditions by pycnidiospores of Phoma lingam as a main source of inoculum. *Canadian*

Journal of Plant Pathology, *33*(3), 355–363.https://doi.org/10.1080/07060661.2011.593189

Ghanbarnia, K., Fudal, I., Larkan, N. J., Links, M. G., Balesdent, M. H., Profotova, B., Fernando, W. G. D., Rouxel, T., & Borhan, M. H. (2015). Rapid identification of the *Leptosphaeria maculans* avirulence gene *AvrLm2* using an intraspecific comparative genomics approach. *Molecular Plant Pathology*, *16*(7), 699–709. https://doi.org/10.1111/mpp.12228

Ghanbarnia, K., Ma, L., Larkan, N. J., Haddadi, P., Fernando, W. G. D., & Borhan, M. H. (2018). *Leptosphaeria maculans AvrLm9*: a new player in the game of hide and seek with *AvrLm4-7*. *Molecular Plant Pathology*, *19*(7), 1754–1764. https://doi.org/10.1111/mpp.12658

Gilbert, J., & Fernando, W. G. D. (2004). Epidemiology and biological control of *Gibberella zeae* /*Fusarium graminearum*. *Canadian Journal of Plant Pathology*, *26*(4), 464–472. https://doi.org/10.1080/07060660409507166

Gilbert, J., & Tekauz, A. (2000). Review: Recent developments in research on Fusarium head blight of wheat in Canada. *Canadian Journal of Plant Pathology*, *22*(1), 1–8. https://doi.org/10.1080/07060660009501155

Gilbert, J., & Tekauz, A. (2011). Strategies for management of Fusarium head blight (FHB) in cereals Varietal Resistance. *Insects and Diseases*, *4*, 97–104. www.prairiesoilsandcrops.ca

Giroux, M. E., Bourgeois, G., Dion, Y., Rioux, S., Pageau, D., Zoghlami, S., Parent, C., Vachon, E., & Vanasse, A. (2016). Evaluation of forecasting models for Fusarium head blight of wheat under growing conditions of Quebec, Canada. *Plant Disease*, *100*(6), 1192–1201. https://doi.org/10.1094/PDIS-04-15-0404-RE

Goswami, R. S., & Kistler, H. C. (2005). Pathogenicity and in planta mycotoxin accumulation among members of the *Fusarium graminearum* species complex on wheat and rice. *Phytopathology*, *95*(12), 1397–1404. https://doi.org/10.1094/PHYTO-95-1397

Gout, L., Fudal, I., Kuhn, M. L., Blaise, F., Eckert, M., Cattolico, L., Balesdent, M. H., & Rouxel, T. (2006). Lost in the middle of nowhere: The *AvrLm1* avirulence gene of the Dothideomycete *Leptosphaeria maculans*. *Molecular Microbiology*, *60*(1), 67–80. https://doi.org/10.1111/j.1365-2958.2006.05076.x

Government of Canada. (2017). *Section 1 - RG-8 Regulatory Guidance: Contaminants in Feed (formerly RG-1, Chapter 7) - Animal health - Canadian Food Inspection Agency*.

Government of Canada. https://www.inspection.gc.ca/animal-health/livestock-feeds/regulatory-guidance/rg-8/eng/1347383943203/1347384015909?chap=1

Grote, U., Fasse, A., Nguyen, T. T., & Erenstein, O. (2021). Food Security and the Dynamics of Wheat and Maize Value Chains in Africa and Asia. *Frontiers in Sustainable Food Systems*, *4*, 317. https://doi.org/10.3389/fsufs.2020.617009

Gugel, R. K., & Petrie, G. A. (1992). History, occurrence, impact, and control of blackleg of rapeseed. *Canadian Journal of Plant Pathology*, *14*(1), 36–45. https://doi.org/10.1080/07060669209500904

Guo, X. W., & Fernando, W. G. D. (2005). Seasonal and diurnal patterns of spore dispersal by *Leptosphaeria maculans* from canola stubble in relation to environmental conditions. *Plant Disease*, *89*(1), 97–104. https://doi.org/10.1094/PD-89-0097

Guo, X. W., Fernando, W. G. D., & Entz, M. (2005). Effects of crop rotation and tillage on blackleg disease of canola. *Canadian Journal of Plant Pathology*, *27*(1), 53–57. https://doi.org/10.1080/07060660509507193

Guo, X. W., Fernando, W. G. D., & Seow-Brock, H. Y. (2008). Population structure, chemotype diversity, and potential chemotype shifting of *Fusarium graminearum* in wheat fields of Manitoba. *Plant Disease*, *92*(5), 756–762. https://doi.org/10.1094/PDIS-92-5-0756

Haddadi, P., Ma, L., Wang, H., & Borhan, M. H. (2016). Genome-wide transcriptomic analyses provide insights into the lifestyle transition and effector repertoire of *Leptosphaeria maculans* during the colonization of *Brassica napus* seedlings. *Molecular Plant Pathology*, *17*(8), 1196–1210. https://doi.org/10.1111/mpp.12356

Hall, R. (1992). Epidemiology of blackleg of oilseed rape. *Canadian Journal of Plant Pathology*, *14*(1), 46–55. https://doi.org/10.1080/07060669209500905

Hooker, D. C., Schaafsma, A. W., & Tamburic-Ilincic, L. (2002). Using weather variables pre- and post-heading to predict deoxynivalenol content in winter wheat. *Plant Disease*, *86*(6), 611–619. https://doi.org/10.1094/PDIS.2002.86.6.611

Hope, R., Aldred, D., & Magan, N. (2005). Comparison of environmental profiles for growth and deoxynivalenol production by *Fusarium culmorum* and *F. graminearum* on wheat grain. *Letters in Applied Microbiology*, *40*(4), 295–300. https://doi.org/10.1111/j.1472-765X.2005.01674.x

Howlett, B. J., Idnurm, A., & Pedras, M. S. C. (2001). *Leptosphaeria maculans*, the causal agent

of blackleg disease of Brassicas. In *Fungal Genetics and Biology* (Vol. 33, Issue 1, pp. 1–14). Academic Press. https://doi.org/10.1006/fgbi.2001.1274

Huang, Y. J., Fitt, B. D. L., & Hall, A. M. (2003). Survival of A-group and B-group *Leptosphaeria maculans* (phoma stem canker) ascospores in air and mycelium on oilseed rape stem debris. *Annals of Applied Biology*, *143*(3), 359–369. https://doi.org/10.1111/j.1744-7348.2003.tb00305.x

Ichinoe, M., Kurata, H., Sugiura, Y., & Ueno, Y. (1983). Chemotaxonomy of *Gibberella zeae* with special reference to production of trichothecenes and zearalenone. *Applied and Environmental Microbiology*, *46*(6), 1364–1367. https://doi.org/10.1128/aem.46.6.1364-1369.1983

Idnurm, A., Bailey, A. M., Cairns, T. C., Elliott, C. E., Foster, G. D., Ianiri, G., & Jeon, J. (2017a). A silver bullet in a golden age of functional genomics: The impact of agrobacterium-mediated transformation of fungi. *Fungal Biology and Biotechnology*, *4*(1), 1–28. https://doi.org/10.1186/s40694-017-0035-0

Idnurm, A., Urquhart, A. S., Vummadi, D. R., Chang, S., Van de Wouw, A. P., & López-ruiz, F. J. (2017b). Spontaneous and crispr/cas9-induced mutation of the osmosensor histidine kinase of the canola pathogen *Leptosphaeria maculans*. *Fungal Biology and Biotechnology*, *4*(1), 1–12. https://doi.org/10.1186/s40694-017-0043-0

Inch, S., Fernando, W. G. D., & Gilbert, J. (2005). Seasonal and daily variation in the airborne concentration of *Gibberella zeae* (Schw.) Petch spores in Manitoba. *Canadian Journal of Plant Pathology*, *27*(3), 357–363. https://doi.org/10.1080/07060660509507233

Jestin, C., Lodé, M., Vallée, P., Domin, C., Falentin, C., Horvais, R., Coedel, S., Manzanares-Dauleux, M. J., & Delourme, R. (2011). Association mapping of quantitative resistance for *Leptosphaeria maculans* in oilseed rape (*Brassica napus* L.). *Molecular Breeding*, *27*(3), 271–287. https://doi.org/10.1007/s11032-010-9429-x

Ji, F., Wu, J., Zhao, H., Xu, J., & Shi, J. (2015). Relationship of deoxynivalenol content in grain, chaff, and straw with Fusarium head blight severity in wheat varieties with various levels of resistance. *Toxins*, *7*(3), 728–742. https://doi.org/10.3390/toxins7030728

Jinek, M., Chylinski, K., Fonfara, I., Hauer, M., Doudna, J. A., & Charpentier, E. (2012). A programmable dual-RNA-guided DNA endonuclease in adaptive bacterial immunity. *Science*, *337*(6096), 816–821. https://doi.org/10.1126/science.1225829

Johnson, D. G. (1999). The growth of demand will limit output growth for food over the next quarter century. *Proceedings of the National Academy of Sciences of the United States of America*, *96*(11), 5915–5920. https://doi.org/10.1073/pnas.96.11.5915

Jurado, M., Vázquez, C., Patiño, B., González-Jaén, & Teresa, M. (2005). PCR detection assays for the trichothecene-producing species *Fusarium graminearum*, *Fusarium culmorum*, *Fusarium poae*, *Fusarium equiseti* and *Fusarium sporotrichioides*. *Systematic and Applied Microbiology*, *28*(6), 562–568. https://doi.org/10.1016/j.syapm.2005.02.003

Kang, Z., Zingen-Sell, I., & Buchenauer, H. (2005). Infection of wheat spikes by *Fusarium avenaceum* and alterations of cell wall components in the infected tissue. *European Journal of Plant Pathology*, *111*(1), 19–28. https://doi.org/10.1007/s10658-004-1983-9

Kannangara, S. K., Bullock, P., Walkowiak, S., & Fernando, W. G. D. (2021). Fusarium Head Blight species diversity and deoxynivalenol (DON) levels in Western Canadian producer wheat fields. *Tri-Society Virtual Conference*, 50. https://phytopath.ca/wp-content/uploads/2021/09/TriSociety-Flipbook.pdf

Karelov, A. V., Borzykh, O. I., Kozub, N. O., Sozinov, I. O., Yanse, L. A., Sozinova, O. I., Tkalenko, H. M., Mishchenko, L. T., & Blume, Y. B. (2021). Current approaches to identification of *Fusarium* fungi infecting wheat. *Cytology and Genetics*, *55*(5), 433–446. https://doi.org/10.3103/S0095452721050030

Kelly, A. C., & Ward, T. J. (2018). Population genomics of *Fusarium graminearum* reveals signatures of divergent evolution within a major cereal pathogen. *PLoS ONE*, *13*(3), e0194616. https://doi.org/10.1371/journal.pone.0194616

Kheiri, A., Moosawi Jorf, S. A., & Malihipour, A. (2019). Infection process and wheat response to Fusarium head blight caused by *Fusarium graminearum*. *European Journal of Plant Pathology*, *153*(2), 489–502. https://doi.org/10.1007/s10658-018-1576-7

Khonga, E. B., & Sutton, J. C. (1988). Inoculum production and survival of *Gibberella zeae* in maize and wheat residues. *Canadian Journal of Plant Pathology*, *10*(3), 232–239. https://doi.org/10.1080/07060668809501730

Khudhair, M., Melloy, P., Lorenz, D. J., Obanor, F., Aitken, E., Datta, S., Luck, J., Fitzgerald, G., & Chakraborty, S. (2014). Fusarium crown rot under continuous cropping of susceptible and partially resistant wheat in microcosms at elevated CO2. *Plant Pathology*, *63*(5), 1033–1043. https://doi.org/10.1111/ppa.12182

Klem, K., Váňová, M., Hajšlová, J., Lancová, K., & Sehnalová, M. (2007). A neural network model for prediction of deoxynivalenol content in wheat grain based on weather data and preceding crop. *Plant, Soil and Environment*, *53*(10), 421–429. https://doi.org/10.17221/2200-pse

Klemsdal, S. S., & Elen, O. (2006). Development of a highly sensitive nested-PCR method using a single closed tube for detection of *Fusarium culmorum* in cereal samples. *Letters in Applied Microbiology*, *42*(5), 544–548. https://doi.org/10.1111/j.1472-765X.2006.01880.x

Krska, R., Baumgartner, S., & Josephs, R. (2001). The state-of-the-art in the analysis of type-A and -B trichothecene mycotoxins in cereals. *Analytical and Bioanalytical Chemistry*, *371*(3), 285–299. https://doi.org/10.1007/S002160100992

Kulik, T., Fordoński, G., Pszczółkowska, A., Płodzień, K., & Łapiński, M. (2004). Development of PCR assay based on ITS2 rDNA polymorphism for the detection and differentiation of *Fusarium sporotrichioides*. *FEMS Microbiology Letters*, *239*(1), 181–186. https://doi.org/10.1016/j.femsle.2004.08.037

Kuscu, C., Arslan, S., Singh, R., Thorpe, J., & Adli, M. (2014). Genome-wide analysis reveals characteristics of off-target sites bound by the Cas9 endonuclease. *Nature Biotechnology*, *32*(7), 677–683. https://doi.org/10.1038/nbt.2916

Kutcher, H. R., Turkington, T. K., & Mclaren, D. L. (2011). Best Management Practices for Blackleg Disease of Canola. *Prairie Soils and Crops Journal*, *4*, 122–134.

Leclair, S., Ansan-Melayah, D., Rouxel, T., & Balesdent, M. H. (1996). Meiotic behaviour of the minichromosome in the phytopathogenic ascomycete *Leptosphaeria maculans*. *Current Genetics*, *30*(6), 541–548. https://doi.org/10.1007/s002940050167

Leonard, K. J., & Bushnell, W. R. (2003). *Fusarium Head Blight of Wheat and Barley*. APS Press.

Liban, S. H., Cross, D. J., Kutcher, H. R., Peng, G., & Fernando, W. G. D. (2016). Race structure and frequency of avirulence genes in the western Canadian *Leptosphaeria maculans* pathogen population, the causal agent of blackleg in *Brassica* species. *Plant Pathology*, *65*(7), 1161–1169. https://doi.org/10.1111/ppa.12489

Liu, F., Selin, C., Zou, Z., & Fernando, W. G. D. (2020a). LmCBP1, a secreted chitin-binding protein, is required for the pathogenicity of *Leptosphaeria maculans* on *Brassica napus*. *Fungal Genetics and Biology*, *136*, 103320. https://doi.org/10.1016/j.fgb.2019.103320

Liu, F., Zou, Z., Huang, S., Parks, P., & Fernando, W. G. D. (2020b). Development of a specific marker for detection of a functional *AvrLm9* allele and validating the interaction between *AvrLm7* and *AvrLm9* in *Leptosphaeria maculans*. *Molecular Biology Reports*, *47*(9), 7115–7123. https://doi.org/10.1007/s11033-020-05779-8

Lowe, R. G. T., Cassin, A., Grandaubert, J., Clark, B. L., Van de Wouw, A. P., Rouxel, T., & Howlett, B. J. (2014). Genomes and transcriptomes of partners in plant-fungal- interactions between canola (*Brassica napus*) and two Leptosphaeria species. *PLoS ONE*, *9*(7), e103098. https://doi.org/10.1371/journal.pone.0103098

Manitoba Agriculture. (2021). *Province of Manitoba | agriculture - Highbush Cranberry Production in Manitoba*. https://www.gov.mb.ca/agriculture/crops/crop-management/fruit-crops/highbush-cranberry-production.html

Maruyama, T., Dougan, S. K., Truttmann, M. C., Bilate, A. M., Ingram, J. R., & Ploegh, H. L. (2015). Increasing the efficiency of precise genome editing with CRISPR-Cas9 by inhibition of nonhomologous end joining. *Nature Biotechnology*, *33*(5), 538–542. https://doi.org/10.1038/nbt.3190

Mateo, J. J., Mateo, R., & Jiménez, M. (2002). Accumulation of type A trichothecenes in maize, wheat and rice by *Fusarium sporotrichioides* isolates under diverse culture conditions. *International Journal of Food Microbiology*, *72*(1–2), 115–123. https://doi.org/10.1016/S0168-1605(01)00625-0

McMullen, M., Bergstrom, G., De Wolf, E., Dill-Macky, R., Hershman, D., Shaner, G., & Van Sanford, D. (2012). A unified effort to fight an enemy of wheat and barley: Fusarium head blight. *Plant Disease*, *96*(12), 1712–1728. https://doi.org/10.1094/PDIS-03-12-0291-FE

McMullen, M., Jones, R., & Gallenberg, D. (1997). Scab of wheat and barley: A re-emerging disease of devastating impact. In *Plant Disease*, *81*(12), 1340–1348. https://doi.org/10.1094/PDIS.1997.81.12.1340

Michielse, C. B., Hooykaas, P. J. J., van den Hondel, C. A. M. J. J., & Ram, A. F. J. (2005). *Agrobacterium*-mediated transformation as a tool for functional genomics in fungi. In *Current Genetics* (Vol. 48, Issue 1, pp. 1–17). Springer. https://doi.org/10.1007/s00294-005-0578-0

Mendes-Pereira, E., Balesdent, M.H., Brun, H., & Rouxel, T. (2003). Molecular phylogeny of the *Leptosphaeria maculans - L. biglobosa* species complex. *Mycological Research*, 107,

1287-1304. https://doi.org/10.1017/s0953756203008554.

Miller, J. D., & Richardson, S. N. (2013). *Mycotoxins in Canada: a perspective for 2013*.

Mishra, P. K., Fox, R. T. ., & Culham, A. (2003). Development of a PCR-based assay for rapid and reliable identification of pathogenic Fusaria. *FEMS Microbiology Letters*, *218*(2), 329–332. https://doi.org/10.1111/j.1574-6968.2003.tb11537.x

Mongrain, D., Couture, L., & Comeau, A. (2000). Natural occurrence of *Fusarium graminearum* on adult wheat midge and transmission to wheat spikes. *Cereal Research Communications*, *28*(1–2), 173–180. https://doi.org/10.1007/bf03543590

Morrall, R. (1982). Epidemiology of sclerotinia stem rot of rapeseed in saskatchewan. *Canadian Journal of Plant Pathology*, *4*(2), 161–168. https://doi.org/10.1080/07060668209501319

Nelson, P. E., Toussoun, T. A., & Marasas, W. F. O. (1983). *Fusarium Species: An Illustrated Manual for Identification*. 206. https://doi.org/10.3/JQUERY-UI.JS

Neik., T. X., Ghanbarnia, K., Ollivier, B., Scheben, A., Severn-Ellis, A., Larkan, N. J., Haddadi, P., Fernando, W. G. D., Rouxe, T., Batley, J., Borhan, H. M., & Balesdent, M. (2022) Two independent approaches converge to the cloning of a new *Leptosphaeria maculans* avirulence 2 effector gene, *AvrLmS-Lep2*. *Molecular Plant Pathology* (In press).

Nicholson, P., Simpson, D. R., Weston, G., Rezanoor, H. N., Lees, A. K., Parry, D. W., & Joyce, D. (1998). Detection and quantification of *Fusarium culmorum* and *Fusarium graminearum* in cereals using PCR assays. *Physiological and Molecular Plant Pathology*, *53*(1), 17–37. https://doi.org/10.1006/pmpp.1998.0170

Nicholson, P., Simpson, D. R., Wilson, A. H., Chandler, E., & Thomsett, M. (2004). Detection and differentiation of trichothecene and enniatin-producing Fusarium species on small-grain cereals. In *Molecular Diversity and PCR-detection of Toxigenic Fusarium Species and Ochratoxigenic Fungi* (Vol. 110, pp. 503–514). Springer, Dordrecht. https://doi.org/10.1007/978-1-4020-2285-2_5

Nicolaisen, M., Suproniene, S., Nielsen, L. K., Lazzaro, I., Spliid, N. H., & Justesen, A. F. (2009). Real-time PCR for quantification of eleven individual Fusarium species in cereals. *Journal of Microbiological Methods*, *76*(3), 234–240. https://doi.org/10.1016/j.mimet.2008.10.016

Nielsen, L. K., Jensen, J. D., Rodríguez, A., Jørgensen, L. N., & Justesen, A. F. (2012). TRI12 based quantitative real-time PCR assays reveal the distribution of trichothecene genotypes

of *F. graminearum* and *F. culmorum* isolates in Danish small grain cereals. *International Journal of Food Microbiology*, *157*(3), 384–392. https://doi.org/10.1016/j.ijfoodmicro.2012.06.010

Nødvig, C. S., Nielsen, J. B., Kogle, M. E., & Mortensen, U. H. (2015). A CRISPR-Cas9 system for genetic engineering of filamentous fungi. *PLoS ONE*, *10*(7), e0133085. https://doi.org/10.1371/journal.pone.0133085

O'Donnell, K., Kistler, H. C., Tacke, B. K., & Casper, H. H. (2000). Gene genealogies reveal global phylogeographic structure and reproductive isolation among lineages of *Fusarium graminearum*, the fungus causing wheat scab. *Proceedings of the National Academy of Sciences of the United States of America*, *97*(14), 7905–7910. https://doi.org/10.1073/pnas.130193297

O'Donnell, K., Ward, T. J., Aberra, D., Kistler, H. C., Aoki, T., Orwig, N., Kimura, M., Bjørnstad, Å., & Klemsdal, S. S. (2008). Multilocus genotyping and molecular phylogenetics resolve a novel head blight pathogen within the *Fusarium graminearum* species complex from Ethiopia. *Fungal Genetics and Biology*, *45*(11), 1514–1522. https://doi.org/10.1016/j.fgb.2008.09.002

O'Donnell, K., Ward, T. J., Geiser, D. M., Kistler, H. C., & Aoki, T. (2004). Genealogical concordance between the mating type locus and seven other nuclear genes supports formal recognition of nine phylogenetically distinct species within the *Fusarium graminearum* clade. *Fungal Genetics and Biology*, *41*(6), 600–623. https://doi.org/10.1016/j.fgb.2004.03.003

Palmero Llamas, D., De Cara Gonzalez, M., Iglesias Gonzalez, C., Ruíz Lopez, G., & Tello Marquina, J. C. (2008). Effects of water potential on spore germination and viability of *Fusarium* species. *Journal of Industrial Microbiology and Biotechnology*, *35*(11), 1411–1418. https://doi.org/10.1007/s10295-008-0441-7

Pang, E. C. K., & Halloran, G. M. (1996). The genetics of adult-plant blackleg (*Leptosphaeria maculans*) resistance from Brassica juncea in B. napus. *Theoretical and Applied Genetics*, *92*(3–4), 382–387. https://doi.org/10.1007/BF00223683

Panthi, A., Hallen-Adams, H., Wegulo, S. N., Hernandez Nopsa, J., & Stephen Baenziger, P. (2014). Chemotype and aggressiveness of isolates of *Fusarium graminearum* causing head blight of wheat in Nebraska. *Canadian Journal of Plant Pathology*, *36*(4), 447–455.

https://doi.org/10.1080/07060661.2014.964775

Parry, D. W., Jenkinson, P., & McLeod, L. (1995). Fusarium ear blight (scab) in small grain cereals—a review. *Plant Pathology*, *44*(2), 207–238. https://doi.org/10.1111/j.1365-3059.1995.tb02773.x

Parry, D. W., & Nicholson, P. (1996). Development of a PCR assay to detect Fusarium poae in wheat. *Plant Pathology*, *45*(2), 383–391. https://doi.org/10.1046/j.1365-3059.1996.d01-133.x

Paul, P. A., El-Allaf, S. M., Lipps, P. E., & Madden, L. V. (2004). Rain splash dispersal of Gibberella zeae within wheat canopies in Ohio. *Phytopathology*, *94*(12), 1342–1349. https://doi.org/10.1094/PHYTO.2004.94.12.1342

Paul, P. A., Lipps, P. E., & Madden, L. V. (2005). Relationship between visual estimates of Fusarium head blight intensity and deoxynivalenol accumulation in harvested wheat grain: A meta-analysis. *Phytopathology*, *95*(10), 1225–1236. https://doi.org/10.1094/PHYTO-95-1225

Peng, G., Lahlali, R., Hwang, S. F., Pageau, D., Hynes, R. K., McDonald, M. R., Gossen, B. D., & Strelkov, S. E. (2014). Special Issue: Crop rotation, cultivar resistance, and fungicides/ biofungicides for managing clubroot (*Plasmodiophora brassicae*) on canola. In *Canadian Journal of Plant Pathology* (Vol. 36, Issue SUPPL. 1, pp. 99–112). Taylor & Francis. https://doi.org/10.1080/07060661.2013.860398

Petrie, G. A., & Lewis, P. A. (1985). Sexual compatibility of isolates of the rapeseed blackleg fungus *Leptosphaeria maculans* from canada, australia, and england. *Canadian Journal of Plant Pathology*, *7*(3), 253–255. https://doi.org/10.1080/07060668509501687

Plissonneau, C., Daverdin, G., Ollivier, B., Blaise, F., Degrave, A., Fudal, I., Rouxel, T., & Balesdent, M. H. (2016). A game of hide and seek between avirulence genes *AvrLm4-7* and *AvrLm3* in *Leptosphaeria maculans*. *New Phytologist*, *209*(4), 1613–1624. https://doi.org/10.1111/nph.13736

Plummer, K. M., & Howlett, B. J. (1993). Major chromosomal length polymorphisms are evident after meiosis in the phytopathogenic fungus *Leptosphaeria maculans*. *Current Genetics*, *24*(1–2), 107–113. https://doi.org/10.1007/BF00324673

Plummer, K. M., & Howlett, B. J. (1995). Inheritance of chromosomal length polymorphisms in the ascomycete *Leptosphaeria maculans*. *MGG Molecular & General Genetics*, *247*(4),

416–422. https://doi.org/10.1007/BF00293142

Prandini, A., Sigolo, S., Filippi, L., Battilani, P., & Piva, G. (2009). Review of predictive models for Fusarium head blight and related mycotoxin contamination in wheat. *Food and Chemical Toxicology*, *47*(5), 927–931. https://doi.org/10.1016/j.fct.2008.06.010

Prescott, J. M., Burnett, P. A., Saari, E. E., Ranson, J., Bowman, J., de Milliano, W., Singh, R. P., & Bekele, G. (2015). *Wheat diseases and pests: a guide for field identification Predicting grain protein content of spring wheat using sensors View project*. International Maize And Wheat Improvement Center. https://www.researchgate.net/publication/38987380

Pritsch, C., Muehlbauer, G. J., Bushnell, W. R., Somers, D. A., & Vance, C. P. (2000). Fungal development and induction of defense response genes during early infection of wheat spikes by *Fusarium graminearum*. In *Molecular Plant-Microbe Interactions* (Vol. 13, Issue 2). https://doi.org/10.1094/MPMI.2000.13.2.159

Rashid, M. H., Liban, S., Zhang, X., Parks, P., Borhan, H., & Fernando, W. G. D. (2021). Impact of *Brassica napus–Leptosphaeria maculans* interaction on the emergence of virulent isolates of *L. maculans*, causal agent of blackleg disease in canola. *Plant Pathology*, *70*(2), 459–474. https://doi.org/10.1111/ppa.13293

Rimmer, S. R., & Van Den Berg, C. G. J. (1992). Resistance of oilseed *Brassica* spp. to blackleg caused by *Leptosphaeria maculans*. *Canadian Journal of Plant Pathology*, *14*(1), 56–66. https://doi.org/10.1080/07060669209500906

Rouxel, T., Grandaubert, J., Hane, J. K., Hoede, C., Van de Wouw, A. P., Couloux, A., Dominguez, V., Anthouard, V., Bally, P., Bourras, S., Cozijnsen, A. J., Ciuffetti, L. M., Degrave, A., Dilmaghani, A., Duret, L., Fudal, I., Goodwin, S. B., Gout, L., Glaser, N., … Howlett, B. J. (2011). Effector diversification within compartments of the *Leptosphaeria maculans* genome affected by repeat-induced point mutations. *Nature Communications*, *2*(1), 1–10. https://doi.org/10.1038/ncomms1189

Rouxel, T., Penaud, A., Pinochet, X., Brun, H., Gout, L., Delourme, R., Schmit, J., & Balesdent, M. H. (2003). A 10-year survey of populations of *Leptosphaeria maculans* in France indicates a rapid adaptation towards the *Rlm1* resistance gene of oilseed rape. *European Journal of Plant Pathology*, *109*(8), 871–881. https://doi.org/10.1023/A:1026189225466

Schroeder, H. W., & Christensen, J. J. (1963). Factors affecting resistance of wheat to scab

caused by Gibberella zeae. *Phytopathology*, *53*, 831–838. https://www.cabdirect.org/cabdirect/abstract/19641100439

Schuster, M., & Kahmann, R. (2019). CRISPR-Cas9 genome editing approaches in filamentous fungi and oomycetes. *Fungal Genetics and Biology*, *130*, 43–53. https://doi.org/10.1016/j.fgb.2019.04.016

Seeling, K., Boguhn, J., Strobel, E., Dänicke, S., Valenta, H., Ueberschär, K. H., & Rodehutscord, M. (2006). On the effects of Fusarium toxin contaminated wheat and wheat chaff on nutrient utilisation and turnover of deoxynivalenol and zearalenone in vitro (Rusitec). *Toxicology in Vitro*, *20*(5), 703–711. https://doi.org/10.1016/j.tiv.2005.10.006

Segalin, M., & Reis, E. M. (2010). Meio semi-seletivo para detecção de *Fusarium graminearum* em amostras de sementes. *Summa Phytopathologica*, *36*(4), 338–341. https://doi.org/10.1590/S0100-54052010000400010

Shahbandeh, M. (2021). *Wheat - statistics & facts | Statista*. Statista. https://www-statista-com.uml.idm.oclc.org/topics/1668/wheat/#dossierKeyfigures

Sinha, R. C., & Savard, M. E. (1997). Concentration of deoxynivalenol in single kernels and various tissues of wheat heads. *Canadian Journal of Plant Pathology*, *19*(1), 8–12. https://doi.org/10.1080/07060669709500578

Sobrova, P., Adam, V., Vasatkova, A., Beklova, M., Zeman, L., & Kizek, R. (2010). Deoxynivalenol and its toxicity. *Interdisciplinary Toxicology*, *3*(3), 94–99. https://doi.org/10.2478/v10102-010-0019-x

Sonah, H., Zhang, X., Deshmukh, R. K., Hossein Borhan, M., Fernando, W. G. D., & Bélanger, R. R. (2016). Comparative transcriptomic analysis of virulence factors in *Leptosphaeria maculans* during compatible and incompatible interactions with canola. *Frontiers in Plant Science*, *7*(DECEMBER2016), 1784. https://doi.org/10.3389/fpls.2016.01784

Song, R., Zhai, Q., Sun, L., Huang, E., Zhang, Y., Zhu, Y., Guo, Q., Tian, Y., Zhao, B., & Lu, H. (2019). CRISPR/Cas9 genome editing technology in filamentous fungi: progress and perspective. *Applied Microbiology and Biotechnology*, *103*(17), 6919–6932. https://doi.org/10.1007/s00253-019-10007-w

Starkey, D. E., Ward, T. J., Aoki, T., Gale, L. R., Kistler, H. C., Geiser, D. M., Suga, H., Tóth, B., Varga, J., & O'Donnell, K. (2007). Global molecular surveillance reveals novel Fusarium head blight species and trichothecene toxin diversity. *Fungal Genetics and*

Biology, *44*(11), 1191–1204. https://doi.org/10.1016/j.fgb.2007.03.001

Statistics Canada. (2021). *Crop production*. https://www150.statcan.gc.ca/n1/en/subjects/agriculture_and_food/crop_production

Stull, R. B., & Ahrens, C. D. (2000). *Meteorology for scientists and engineers*. *I*, 10–12. https://doi.org/10.3/JQUERY-UI.JS

Sun, S. J., Gao, W., Lin, S. Q., Zhu, J., Xie, B. G., & Lin, Z. Bin. (2006). Analysis of genetic diversity in Ganoderma population with a novel molecular marker SRAP. *Applied Microbiology and Biotechnology*, *72*(3), 537–543. https://doi.org/10.1007/s00253-005-0299-9

Sung, J.-M., & Cook, R. . (1981). Effect of water potential on reproduction and spore germination by *Fusarium roseum* "*graminearum*," "*culmorum*," and "*avenaceum*" . *Phytopathology*, *71*(5), 499. https://doi.org/10.1094/PHYTO-71-499

Sutton, J. C. (1982). Epidemiology of wheat head blight and maize ear rot caused by *Fusarium graminearum*. *Canadian Journal of Plant Pathology*, *4*(2), 195–209. https://doi.org/10.1080/07060668209501326

Tack, J., Barkley, A., & Nalley, L. L. (2015). Effect of warming temperatures on US wheat yields. *Proceedings of the National Academy of Sciences of the United States of America*, *112*(22), 6931–6936. https://doi.org/10.1073/pnas.1415181112

Tagami, K., Minami, A., Fujii, R., Liu, C., Tanaka, M., Gomi, K., Dairi, T., & Oikawa, H. (2015). Rapid reconstitution of biosynthetic machinery for fungal metabolites in *Aspergillus oryzae*: Total biosynthesis of aflatrem. *ChemBioChem*, *16*(17), 2076–2080. https://doi.org/10.1002/cbic.201402195

Tillmann, M., von Tiedemann, A., & Winter, M. (2017). Crop rotation effects on incidence and diversity of *Fusarium* species colonizing stem bases and grains of winter wheat. *Journal of Plant Diseases and Protection*, *124*(2), 121–130. https://doi.org/10.1007/s41348-016-0064-6

Tittlemier, S. A., Arsiuta, J., Mohammad, U., Hainrich, C., Bowler, K., Croom, R., Olubodun, A., Blagden, R., Mckendry, T., Gräfenhan, T., & Pleskach, K. (2020). Variable relationships between *Fusarium* damage and deoxynivalenol concentrations in wheat in western Canada in 2016. *Canadian Journal of Plant Pathology*, *42*(1), 41–51. https://doi.org/10.1080/07060661.2019.1620861

Turkington, T. K., Clear, R. M., Demeke, T., Lange, R., Xi, K., & Kumar, K. (2011). Isolation of *Fusarium graminearum* from cereal, grass and corn residues from Alberta, 2001-2003. *Canadian Journal of Plant Pathology*, *33*(2), 179–186. https://doi.org/10.1080/07060661.2011.560189

Turner, A. S., Lees, A. K., Rezanoor, H. N., & Nicholson, P. (1998). Refinement of PCR-detection of *Fusarium avenaceum* and evidence from DNA marker studies for phenetic relatedness to *Fusarium tricinctum*. *Plant Pathology*, *47*(3), 278–288. https://doi.org/10.1046/j.1365-3059.1998.00250.x

Urquhart, A. S., & Idnurm, A. (2019). Limitations of transcriptome-based prediction of pathogenicity genes in the plant pathogen *Leptosphaeria maculans*. *FEMS Microbiology Letters*, *366*(7), 80. https://doi.org/10.1093/femsle/fnz080

US Food and Drug Administration. (2010). Guidance for industry and FDA: advisory levels for deoxynivalenol (DON) in finished wheat products for human consumption and grains and grain by-products used for animal feed. Silver Spring, MD: USFDA.

Van de Wouw, A. P., Elliott, C. E., Popa, K. M., & Idnurm, A. (2019). Analysis of Repeat Induced Point (RIP) Mutations in *Leptosphaeria maculans* Indicates Variability in the RIP Process Between Fungal Species. *Genetics*, *211*(1), 89–104. https://doi.org/10.1534/GENETICS.118.301712

Van de Wouw, A. P., Idnurm, A., Davidson, J. A., Sprague, S. J., Khangura, R. K., Ware, A. H., Lindbeck, K. D., & Marcroft, S. J. (2016). Fungal diseases of canola in Australia: identification of trends, threats and potential therapies. *Australasian Plant Pathology*, *45*(4), 415–423. https://doi.org/10.1007/s13313-016-0428-1

Van de Wouw, A. P., Lowe, R. G. T., Elliott, C. E., Dubois, D. J., & Howlett, B. J. (2014a). An avirulence gene, *AvrLmJ1*, from the blackleg fungus, *Leptosphaeria maculans*, confers avirulence to *Brassica juncea* cultivars. *Molecular Plant Pathology*, *15*(5), 523–530. https://doi.org/10.1111/mpp.12105

Van de Wouw, A. P., Marcroft, S. J., Ware, A., Lindbeck, K., Khangura, R., & Howlett, B. J. (2014b). Breakdown of resistance to the fungal disease, blackleg, is averted in commercial canola (*Brassica napus*) crops in Australia. *Field Crops Research*, *166*, 144–151. https://doi.org/10.1016/j.fcr.2014.06.023

Waalwijk, C., van der Heide, R., de Vries, I., van der Lee, T., Schoen, C., Corainville, G. C.,

Häuser-Hahn, I., Kastelein, P., Köhl, J., Lonnet, P., Demarquet, T., & Kema, G. H. J. (2004). Quantitative detection of Fusarium species in wheat using TaqMan. *Molecular Diversity and PCR-Detection of Toxigenic Fusarium Species and Ochratoxigenic Fungi*, 481–494. https://doi.org/10.1007/978-1-4020-2285-2_3

Wang, J. H., Ndoye, M., Zhang, J. B., Li, H. P., & Liao, Y. C. (2011). Population structure and genetic diversity of the *Fusarium graminearum* species complex. *Toxins*, *3*(8), 1020–1037. https://doi.org/10.3390/toxins3081020

Wang, Q., & Coleman, J. J. (2019). Progress and Challenges: Development and Implementation of CRISPR/Cas9 Technology in Filamentous Fungi. *Computational and Structural Biotechnology Journal*, *17*, 761–769. https://doi.org/10.1016/j.csbj.2019.06.007

Ward, T. J., Bielawski, J. P., Corby Kistler, H., Sullivan, E., & O'Donnell, K. (2002). Ancestral polymorphism and adaptive evolution in the trichothecene mycotoxin gene cluster of phytopathogenic *Fusarium*. *Proceedings of the National Academy of Sciences of the United States of America*, *99*(14), 9278–9283. https://doi.org/10.1073/pnas.142307199

Ward, T. J., Clear, R. M., Rooney, A. P., O'Donnell, K., Gaba, D., Patrick, S., Starkey, D. E., Gilbert, J., Geiser, D. M., & Nowicki, T. W. (2008). An adaptive evolutionary shift in Fusarium head blight pathogen populations is driving the rapid spread of more toxigenic *Fusarium graminearum* in North America. *Fungal Genetics and Biology*, *45*(4), 473–484. https://doi.org/10.1016/j.fgb.2007.10.003

Wegulo, S. N. (2012). Factors influencing deoxynivalenol accumulation in small grain cereals. *Toxins*, *4*(11), 1157–1180. https://doi.org/10.3390/toxins4111157

West, J. S., & Fitt, B. D. L. (2005). Population dynamics and dispersal of *Leptosphaeria maculans* (blackleg of canola): Adapted from a keynote address at the 15th Biennial Conference of the Australasian Plant Pathology Society, 26-29 September 2005, Geelong. *Australasian Plant Pathology*, *34*(4), 457–461. https://doi.org/10.1071/AP05086

West, J. S., Kharbanda, P. D., Barbetti, M. J., & Fitt, B. D. L. (2001). Epidemiology and management of *Leptosphaeria maculans* (phoma stem canker) on oilseed rape in Australia, Canada and Europe. In *Plant Pathology*, *50*(1), 10–27. https://doi.org/10.1046/j.1365-3059.2001.00546.x

Wiedenheft, B., Lander, G. C., Zhou, K., Jore, M. M., Brouns, S. J. J., Van Der Oost, J., Doudna, J. A., & Nogales, E. (2011). Structures of the RNA-guided surveillance complex from a

bacterial immune system. *Nature*, *477*(7365), 486–489. https://doi.org/10.1038/nature10402

Wiedenheft, B., Sternberg, S. H., & Doudna, J. A. (2012). RNA-guided genetic silencing systems in bacteria and archaea. *Nature*, *482*(7385), 331–338. https://doi.org/10.1038/nature10886

Williams, P. H., & Delwiche, P. A. (1980). Screening for resistance to blackleg of crucifers in the seedling stage. In *Eucarpia "Cruciferae 1979" conference, 1-3 October 1979, Wageningen.* (pp. 164–170). https://www.cabdirect.org/cabdirect/abstract/19801693993

Yin, Y., Liu, X., Li, B., & Ma, Z. (2009). Characterization of sterol demethylation inhibitor-resistant isolates of *Fusarium asiaticum* and *F. graminearum* collected from wheat in china. *Phytopathology*, *99*(5), 487–497. https://doi.org/10.1094/PHYTO-99-5-0487

Yli-Mattila, T., Gagkaeva, T., Ward, T. J., Aoki, T., Kistler, H. C., & O'Donnell, K. (2009). A novel Asian clade within the *Fusarium graminearum* species complex includes a newly discovered cereal head blight pathogen from the Russian Far East. *Mycologia*, *101*(6), 841–852. https://doi.org/10.3852/08-217

Zhang, X., Peng, G., Parks, P., Hu, B., Li, Q., Jiang, L., Niu, Y., Huang, S., & Fernando, W. G. D. (2017). Identifying seedling and adult plant resistance of Chinese *Brassica napus* germplasm to *Leptosphaeria maculans*. *Plant Pathology*, *66*(5), 752–762. https://doi.org/10.1111/ppa.12626

Zhang, Xuehua, & Fernando, W. G. D. (2018). Insights into fighting against blackleg disease of *Brassica napus* in Canada. *Crop and Pasture Science*, *69*(1), 40–47. https://doi.org/10.1071/CP16401

Zhang, Xuehua, Peng, G., Kutcher, H. R., Balesdent, M. H., Delourme, R., & Fernando, W. G. D. (2016). Breakdown of *Rlm3* resistance in the *Brassica napus–Leptosphaeria maculans* pathosystem in western Canada. *European Journal of Plant Pathology*, *145*(3), 659–674. https://doi.org/10.1007/s10658-015-0819-0

Zhu, B., Cai, G., Hall, E. O., & Freeman, G. J. (2007). In-Fusion™ assembly: Seamless engineering of multidomain fusion proteins, modular vectors, and mutations. *BioTechniques*, *43*(3), 354–359. https://doi.org/10.2144/000112536

Zou, Z., Liu, F., & Fernando, W. G. D. (2018a). Rapid detection of *Leptosphaeria maculans* avirulence gene *AvrLm4-7* conferring the avirulence/virulence specificity on *Brassica napus* using a tetra-primer ARMS-PCR. *European Journal of Plant Pathology*, *152*(2), 515–520.

https://doi.org/10.1007/s10658-018-1465-0

Zou, Z., Liu, F., Selin, C., & Fernando, W. G. D. (2020). Generation and characterization of a virulent *Leptosphaeria maculans* isolate carrying a mutated *AvrLm7* gene using the CRISPR/Cas9 System. *Frontiers in Microbiology*, *11*. https://doi.org/10.3389/fmicb.2020.01969

Zou, Z., Zhang, X., & Fernando, W. G. D. (2018b). Distribution of mating-type alleles and genetic variability in field populations of *Leptosphaeria maculans* in western Canada. *Journal of Phytopathology*, *166*(6), 438–447. https://doi.org/10.1111/jph.12706

7.0 Appendices

7.1 Appendix A

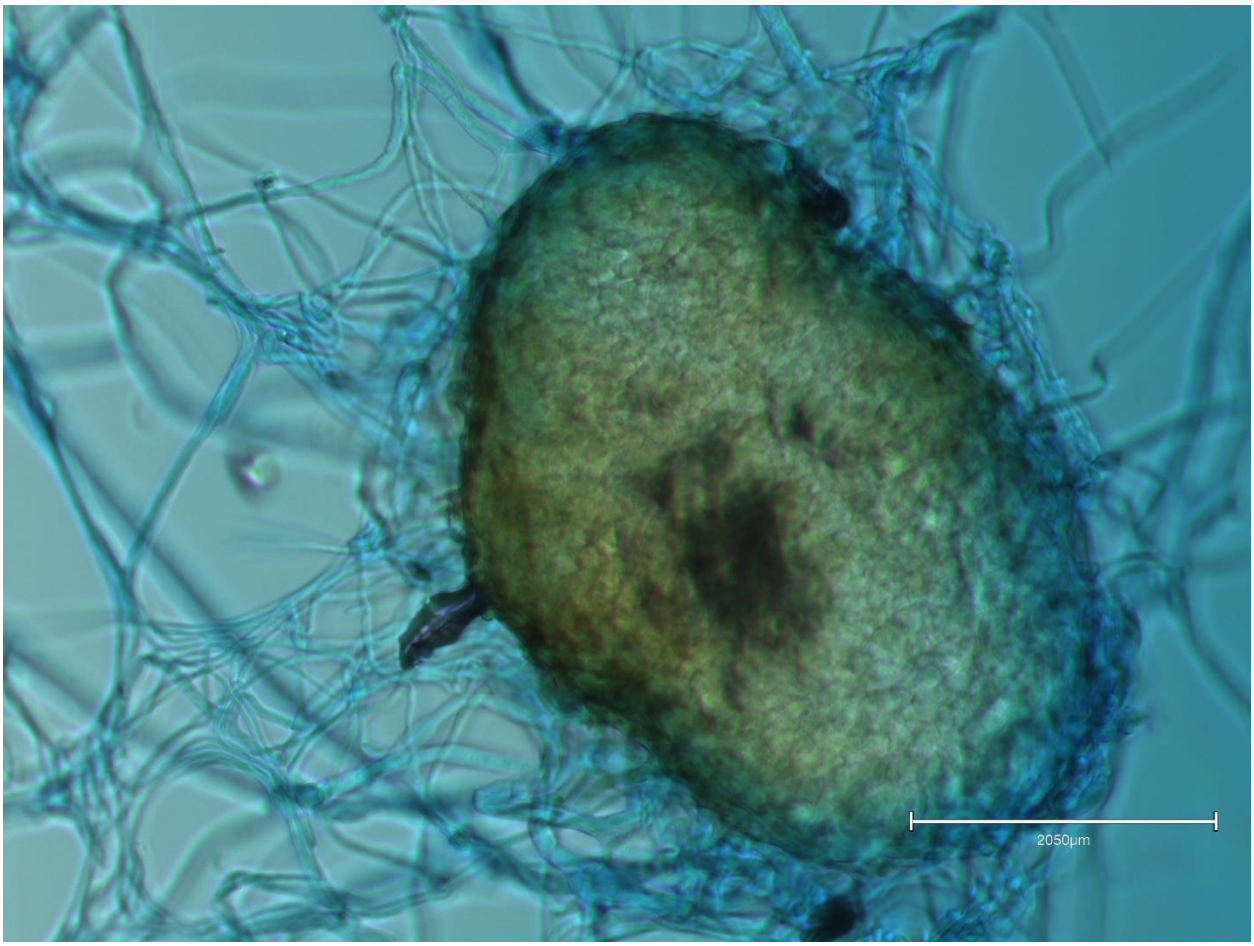

Figure 7.1 Microscopic image of pycnidia produced by *L. maculans* stained with lactophenol (magnification ×100 and scale bar illustrate 2050 µm). Pycnidia produce pycnidiospores, the main inoculum in blackleg in western Canadian canola fields.

7.2 Appendix B

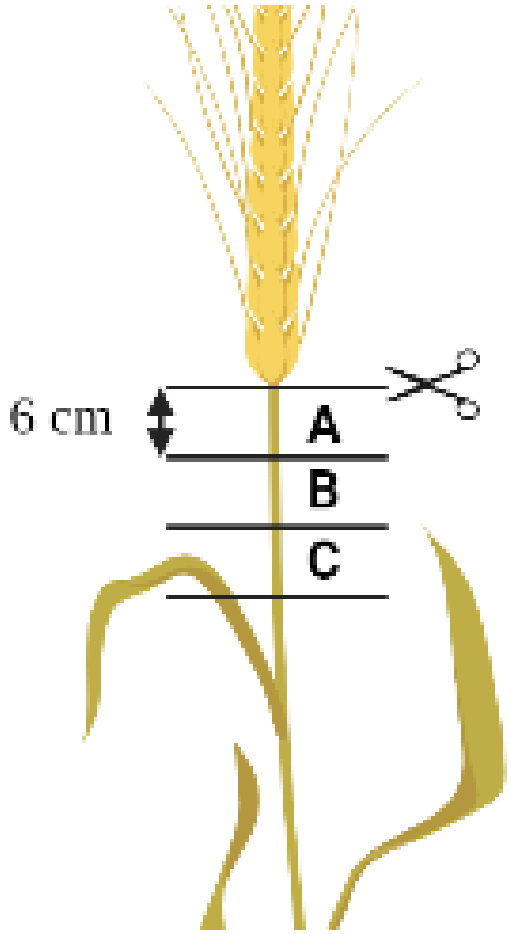

Figure 7.2 Image explaining the sample preparation for determining F. *graminearum* abundance in spring wheat stalks. Image created using BioRender.com.

Table 7.1 The primer sequences of PCR assays used to identify *Fusarium* species and chemotypes with SmartChip PCR technique (Canadian Grain Commission)

Species/chemotype	F Primer	F Primer Sequence	R Primer	R Primer Sequence	Reference
15ADON	15ADONfwd	GTTTCGATATTCATTGGAAAGCTAC	15ADONrev	CAAATAAGTATCGTCTGAAATTGGAAA	Nielsen et al., 2012
3ADON	3ADONfwd	AACATGATCGGTGAGGTATCGA	3ADONrev	CCATGGCGCTGGGAGTT	Nielsen et al., 2012
F. avenaceum	JiAf	GCTAATTCTTAACTTACTAGGGGCC	JiAr	CTGTAATAGGTTATTTACATGGGCG	Turner et al., 1998
F. asiaticum	FaF	CAGCTTCCTCGAAGACCT	FaR	GGACCGTAAATTTCTTCAGTG	Yin et al., 2009
F. avenaceum, acuminatum, tricinctum	avenMGB-fwd	CCATCGCCGTGGCTTTC	avenMGB-rev	CAAGCCCACAGACACGTTGT	Waalwijk et al., 2004
F. crookwellense/cerealis	Fcerf1	AGTGCCACCATCCCACACG	Fcerr1	CTGTTCGATGTGAACCAATCGA	Waalwijk et al., 2004
F. culmorum	FculBF	TTGATCAAACCATCATCATC	FculBR	AGAAAGGGTTAGAATCATGC	Klemsdal & Elen, 2006
F. equiseti	FequiB569 fwd	CACCGTCATTGGTATGTTGTCATC	FequiB598 rev	TGTTAGCATGAGAAGGTCATGAGTG	Nicolaisen et al., 2009
F. graminearum	Fg16N-F	ACAGATGACAAGATTCAGGCACA	Fg16N-R	TTCTTTGACATCTGTTCAACCCA	Nicholson et al., 1998
F. graminearum	FgramB379 fwd	CCATTCCCTGGGCGCT	FgramB411 rev	CCTATTGACAGGTGGTTAGTGACTGG	Nicolaisen et al., 2009
F. poae	FpoaeA51 fwd	ACCGAATCTCAACTCCGCTTT	FpoaeA98 rev	GTCTGTCAAGCATGTTAGCACAAGT	Nicolaisen et al., 2009
F. *pseudograminearum*	Fptri3e F	CAAGTTTGATCCAGGGTAATCC	Fptri3e R	GCTGTTTCTCTTAGTCTTCCTCA	Khudhair et al., 2014
F. tricinctum	Ftri573 fwd	TTGGTATGTTGTCACTGTCTCACACTAT	Ftri630 rev	TGACAGAGATGTTAGCATGATGCA	Nicolaisen et al., 2009
NIV	NIVfwd	GCCCATATTCGCGACAATGT	NIVrev	GGCGAACTGATGAGTAACAAAACC	Nielsen et al., 2012
Nx producer	NX1242tri1-fwd	TCGATGTTAATTGTTTTTGTGTA	NX1243tri1-rev	AGCCAGCTGGGTTTCTTG	Dr. Walkowiak (personal communication)
F. sporotrichioides	PfusF	CCGCGCCCCGTAAAACG	FspoR	ACTGTGTTTGCACACAGATC	Yli-Mattila et al., 2009

7.3 Appendix C

Table 7.2 Spring wheat samples in western Canada from participating farmers with the wheat variety, FHB resistance rating and observed DON levels in the grains

Field Code	Year	Variety	FHB rating	DON (ppm)
MB-SW09	2019	AAC Brandon	MR	0
MB-SW10	2019	SY Rowyn	MR	0.03
MB-SW11	2019	AAC Brandon	MR	0.43
MB-SW12	2019	Redberry	I	1.06
MB-SW13	2019	AAC Brandon	MR	0.01
MB-SW14	2019	AAC Viewfield	I	0
MB-SW15	2019	AAC Brandon	MR	0
MB-SW16	2019	AAC Brandon	MR	0.092
MB-SW17	2019	AAC Brandon	MR	0.08
MB-SW18	2019	AAC Brandon	MR	0.009
MB-SW19	2019	AAC Cameron	I	1.702
MB-SW20	2019	AAC Brandon	MR	0.015
MB-SW21	2019	AAC Brandon	MR	0.033
MB-SW22	2019	Prosper	I	0.019
MB-SW23	2019	AAC Brandon	MR	0.004
MB-SW24	2019	AAC Alida	MR	0.265
MB-SW25	2019	AAC Redberry	I	0.729
MB-SW26	2019	Titanium	MR	0.024
MB-SW27	2019	AAC Tisdale	MR	0
MB-SW28	2019	AAC Brandon	MR	0
MB-SW29	2019	AAC Brandon	MR	0.43
SK-SW01	2019	Plentiful	MR	0.015
SK-SW03	2019	AAC Brandon	MR	0.015
SK-SW04	2019			0.231
SK-SW05	2019	AAC Brandon	MR	0.086
SK-SW06	2019	AAC Brandon	MR	0.141
SK-SW07	2019	Morris	MR	0.13
SK-SW08	2019	AAC Brandon	MR	0.011
SK-SW09	2019	AAC Viewfield	I	1.124
SK-SW11	2019	Utmost	MS	2.613
SK-SW12	2019	Landmark	I	0.009
SK-SW14	2019	Landmark	I	0.081
SK-SW15	2019	Landmark	I	0.086
SK-SW16	2019	Utmost	MS	8.533
SK-SW17	2019	Shaw	MS	0.054

AB-SW01	2019	AAC Brandon	MR	0.014
AB-SW02	2019	AAC Viewfield	I	0.007
AB-SW03	2019	AAC Brandon	MR	0
AB-SW04	2019	AAC Elie	I	0
AB-SW05	2019	Sadash	S	1.742
AB-SW06	2019	AAC Brandon	MR	0.644
AB-SW07	2019	AAC Brandon	MR	0
AB-SW08	2019	AAC Brandon	MR	0
AB-SW09	2019	Chiffon	S	0.014
AB-SW11	2019	AAC Elie	I	0.012
MB-SW09	2020	AAC Brandon	MR	0.1
MB-SW10	2020	Redberry	I	1.6
MB-SW11	2020	AC Cardale	MR	0.1
MB-SW12	2020	AAC Brandon	MR	0
MB-SW13	2020	AAC Brandon	MR	0.1
MB-SW14	2020	AAC Brandon	MR	0.1
MB-SW15	2020	AAC Brandon	MR	0.9
MB-SW16	2020	AAC Brandon	MR	0.1
MB-SW17	2020	AAC Elie	I	0.1
MB-SW18	2020	AAC Starbuck - AAC Brandon VB	MR	0.2
MB-SW19	2020	AAC Cameron	I	0
MB-SW20	2020	AAC Brandon	MR	0.1
MB-SW21	2020	SY Rowyn	MR	0.1
MB-SW22	2020	ACC Viewfield	I	0
MB-SW23	2020	Penhold	MR	0.2
MB-SW24	2020	AAC Redberry	I	0.3
MB-SW25	2020	Landmark	I	0.2
MB-SW26	2020	AAC Brandon	MR	0
MB-SW27	2020	AAC Elie	I	0.5
MB-SW28	2020	AAC Brandon	MR	0
MB-SW29	2020	AAC Brandon	MR	1
SK-SW01	2020	AAC Brandon	MR	0.5
SK-SW03	2020	Alida	MR	0
SK-SW04	2020	AAC Brandon	MR	0
SK-SW05	2020	Redberry	I	0.1
SK-SW06	2020	Landmark	I	0.2
SK-SW07	2020	Morris	MR	0
SK-SW08	2020	Viewfield	I	0
SK-SW10	2020	Utmost	MS	0.1
SK-SW11	2020	Landmark	I	0.4

AB-SW01	2020	AAC Brandon	MR	0
AB-SW02	2020	AAC Viewfield	I	0
AB-SW03	2020	CDC Go	MS	0
AB-SW04	2020	AAC Elie	I	0
AB-SW05	2020	AAC Viewfield	I	0
AB-SW06	2020	Sadash	S	0.1
AB-SW08	2020	AAC Starbuck	MR	0
AB-SW09	2020	Glenn	I	0
AB-SW11	2020	AAC Viewfield	I	0.1

7.4 Appendix D

Table 7.3 Winter wheat samples in western Canada from participating farmers with the wheat variety, FHB resistance rating and observed DON levels in the grains

Field Code	Year	Variety	FHB rating	DON (ppm)
MBWW-30	2019	Emerson	R	0.01
MBWW-31	2019	Gateway	I	0
MBWW-32	2019	Elevate	I	0
MBWW-33	2019	Emerson	R	0
MBWW-34	2019	Gateway	I	0.01
MBWW-35	2019	Gateway	I	0
SKWW-01	2019	Buteo	MR	
SKWW-02	2019	Moats	S	0.09
SKWW-03	2019	Ptarmigan	I	0
SKWW-04	2019	AAC Wildfire	MR	0.15
SKWW-05	2019	Buteo	MR	0
SKWW-06	2019	Moats	S	
SKWW-07	2019	Wildfire	MR	0
SKWW-08	2019	Moats	S	0
SKWW-09	2019	Goldrush	I	0
SKWW-10	2019	Emerson	R	0
SKWW-11	2019	Moats	S	0
ABWW-01	2019	Pintail	S	0
ABWW-02	2019	Pintail	S	0
ABWW-03	2019	CDC Chase	MS	0.01
ABWW-04	2019	Moats	S	0
ABWW-05	2019	Wildfire	MR	0.01
ABWW-06	2019	Elevate	I	0
ABWW-07	2019	Elevate	I	0
MB-WW31	2020	Gateway	I	0
MB-WW32	2020	AAC Wildfire	MR	0.1
MB-WW33	2020	Emerson	R	0
MB-WW34	2020	Elevate	I	0
MB-WW35	2020	Gateway	I	0.1
MB-WW36	2020	Gateway	I	0
SK-WW01	2020	AAC Wildfire	MR	0.3
SK-WW02	2020	AAC Wildfire	MR	0.5
SK-WW03	2020	Moats	MS	0.1
SK-WW04	2020	Buteo	MR	0.1
SK-WW05	2020	Buteo	MR	0

SK-WW06	2020	Buteo	MR	0
SK-WW07	2020	Goldrush	I	0
SK-WW08	2020	Ptarmigan	I	0.2
SK-WW09	2020	AAC Wildfire	MR	0.3
SK-WW10	2020	AAC Wildfire	MR	0.2
SK-WW11	2020	Emerson	R	0
AB-WW01	2020	AAC Elevate	I	0
AB-WW02	2020	AAC Wildfire	MR	0
AB-WW03	2020	AAC Wildfire	MR	0
AB-WW05	2020	AAC Wildfire	MR	0
AB-WW07	2020	AAC Gateway	I	0
AB-WW09	2020	AAC Wildfire	MR	0
AB-WW12	2020	AAC Wildfire	MR	0

7.5 Appendix E

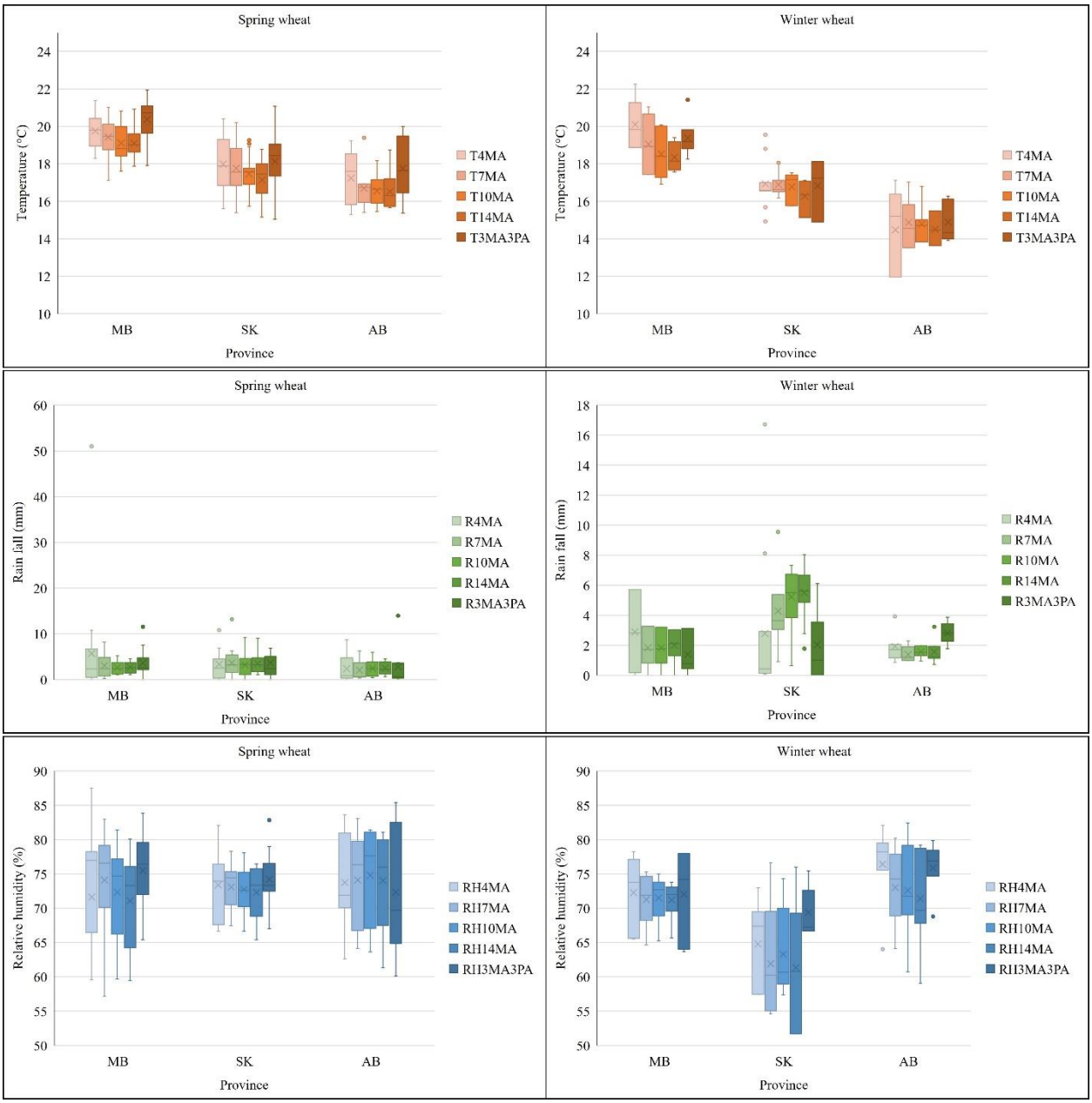

Figure 7.3 Box plots of the mean temperature (T), relative humidity (RH), and rainfall (R) data for each producer field retrieved from the nearest weather stations in 2019 to detect environmental conditions associated with FHB (data collected by Dr. Manasah Mkhabela). Data were collected for 4 days (4MA), 7 days (7MA), 10 days (10MA), 14 days pre-mid anthesis (14MA) and 3 days pre-mid anthesis to 3 days post-anthesis (3MA3PA).

7.6 Appendix F

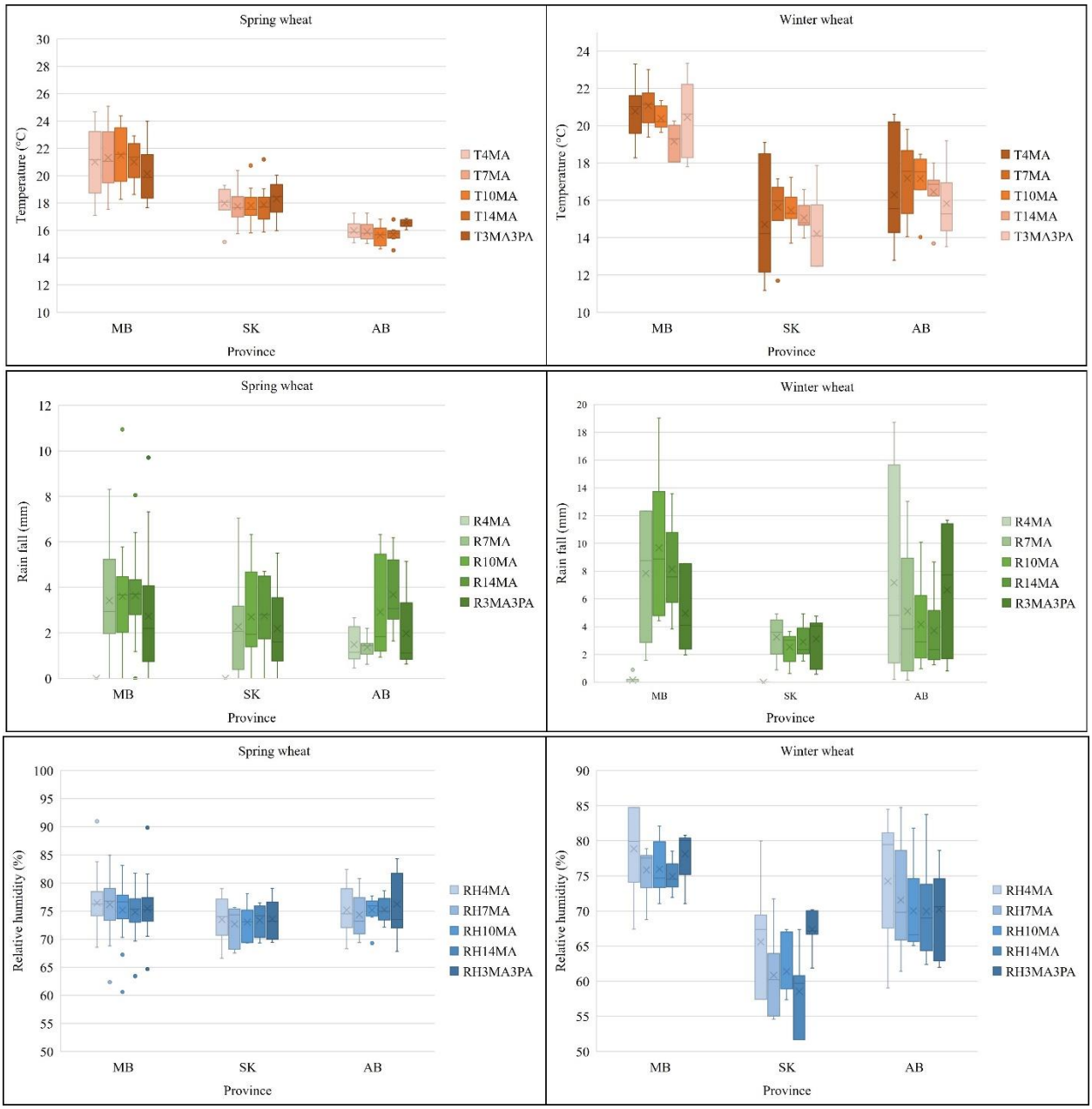

Figure 7.4 Box plots of the mean temperature (T), relative humidity (RH), and rainfall (R) data for each producer field retrieved from the nearest weather stations in 2020 to detect environmental conditions associated with FHB (data collected by Dr. Manasah Mkhabela). Data were collected for 4 days (4MA), 7 days (7MA), 10 days (10MA), 14 days pre-mid anthesis (14MA) and 3 days pre-mid anthesis to 3 days post-anthesis (3MA3PA).

7.7 List of abbreviations

AAFC	Agriculture and agri-food Canada
AB	Alberta
Avr	Avirulent
CRISPR	Clustered regularly interspaced short palindromic repeats
DNA	Deoxyribonucleic acid
DON	Deoxynivalenol
DSB	Double-strand break
ELISA	Enzyme-linked immunosorbent assay
FDK	*Fusarium* damaged kernels
Fg	*Fusarium graminearum*
FHB	Fusarium head blight
GDP	Gross domestic product
ITS	Internal transcribed spacer
MB	Manitoba
NIV	Nivalenol
qPCR	Quantitative PCR
RNA	Ribonucleic acid
RT-PCR	Real-time PCR
SgRNA	Single guide RNA
SK	Saskatchewan